

July 2020

# Design and Fabrication of Colloidal Delivery Systems to Encapsulate and Protect Curcumin: An Important Hydrophobic Nutraceutical

Mahesh Kharat

Follow this and additional works at: [https://scholarworks.umass.edu/dissertations\\_2](https://scholarworks.umass.edu/dissertations_2)



Part of the [Food Chemistry Commons](#)

---

## Recommended Citation

Kharat, Mahesh, "Design and Fabrication of Colloidal Delivery Systems to Encapsulate and Protect Curcumin: An Important Hydrophobic Nutraceutical" (2020). *Doctoral Dissertations*. 1930.  
[https://scholarworks.umass.edu/dissertations\\_2/1930](https://scholarworks.umass.edu/dissertations_2/1930)

This Open Access Dissertation is brought to you for free and open access by the Dissertations and Theses at ScholarWorks@UMass Amherst. It has been accepted for inclusion in Doctoral Dissertations by an authorized administrator of ScholarWorks@UMass Amherst. For more information, please contact [scholarworks@library.umass.edu](mailto:scholarworks@library.umass.edu).

**DESIGN AND FABRICATION OF COLLOIDAL DELIVERY SYSTEMS TO  
ENCAPSULATE AND PROTECT CURCUMIN: AN IMPORTANT  
HYDROPHOBIC NUTRACEUTICAL**

A Dissertation Presented

by

MAHESH M. KHARAT

Submitted to the Graduate School of the  
University of Massachusetts Amherst in partial fulfillment  
of the requirements for the degree of

DOCTOR OF PHILOSOPHY

May 2020

Food Science

© Copyright by Mahesh M. Kharat 2020

All Rights Reserved

**DESIGN AND FABRICATION OF COLLOIDAL DELIVERY SYSTEMS TO  
ENCAPSULATE AND PROTECT CURCUMIN: AN IMPORTANT  
HYDROPHOBIC NUTRACEUTICAL**

A Dissertation Presented

by

MAHESH M. KHARAT

Approved as to style and content by:

---

David Julian McClements, Chair

---

Hang Xiao, Member

---

Zhenhua Liu, Member

---

Eric Decker, Department Head  
Food Science

## *To the greatest warrior, Arjuna*

who, in the middle of the battlefield,  
asked Lord Krishna this remarkable question-

*स्थितप्रज्ञस्य का भाषा समाधिस्थस्य केशव |  
स्थितधीः किं प्रभाषेत किमासीत ब्रजेत किम् ॥*

भगवद्गीता अध्याय २, श्लोक ५४

*Sthita-prajnasya ka bhasa samadhi-sthasya kesava |  
Sthita-dhih kim prabhaseta kim asita vrajeta kim ॥*

Bhagavadgeeta Chapter 2, Verse 54

## ACKNOWLEDGMENTS

I would like to express my sincere gratitude to my advisor and mentor, Prof. Julian McClements, for his guidance and enormous support throughout my graduate studies. His efforts, knowledge, and encouragement have the greatest contribution to shaping my career as a young scientist. Every discussion I had with Julian was a stress reliever and an intellectual delight!

I would like to thank my dissertation committee members, Dr. Hang Xiao and Dr. Zhenhua Liu. Their suggestions and feedback have greatly contributed to guiding my thesis work. I would like to thank Dr. Decker for the help and support in my research, teaching and co-curricular pursuits, and I am grateful for all of his assistance throughout my time at the University of Massachusetts. I would like to thank Fran, Mary, and Deby, for the help and coordination with the paperwork. A big thanks to Dave for assisting with activities in the pilot plant. I would also like to thank all of my past and current lab mates in the Biopolymers and Colloids Research Laboratory for their support, Anna, Bai, Cansu, Charmaine, Cheryl, Chengzhen, Feng, HaYoun, Irene, Jennie, Jorge, Jun, Kevin, Kubra, Li, Lu, Maria, Minqi, Nat, Ruyi, Sandra, Shelly, Sisie, Vanessa, Ye, Yeye, and Zach. It was a wonderful experience to be able to meet and share the workplace with people from around the world. I am indebted to Bing, and Tao for their love and care. I am grateful to Joy and Matt for their help in conducting and completing the lab work.

I cannot adequately thank Jean Alamed for her support- my research work was not possible without her. Every time I entered Jean's office with questions, concerns, and stress, I came out with answers, encouragement, and relief.

I would like to thank all my friends. They continue to be a source of endless support and unconditional love. Their thoughts always keep my spirit bright.

As I am writing this, I am thinking of my family, its struggle and sacrifices. Their thoughts, teachings, and values are the source of my integrity and wisdom.

## ABSTRACT

### DESIGN AND FABRICATION OF COLLOIDAL DELIVERY SYSTEMS TO ENCAPSULATE AND PROTECT CURCUMIN: AN IMPORTANT HYDROPHOBIC NUTRACEUTICAL

May 2020

MAHESH KHARAT, B.Tech., UNIVERSITY INSTITUTE OF CHEMICAL TECHNOLOGY MUMBAI

M.Tech., INSTITUTE OF CHEMICAL TECHNOLOGY MUMBAI

Ph.D., UNIVERSITY OF MASSACHUSETTS AMHERST

Directed by: Professor David Julian McClements

Curcumin is a polyphenolic compound found in Turmeric (*Curcuma longa*) rhizome that has excellent biological benefits such as antioxidant, anti-inflammatory, and anti-cancer properties to name a few. However, its incorporation in food and pharmaceuticals is difficult due to low water solubility and chemical instability. This study focuses on developing colloidal delivery systems for efficient encapsulation and increased protection of curcumin for maximizing the proposed health benefits of curcumin.

It was found that the physical and chemical stability of pure curcumin is impacted by pH, storage temperature, and molecular environment both in aqueous solutions and in oil-in-water emulsions. Pure curcumin was highly unstable to chemical degradation in neutral and alkaline aqueous solutions ( $\text{pH} \geq 7.0$ ) and it was most stable in acidic oil-in-water emulsions. Curcumin stability in emulsions depended on the emulsifier type, and the extent of curcumin degradation decreased in the following order: saponins  $\gg$  gum arabic  $\approx$  caseinate  $\approx$  Tween 80. These results suggest that saponin accelerated curcumin degradation, which may be due to their ability to promote peroxidation reactions or it

may be due to the presence of impurities in them, such as metals. The kinetics of curcumin degradation was significantly impacted by the mean droplet diameters ( $d_{32}$ ). The more rapid chemical degradation of the curcumin in the smaller droplets can be attributed to the fact that curcumin exchange between the interior and exterior of the droplets occurs more rapidly as the droplet dimensions decrease. Antioxidants were incorporated to protect curcumin in an emulsion having small droplets. The water-soluble antioxidants were more effective at protecting curcumin from degradation than the oil-soluble ones, which may have been because curcumin degrades faster in water than in oil, while the oil-soluble antioxidant actually slightly promoted curcumin degradation. Finally, the formation of nanostructured lipid carriers (NLCs) was optimized which, unlike O/W emulsion, consists of a solidified fat phase. NLCs were formulated using a hot-homogenization approach using fully hydrogenated soybean oil as the lipid phase and quillaja saponins as a natural surfactant. Characterization and stability studies revealed that NLCs have the potential to replace oil-in-water emulsions in commercial foods. Future studies are needed to establish their functional performance for curcumin encapsulation and protection. In summary, this study showed that the stability of curcumin in emulsions depends on various physicochemical parameters. This knowledge is important in designing and fabrication of colloidal systems for curcumin delivery.

**Keywords:** Curcumin; emulsion; degradation, emulsifier type; droplet size; oil-water interfacial area; ascorbic acid; antioxidant; nanostructured lipid carrier



# TABLE OF CONTENTS

	Page
ACKNOWLEDGMENTS .....	v
ABSTRACT .....	vi
LIST OF TABLES .....	xii
LIST OF FIGURES .....	xiii
CHAPTER	
1. LITERATURE REVIEW .....	1
1.1 Introduction .....	1
1.2 Delivery by Design Approach .....	2
1.2.1 Stage 1: Active agent definition.....	3
1.2.1.1. Molecular and physicochemical characteristics.....	3
1.2.1.1.1 Chemical formula and structure .....	3
1.2.1.1.2. Molar mass and density .....	4
1.2.1.1.3. Refractive index .....	4
1.2.1.1.4. Melting and boiling properties .....	4
1.2.1.1.5. Partitioning .....	5
1.2.1.1.6. Diffusion coefficient.....	5
1.2.1.1.7. Surface tension .....	6
1.2.1.1.8. Solubility .....	6
1.2.1.1.9. Acid dissociation constants (pKa).....	7
1.2.1.1.10. Hydrogen bond acceptors and donors .....	7
1.2.1.2. Stability characteristics .....	8
1.2.2. Stage 2: End-product definition .....	9
1.2.3. Stage 3: Delivery system specification .....	13
1.2.4. Stage 4: Particle specification and delivery system specification .....	15
1.2.4.1. Micelles and microemulsions .....	17
1.2.4.2. Liposomes .....	20
1.2.4.3. Emulsions and nanoemulsions .....	22
1.2.4.4. Solid lipid nanoparticles and nanostructured lipid carriers.....	24
1.2.4.5. Biopolymer particles .....	27
1.2.5. Stage 5: Process specification .....	30
1.2.6. Stage 6: Performance testing .....	32
1.2.7. Stage 7: System optimization.....	32
1.3. Conclusion.....	33
2. PHYSICAL AND CHEMICAL STABILITY OF CURCUMIN IN AQUEOUS SOLUTIONS AND EMULSIONS: IMPACT OF PH, TEMPERATURE, AND MOLECULAR ENVIRONMENT.....	34
2.1. Introduction .....	34

2.2. Materials and methods.....	36
2.2.1. Dissolution and Stability of Curcumin in Aqueous Buffer Solutions.....	36
2.2.2. Turbidity Measurements .....	37
2.2.3. Oil Solubility of Curcumin .....	37
2.2.4. Preparation of Curcumin Emulsions .....	37
2.2.5. Curcumin Concentration Measurements.....	38
2.2.6. Color Measurements .....	39
2.2.7. Particle Size and Charge Measurements .....	39
2.2.8. Microstructure Analysis.....	39
2.2.9. Statistical Analysis.....	40
2.3. Results and discussion.....	40
2.3.1 Physical and Chemical Stabilities of Curcumin in Aqueous Solutions .....	40
2.3.2 Crystallization of Curcumin in Aqueous Solutions .....	43
2.3.3 Oil Solubility of Curcumin .....	45
2.3.4 Chemical Stability of Curcumin in Emulsion Systems.....	45
2.3.5 Changes in Emulsion Appearance during Storage.....	48
2.3.6 Detection of Curcumin Crystals in Emulsions.....	52
2.3.7 Physical Properties of Emulsions during Storage.....	53
3. STABILITY OF CURCUMIN IN OIL-IN-WATER EMULSIONS: IMPACT OF EMULSIFIER TYPE AND CONCENTRATION ON CHEMICAL DEGRADATION.....	55
3.1. Introduction .....	55
3.2. Materials and methods.....	56
3.2.1. Materials .....	56
3.2.2. Determination of emulsifier surface load .....	56
3.2.3. Preparation of curcumin-loaded emulsions .....	57
3.2.4. Curcumin concentration measurements .....	58
3.2.5. Color measurements.....	59
3.2.6. Particle size and charge measurements .....	59
3.2.7. Microstructure analysis.....	60
3.2.8. Statistical analysis .....	60
3.3. Results and Discussions .....	61
3.3.1. Impact of emulsifier type on emulsion formation.....	61
3.3.2. Impact of emulsifier on color fading of curcumin-loaded emulsions.....	66
3.3.2.1. Preliminary experiments .....	66
3.3.2.2. Color stability.....	68
3.3.3. Impact of emulsifier on chemical stability of curcumin in emulsion systems	71
3.3.4. Impact of emulsifier on physical stability of curcumin-loaded emulsions .....	74
3.3.5. Electrical characteristics of emulsion droplets .....	78
3.4. Conclusions .....	79
4. STABILITY OF CURCUMIN-ENRICHED OIL-IN-WATER EMULSIONS: ROLE OF INTERFACIAL SURFACE AREA.....	81
4.1. Introduction .....	81
4.2. Materials and methods.....	82
4.2.1. Materials .....	82

4.2.2. Preparation of curcumin-loaded emulsions .....	82
4.2.3. Appearance .....	83
4.2.4. Curcumin concentration measurements .....	84
4.2.5. Particle characterization .....	84
4.2.6. Particle morphology .....	85
4.2.7. Statistical analysis .....	85
4.3. Results and discussions .....	85
4.3.1. Emulsion droplet characteristics .....	85
4.3.2. Microstructure analysis .....	89
4.3.3. Impact of droplet size on emulsion appearance .....	90
4.3.4. Impact of droplet size on color fading .....	92
4.3.5. Impact of droplet size on chemical stability of curcumin .....	95
4.4. Conclusions .....	101
5. ENHANCEMENT OF CHEMICAL STABILITY OF CURCUMIN-ENRICHED OIL-IN-WATER EMULSIONS: IMPACT OF ANTIOXIDANT TYPE AND CONCENTRATION .....	103
5.1. Introduction .....	103
5.2. Materials and methods.....	103
5.2.1. Materials .....	103
5.2.2. Preparation of curcumin-loaded emulsions .....	105
5.2.3. Appearance .....	106
5.2.4. Curcumin concentration measurements .....	106
5.2.5. Particle characterization .....	107
5.2.6. Particle morphology .....	107
5.2.7. Statistical analysis .....	108
5.3. Results and discussions .....	108
5.3.1. Impact of Antioxidants on appearance of curcumin loaded emulsions .....	108
5.3.2. Impact of antioxidant type on chemical stability of curcumin .....	110
5.3.3. Impact of antioxidant concentration on chemical stability of curcumin.....	114
5.3.4. Impact of antioxidant addition on physical stability of curcumin-loaded emulsion .....	115
5.3.5. Microstructure analysis .....	117
5.4. Conclusions .....	118
6. FABRICATION AND CHARACTERIZATION OF NANOSTRUCTURED LIPID CARRIERS (NLC) USING A PLANT-BASED EMULSIFIER: QUILLAJA SAPONINS .....	119
6.1. Introduction .....	119
6.2 Materials and methods.....	122
6.2.1 Materials .....	122
6.2.2. Differential scanning calorimetry (DSC).....	123
6.2.3 Preparation of NLC.....	123
6.2.4 Droplet size and charge measurements .....	125
6.2.5. Thermal analysis of NLC and estimation of solid fat content .....	126
6.2.6. Turbidity measurements.....	126
6.2.7. Rheology analysis .....	127

6.2.8. Color measurements and physical appearance .....	127
6.2.9. Aggregation stability .....	127
6.2.10. Transmission electron microscopy (TEM) .....	128
6.2.11. Temperature-dependent optical microscopy analysis .....	128
6.2.12. Statistical analysis .....	129
6.3 Results and discussions .....	129
6.3.1. Thermal behavior of lipid phase .....	129
6.3.2. Optimizing NLC formation.....	131
6.3.2.1. Number of passes through microfluidizer.....	131
6.3.2.2. Cooling rate and stirring conditions.....	131
6.3.2.3. Effect of emulsifier concentration on droplet size.....	133
6.3.3. Properties of NLC suspensions .....	134
6.3.3.1. Thermal behavior of NLC.....	134
6.3.3.2. Rheology of NLC.....	140
6.3.3.3. Appearance of NLC suspensions .....	140
6.3.3.4. Microstructure of coarse NLCs during thermal transitions .....	141
6.3.3.5. Transition electron microscopy.....	144
6.3.4. Stability of NLC to thermal stress .....	145
6.4 Conclusions .....	147
7. CONCLUSION AND FUTURE STUDIES .....	148
APPENDIX .....	149
BIBLIOGRAPHY.....	161

## LIST OF TABLES

Table	Page
1. Compositional and physicochemical properties of some commercial food products.....	11
2. Physicochemical parameters defining model plant-based ‘Golden Milk’.....	12
3. Examples of biopolymer-based delivery systems for delivery of curcumin.....	28
4. Yellowness ( $b^*$ ), Mean Particle Diameter, and Electrical Characteristics ( $\zeta$ -Potentials) of Emulsions at Days 1 and 31.....	51
5. Mean droplet diameter (D32) and electrical characteristics ( $\zeta$ -potentials) of curcumin emulsions at Day 1 and Day 15 (37 °C).....	76
6. Different emulsion types, and their preparation.....	83
7. Emulsion droplet characteristics after emulsion preparation (Day 0).....	87
8. Molecular structure and partition coefficients of antioxidants used in this study.....	104
9. Enthalpy changes and onset temperatures for the melting and crystallization of hydrogenated bulk fats.....	130
10. Comparison of thermal behavior (transition enthalpies and onset temperatures) of NLCs and bulk fats formulated from hydrogenated soybean oil. The NLCs were formulated using different Q-naturale levels.....	137

## LIST OF FIGURES

Figure	Page
1. Structure of curcumin .....	3
2. Properties of curcumin as a function of pH.....	7
3. Stability of curcumin in MCT oil, and tween 80 solution (1 wt. % tween 80, pH 6.5).....	15
4. Different colloidal system for encapsulation and delivery of curcumin.....	17
5. Stability of curcumin (40 $\mu$ M) in phosphate buffer solutions (10 mM) of various pH values when the system was unmixed (A) and mixed (B).....	42
6. Turbidity of aqueous curcumin buffer solutions (40 $\mu$ M) measured at 600 nm: (A) effect of pH on turbidity of unmixed samples over a period of 60 min; (B) difference in turbidity values after 15 min as affected by agitation.....	44
7. Stability of curcumin in oil-in-water emulsions (30 wt % oil) at 37 °C: (A) change in curcumin concentration; (B) curcumin retention in emulsions after 1 month of storage; (C) comparison of residual curcumin in emulsions stored at different pH values and temperatures.....	48
8. Visual appearance of curcumin buffer solution (40 $\mu$ M) incubated at 37 °C for 15 min (A) and MCT-in-water emulsion (30 wt % oil) incubated at 37 °C taken on day 1 (B) and day 31 (C). The labels on day 31 are the same as those on day 1.....	50
9. Micrographs showing curcumin crystals in (A) unmixed aqueous buffers (scale bar = 10 $\mu$ m), (B) emulsions (scale bar = 10 $\mu$ m), and (C) mixed aqueous buffers (images taken using cross-polarizer, scale bar = 20 $\mu$ m; (i–iii) pH 3.0, 5.0, and 7.0, respectively.....	53
10. Effect of emulsifier type and concentration on the mean droplet diameter ( $D_{32}$ ) of MCT oil-in-water emulsions produced using a high-pressure homogenizer (microfluidizer).....	62
11. Photographs of curcumin-loaded oil-in-water emulsions prepared at the critical emulsifier concentration when stored under different conditions (pH 7.0). Emulsions were stabilized by sodium caseinate (NaC), Tween 80 (T80), quillaja saponins (SAP) or gum.....	67
12. Change in tristimulus color coordinates ( $L^*$ , $a^*$ , $b^*$ ) of curcumin-loaded oil-in-water emulsions during storage at pH 7 and 55 °C.....	69
13. Impact of emulsifier type and concentration on the yellowness ( $b^*$ -values) of emulsions stored at pH 7 and 55 °C for 15 days.....	70
14. Impact of emulsifier type and concentration on curcumin retention in emulsions stored at pH 3 and 7 at 37 °C for 15 days.....	72

15. Impact of emulsifier type on curcumin retention in emulsions during storage at pH 7 and 55 °C.....	73
16. Impact of emulsifier type and concentration on curcumin retention in emulsions stored at pH 7 and 55 °C.....	74
17. Micrographs of curcumin-loaded emulsions after storage at pH 7 and 55 °C at Day 1 and 15.....	78
18. Droplet size distribution of different emulsion types.....	88
19. Change in the electrical characteristics of droplets before and after storage....	88
20. Micrographs of curcumin-loaded emulsions having different specific surface area taken at Day 0 (Initial) and Day 17 (After storage, pH 7, 55 °C). Scale bars represent 20 µm.....	90
21. Photographs of curcumin-loaded oil-in-water emulsions with different specific surface area of droplets (300, 2500, 2400, 80000 m <sup>2</sup> , left to right) during storage (55 °C). Emulsions composition: oil 10 wt.%, curcumin 0.01 wt.%, Quillaja saponin extract 1 wt.%, and rest phosphate buffer (pH 7.0, 5 mM).....	92
22. Impact of specific surface area of droplets on change (A) and retention (B) in tristimulus color coordinate (b*) of curcumin-loaded oil-in-water emulsions during storage at pH 7 and 55 °C.....	94
23. Impact of specific surface area of droplets on change (A) and retention (B) in curcumin concentration, and (C) rate of curcumin degradation, k, in oil-in-water emulsions during storage at pH 7 and 55 °C.....	97
24. Effect of droplet size on the release profiles of curcumin from a spherical oil droplet as derived from the Crank model.....	100
25. Hydrophobic curcumin is distributed between the oil and water phases according to its LogP value (3.29). The rate of exchange is faster in emulsions with smaller droplet, leading to faster degradation since each curcumin molecule spends more time in the water.....	101
26. Photographs of curcumin-loaded oil-in-water emulsions incorporated with different antioxidants. Emulsions composition: oil 10 wt.%, curcumin 0.01 wt.%, Quillaja saponin extract 1 wt.%, antioxidants (600 µM), and rest phosphate buffer (pH 7.0, 5 mM).....	109
27. Impact of antioxidant type on change (A) and retention (B) in tristimulus color coordinate (b*) of curcumin-loaded oil-in-water emulsions during storage at pH 7 and 55 °C. Antioxidant concentration, 600 µM.....	110
28. Impact of antioxidant type on change (A) and retention (B) in curcumin concentration of oil-in-water emulsions during storage at pH 7 and 55 °C. Antioxidant concentration, 600 µM.....	113
29. Impact of antioxidant concentration on curcumin concentration (A) and retention (B) in oil-in-water emulsions during storage at pH 7 and 55 °C.....	115

30. Effect of antioxidant type (A) and ascorbic acid concentration (B) on the mean droplet diameter ( $D_{32}$ ) of MCT oil-in-water emulsions produced using a high-pressure homogenizer (microfluidizer).....	117
31. Micrographs of curcumin-loaded emulsions added without and with different antioxidants at Day 1 and Day 17 (pH 7, 55 °C). Scale bars represent 20 $\mu$ m.	118
32. Potential loss of bioactive agents by simple diffusion from liquid oil droplets in nanoemulsions (a) or expulsion from homogeneous crystal matrices in solid lipid nanoparticles (b). Potential entrapment of bioactives in heterogeneous crystal matrix in nanostructured lipid carriers (c). Modified from (Müller et al., 2002).....	120
33. Effect of emulsifier concentration on the mean particle diameter (A) and particle size distribution (B) of 30 wt% fully hydrogenated soybean oil-in-water emulsions prepared using a high-pressure homogenizer (microfluidizer).....	133
34. DSC profiles of hydrogenated soybean oil (HSO) in bulk form and NLC suspension form (30% HSO, 6% QN) during heating and cooling at a controlled rate of 10 °C min <sup>-1</sup> ; (B) Turbidity analysis of the same NLC suspensions.....	135
35. DSC profiles (A), and solid fat content as a function of temperature (B) in emulsified HSO (30 wt. %) prepared with varying emulsifier concentrations. Samples were analyzed at a rate of 10 °C min <sup>-1</sup> .....	138
36. Rheological properties of NLC suspensions. (A) Flow behavior studied by measuring shear stress at variable shear rates; (B) Effect of emulsifier concentration on shear viscosity of NLC suspensions.....	140
37. Visual appearance of NLC suspensions with QN contents of 3, 6, 9, and 12 wt. % (left to right). L* values represent lightness of dispersion.....	141
38. Microscopy images of coarse NLC suspensions during heating and cooling on an optical microscopy stage with crossed-polarizers (30% HSO, 6% QN, 64% phosphate buffer).....	143
39. Mean Grey Value analysis of optical microscopy images (A) and DSC analysis (B) of coarse NLC (30% HSO, 6% QN, 64% phosphate buffer).....	144
40. Transmission electron microscopy images of NLC suspensions (30% HSO, 6% QN). The scale bar represents 500 nm.....	145



# CHAPTER 1

## LITERATURE REVIEW

### 1.1 Introduction

Curcumin is a natural, yellow colored polyphenol present in turmeric, the rhizome of perennial herb *Curcuma longa*. For many centuries, dried and powdered turmeric has been used as spice for its specific color and flavor. It has been a major ingredient in Ayurvedic remedies as well as in Chinese medicine. With over 7000 research publications in last five years, the consensus amongst scientist on curcumin's health benefits has grown only stronger (Web of Science, © 2019 Clarivate). Many *in vitro* and *in vivo* studies have recognized antioxidant, anti-inflammatory, and anticancer properties of curcumin to name a few. Moreover, curcumin is shown to selectively attack cancer cells and not produce any cytotoxic effects on normal cells (Vecchione et al., 2016). Despite its benefits that are proven *in vitro* and *in vivo*, poor oral bioavailability of curcumin is the biggest challenge in deriving its positive effects in humans (Anand, Kunnumakkara, Newman, & Aggarwal, 2007). For example, when 8g of curcumin was given to human subjects, curcumin present in plasma as free or unconjugated form was mainly undetectable. The highest concentration of curcumin detected after being released from its conjugated form was found to be about 41 ng/mL after 6 h (Dhillon et al., 2008). This clearly indicates poor absorption and rapid metabolism of curcumin under physiological conditions. Moreover, the efficacy of curcumin varies across individuals and its bioavailability is greatly dependent on sex (Barber-Chamoux et al., 2018; Schiborr, Kocher, Behnam, Jandasek, Toelstede, & Frank, 2014).

## **1.2 Delivery by Design Approach**

To address the challenges of low water solubility, high chemical instability, and poor bioavailability, a great number of studies have been carried out to develop delivery systems for curcumin. Surfactant micelles and microemulsions, oil-in-water nanoemulsions, solid-lipid nanoparticles, nanostructured lipid carriers, and biopolymer particles have been shown to increase water dispersibility, enhance chemical stability, and improve bioavailability of curcumin. Each of these systems have different physicochemical properties like particle size, particle composition, stability, appearance and optical properties, and sensory attributes. Also, each system has its own advantages and drawbacks which limits application of a single system in broad category of food products. Consequently, a delivery system must be composed, and selected according to desired properties in the end-product. In this review, we have discussed ‘Delivery by Design (DbD)’- a new standardized approach that could facilitate identification and selection of a specific delivery system which is aimed at delivering curcumin through specific food products (McClements, 2018). This stepwise approach can be discussed in several stages: 1. definition of the molecular and physicochemical properties of the active agent; 2. definition of the required physicochemical, sensory, and functional attributes of the end-product; 3. specification of the required attributes of the colloidal delivery system; 4. specification of particle properties and delivery system selection; 5. optimization of delivery system manufacturing process; 6. establishment and implementation of delivery system testing protocol; and 7. optimization of delivery system performance.

## 1.2.1 Stage 1: Active agent definition

### 1.2.1.1 Molecular and physicochemical characteristics

#### 1.2.1.1.1 Chemical formula and structure

Curcumin has a molecular formula of  $C_{21}H_{20}O_6$ . Structurally, it has two methoxy substituted phenol rings bound through a heptadiene chain having carbonyl moiety at positions 3, and 5 (**Figure 1**). Curcumin is a powerful antioxidant and its mechanism of action is highly pH dependent. In acidic conditions, keto form is predominant and the central methylene ( $-CH_2$ ) group acts as a hydrogen donor (Jovanovic, Steenken, Boone, & Simic, 1999). At alkaline pH, antioxidant properties of curcumin are mainly associated to phenolic hydroxyl groups (Priyadarsini et al., 2003). Methoxy groups present at ortho position further increase the antioxidative effect (Cuvelier, Richard, & Berset, 1992). Moreover, methoxy groups are believed to have an important role in some of the biological activities associated with curcumin (Yang et al., 2017). In keto form, due to the presence of  $\alpha,\beta$ -unsaturated carbonyl group, curcumin can act as Michael acceptor which is basis for its reactivity towards many molecular targets, mainly proteins having cysteine residues. (Heger, van Golen, Broekgaarden, & Michel, 2014).



**Figure 1.** Structure of curcumin

#### **1.2.1.1.2. Molar mass and density**

Absorption of bioactives in humans is affected by their molecular weight (Fisher, Brown, Davis, Parr, & Smith, 1987). Molecular weight of curcumin is 368.38 Da, hence it can be considered as low molecular weight compound. Curcumin occurs as yellow-orange crystalline powder with density of 1.3 g cm<sup>-3</sup>.

#### **1.2.1.1.3. Refractive index**

Its predicted refractive index in powder form is 1.643. This is important in delivery systems stabilized by curcumin particles. For example, 'pickering emulsions' are stabilized by solid particles which will scatter or reflect light and influence optical properties in a different way than a lipid droplet stabilized by dissolved emulsifier would. In many delivery systems, curcumin would be in dissolved form. For example, curcumin may be dissolved in medium chain triglyceride (MCT) before preparing curcumin encapsulated MCT oil-in water emulsion (Shah, Zhang, Li, & Li, 2016). In this case, refractive index of MCT oil-curcumin solution is more important which is 1.447 (1 mg curcumin/g MCT oil).

#### **1.2.1.1.4. Melting and boiling properties**

Curcumin crystals melt around 183 °C and vaporizes at 521 °C. Such high temperatures are rarely experienced in food manufacturing. Usually, curcumin is dissolved in oil or aqueous phase at temperatures below 100 °C for its incorporation in delivery systems.

#### 1.2.1.1.5. Partitioning

In a heterogeneous system such as oil-in-water emulsion, curcumin can be distributed in both oil (nonpolar region), and water (polar region) depending on its affinity toward both phases. It is represented by the partition co-efficient which is logarithm of ratios of curcumin concentration in oil and that in water. As a result, partition co-efficient of curcumin changes if either or both the phases are changed. For example, octanol-water partition coefficient of curcumin is about 4.12, while that for MCT-tween 80 solution (1 wt. %) system is 1.13.

$$\log P = \log \frac{[\text{curcumin}]_{\text{oil}}}{[\text{curcumin}]_{\text{water}}}$$

#### 1.2.1.1.6. Diffusion coefficient

Process of diffusion is driven by the concentration gradient. Diffusion of curcumin through oil, or water, or the oil-water interface would affect its distribution and release characteristics. Theoretical prediction of diffusion co-efficient can be obtained by following equation

$$D = kT / (6\pi \eta r)$$

where,  $k$  is Boltzmann's constant,  $T$  is the absolute temperature ( $^{\circ}\text{K}$ ),  $\eta$  is the shear viscosity of the solvent (mPa.s), and  $r$  is the effective radius of curcumin molecule ( $4.3 \times 10^{-10}$  m). Process of diffusion can also be a key to degradation of curcumin in emulsions. Curcumin is known to be very stable in oils whereas it degrades quickly in aqueous systems at  $\text{pH} \geq 7.0$  (Kharat, Du, Zhang, & McClements, 2017). In emulsion systems, as

curcumin degradation proceeds in the aqueous phase, more curcumin can diffuse from oil to the aqueous phase as a result of the concentration gradient.

#### **1.2.1.1.7. Surface tension**

Curcumin has a backbone of two phenol rings connected through heptadiene chain giving it a hydrophobic characteristic (Balasubramanian, 2006), while hydroxyl groups in phenol rings are hydrophilic in nature (**Figure 1**). Therefore, curcumin can be surface active. Its surface tension is about 54 dyne/cm.

#### **1.2.1.1.8. Solubility**

As mentioned, curcumin has a log  $P$  of 4.12 indicating that it is mainly of hydrophobic nature and poorly soluble in water. Hence, it is difficult to incorporate curcumin in aqueous based food, such as a beverage. Also, the water solubility of curcumin is highly influenced by the pH, which in turn affects its partitioning behavior in foods containing both oil and water, for example a dairy beverage. As shown in **Figure 2**, it has negligible charge and is very sparingly soluble in acidic pH. At pH 7.0, its predicted water solubility is 24 mg/L.

Solubility of curcumin in oils and fat is more important when encapsulating it in delivery systems like nanoemulsion, and solid-lipid nanoparticles. For example, its solubility in corn oil (3 mg/g), medium chain triglyceride (7.9 mg/g), tributyrin (29.8 mg/g), olive oil (1.18 mg/mL), sunflower oil (1.08 mg/mL) has been reported (Ahmed, Li, McClements, & Xiao, 2012; Bergonzi, Hamdouch, Mazzacuva, Isacchi, & Bilia, 2014). (Ahmed et al.) also found that the solubility increases as the molecular weight of

the carrier oil decreases. This was attributed to differential interaction and excluded volume effects (Huyskens & Haulaitpirson, 1985). Application of physical treatments such as heating, and ultrasonication may also improve the oil solubility of curcumin (Ma et al., 2017).

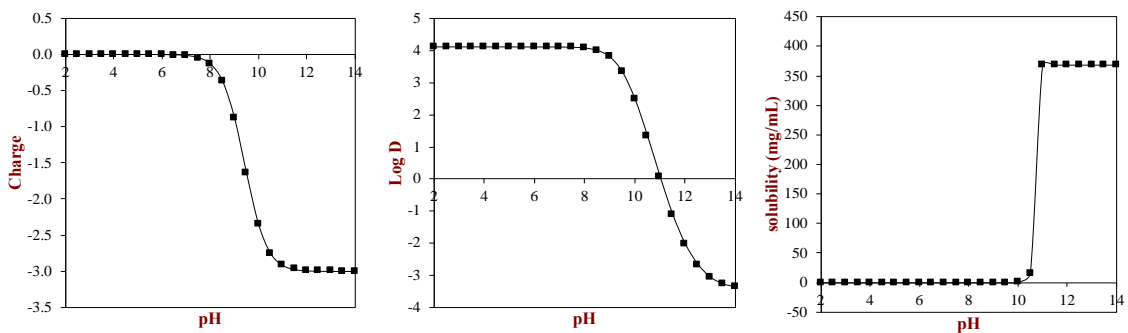


**Figure 2.** Properties of curcumin as a function of pH

#### 1.2.1.1.9. Acid dissociation constants (pKa)

In curcumin, three hydrogen atoms are dissociable with dissociation constant (pKa) values of 8.38 (enolic hydrogen), 9.88, and 10.51 (phenyl hydrogens) (Bernabe-Pineda, Ramirez-Silva, Romero-Romo, Gonzadlez-Vergara, & Rojas-Hernandez, 2004) which explains curcumin's variable solubility and partitioning behavior with pH.

#### 1.2.1.1.10. Hydrogen bond acceptors and donors

Oxygen atoms (total 6) present in dicarbonyl, methoxyl, and phenyl hydroxyl groups in curcumin can accept hydrogen bonds, whereas hydrogen atoms (total 2) present in phenyl hydroxyl groups can donate hydrogen bonds (Heger et al., 2014).

### 1.2.1.2. Stability characteristics

Stability of curcumin is affected by both physical parameters such as time, temperature, and radiation as well as chemical nature of the environment like pH (hydroxyl ions), oxygen, metal ions, and antioxidants to mention a few. In acidic aqueous solutions, curcumin has relatively low solubility and higher stability. For example, its half-life is 4200 h at pH 5.97. However, the degradation rate increases as enolic hydrogen dissociates at around  $\text{pH} \geq 7.0$  (Tonnesen & Karlsen, 1985b). As a result, the half-life of curcumin at pH 7.98 sharply decreases to 2.1 min. Vanillin, ferulic acid, and feruloylmethane were believed to be the major alkaline degradation products (Roughley & Whiting, 1973; Tonnesen & Karlsen, 1985a). Recently, bicyclopentadione was isolated and identified as the major degradation product of curcumin formed through autoxidative pathway (O. N. Gordon & Schneider, 2012). On exposure to visible light, curcumin undergoes photodegradation at a higher rate than that due to UV radiation (Ansari, Ahmad, Kohli, Ali, & Khar, 2005). Presence of other components such as surfactants may promote photodecomposition of curcumin (Tonnesen, 2002). Though high temperatures can solubilize more amounts of curcumin (Jagannathan, Abraham, & Poddar, 2012), it has significant impact on curcumin stability in aqueous solutions and in delivery systems where higher temperature leads to more loss (Mondal, Ghosh, & Moulik, 2016; Niu, Ke, et al., 2012). Curcumin can interact with other components present in the system which would affect its stability. For example, proteins (Tapal & Tikku, 2012), metals like iron, copper, zinc are known to form complexes and improve curcumin stability (Wanninger, Lorenz, Subhan, & Edelmann, 2015). Moreover, rate of curcumin degradation is significantly reduced in presence of antioxidants like ascorbic



acid, and rosmarinic acid (Nimiya et al., 2015). As compared to aqueous solutions, curcumin remains much more stable in oils where it is protected from hydroxyl ions, and oxygen as they have significantly lower solubility in oils.

### **1.2.2. Stage 2: End-product definition**

Food products constitute a wide range such as bread, pasta, dairy, fruit and vegetable products, frozen foods, meat and poultry, and so on. Each food type has different physical and chemical properties which need to be in certain range for a specific food product (**Table 1**). Physical properties like appearance, color, texture and mouthfeel, and viscosity depend on particle size as well as intermolecular interactions. Chemical properties such as pH, moisture content and water activity, and ionic strength depend on concentration of hydrogen ions, and salts. Other ingredients like minerals, antioxidants, surfactants, and emulsifiers would also affect these properties. When delivery system containing curcumin is incorporated in to food product, it is likely to affect its physicochemical parameters, and components present in the food product may also have impact on stability of curcumin and the delivery system itself. Compositional parameters of product like pH, and presence of other ingredients (e.g. fat, proteins) would considerably impact stability of curcumin. For example, curcumin is likely to be more unstable in aqueous beverages having neutral pH than an acidic pH. Also, it will be more unstable in an aqueous beverage than a yogurt drink because fat and proteins present in latter can solubilize more curcumin and stabilize it against hydrolytic degradation. Moreover, storage stability of curcumin in such yogurt drink would likely be higher in a container that prevents exposure of inner contents to light (for example by applying an

opaque packaging label) compared to a transparent container. Thermal stress and exposure to radiation during manufacturing and storage may also have significant effect on curcumin stability. For instance, stability of curcumin in a pasteurized beverage product is likely to be higher than that in a sterilized product. At the same time, incorporation of the delivery system should not significantly affect the viscosity, flavor profile, stability, and appearance of the product. For example, curcumin imparts strong yellow color to the food. Hence the delivery system could be incorporated easily in a product that is expected to have such color or in a product where delivery system would positively contribute to the color e.g. mango or orange flavored beverage. On the other hand, delivering curcumin through a vanilla flavored beverage may be a challenge as the product would not appeal to the consumer's eyes. Also, curcumin has an earthy, spicy flavor which may be a challenge in developing food products. For instance, it would be easier to incorporate curcumin in to spice-flavored beverage as compared to a mango flavored beverage. Depending on product type, earthy flavor from curcumin could be masked or neutralized with use of other ingredients like acids, sugars and gums (Roberts, Elmore, Langley, & Bakker, 1996). For these reasons, it is important to identify and define properties of the end product. A relatively stable delivery system that do not significantly alter the end-product characteristics and provides maximum protection to curcumin could then be chosen. To discuss the DbD approach, encapsulation of curcumin in a plant-based 'Golden Milk' is considered in following sections and its characteristics are defined as in **Table 2**.

**Table 1.** Compositional and physicochemical properties of some commercial food products

	Compositional parameters		Environmental stress parameters		Physicochemical properties				Optical properties
	<i>pH</i>	<i>Important components</i>	<i>processing</i>	<i>Light exposure</i>	<i>State</i>	<i>Viscosity (mPa.s)</i>	<i>Flavor and texture</i>	<i>Stability</i>	
Beverage	< 4.0	water, sugar	HTST	yes	liquid	5-15	smooth	no phase separation	cloudy/ transparent
Ice cream	5.5-6.0	milk fat	HTST (79 °C)	no	viscoelastic solid	>1×10 <sup>5</sup>	creamy, smooth	non- grainy, non-greasy	color
Yogurt	4.4	casein	UHT (140 °C)	no	viscoelastic gel	>4×10 <sup>3</sup>	dairy aroma, creamy	no wheying-off	variable
Yellow mustard	3.5-6	mustard oil	-	yes	viscous solid	>1×10 <sup>5</sup>	pungent flavor	lipid oxidation	yellow
Dry creamer	-	emulsifiers, sugars	spray drying (>150 °C)	no	granular solid	-	free flowing powder	no lumps	white
Liquid creamer	6.75-7	water, emulsifiers	sterilization	no	liquid	20-60	uniform consistency	lipid oxidation	uniform, cloudy
Sauce	3.0-6.0	acids, pepper	sterilization	yes	viscous liquid	>1×10 <sup>3</sup>	uniform flavor and consistency	phase separation	variable

**Table 2.** Physicochemical parameters defining model plant-based ‘Golden Milk’

<b>Property</b>	<b>Requirement</b>
Physical form	Ideal liquid having a shear viscosity of 2 to 4 mPa.s
Optical properties	Color and opacity- Uniform milky yellow appearance with initial tristimulus color coordinates ranging 85 to 90 (L*), -16 to -12 (a*), and 58 to 62 (b*).
Stability characteristics	Physical stability: No visible phase separation and increase in mean particle size > 20% during manufacturing, storage, and consumption Chemical stability: 1. Curcumin content should not decrease by > 15 % during manufacturing, storage, and consumption. 2. The yellowness (b*) should not reduce by > 5% at 20 °C or by > 10 % at 30 °C (6 months, in light exposure)
Functional attributes	The product should be fabricated to protect curcumin during digestion so that the total amount reaching the blood is more than 50 ng/mL
Compositional factors	The product should be formulated from plant-based ingredients with following compositional characteristics: pH (6.3-6.8), total carbohydrates ( $\leq$ 10%) including dietary fibers ( $\geq$ 0.25%), total fat ( $\leq$ 5%), protein ( $\geq$ 3%), minerals (ionic strength of 90-110 mM), curcumin (150 mg/100g)
Processing conditions	The product should be stable after heat treatment at 72 °C for 15 s
Storage conditions	The product should stay physically and chemically stable at temperatures 0-45 °C for 12 months storage
Economic aspect	The cost of finished product should not be greater than 20 cents per unit

### **1.2.3. Stage 3: Delivery system specification**

After deciding a product through which curcumin is to be delivered, it is essential to identify the functional characteristics of delivery system so that it is suitable for application in a particular product. Physical form (solid, semisolid, or liquid) and rheological attributes (low, medium, or high viscosity) of the delivery system may impact end product properties. For instance, if curcumin is to be delivered through a nutritional beverage then a delivery system should either be a miscible liquid or a solid powder that could be easily dispersed in the liquid. Moreover, the delivery system should either enhance optical properties of the desired product or should not change them significantly so that the end product is still acceptable to consumers. For instance, curcumin has yellow color which may limit the choices of foods that could be used for its delivery.

Functional attributes of a delivery systems such as loading capacity, encapsulation efficiency, protection, retention and release profile, dispersibility are the most important. Loading capacity can be defined as maximum amount of the active agent that can be encapsulated per unit mass of the carrier. Therefore, loading capacity in turn depends on the solubility of curcumin in a specific carrier. For example, solubility of curcumin in corn oil is about 3 mg/g, and that in MCT is about 7.9 mg/g. Hence, a delivery system fabricated using MCT could have a loading capacity of about 2.5 times more than that formulated using corn oil. Alternatively, for a specific amount of curcumin to be delivered, about 2.5 times less MCT would be needed. This could be significant as it will reduce the fat content and calories in the product. Furthermore, it is also important to ensure that the delivery system would provide necessary protection from chemical

degradation of curcumin by agents like hydroxyl ions, and oxygen. For example, curcumin is more stable when dissolved in edible oil (like MCT oil) than in aqueous surfactant solution (**Figure 3**). This is because hydroxyl ion, and oxygen have much lower solubility in oil. Also, retention percent of curcumin inside the delivery system and its release characteristics will be different for various delivery systems. For example, it is likely that more curcumin would remain encapsulated within a liquid oil droplet than in a solid oil droplet, as crystallization would expel curcumin out of the solidified fat core over storage (Tamjidi, Shahedi, Varshosaz, & Nasirpour, 2013). Finally, release profile for curcumin will depend on particle nature. For instance, release of curcumin will be much quicker from surfactant micelles and liposomes, while curcumin in an oil droplet would be released slowly over time as lipid droplet need to be digested first in order to release curcumin (Li, Liu, Tan, Zhao, Yang, & Pan, 2016).

To develop a plant-based ‘Golden Milk’ as defined in **Table 2**, the delivery system could be a liquid or dispersible powder that develops yellow milky appearance in the final product. It should be stable at pH 6.5, and to presence of salts (90-110 mM), and it should not break down inside the product during various manufacturing steps including shear mixing, thermal processing (72 °C for 15 s), and storage (0-45 °C for 12 months). Importantly, the delivery system should provide maximum protection to curcumin during its fabrication, product manufacturing, and storage so that curcumin content at the time of consumption is not less than 150 mg/100 g of product. It should also be designed such that it releases most of the encapsulated curcumin during digestion. The ingredients chosen to fabricate such delivery system should ensure high curcumin bioavailability so that total amount reaching the blood after digestion is more than 50 ng/mL.

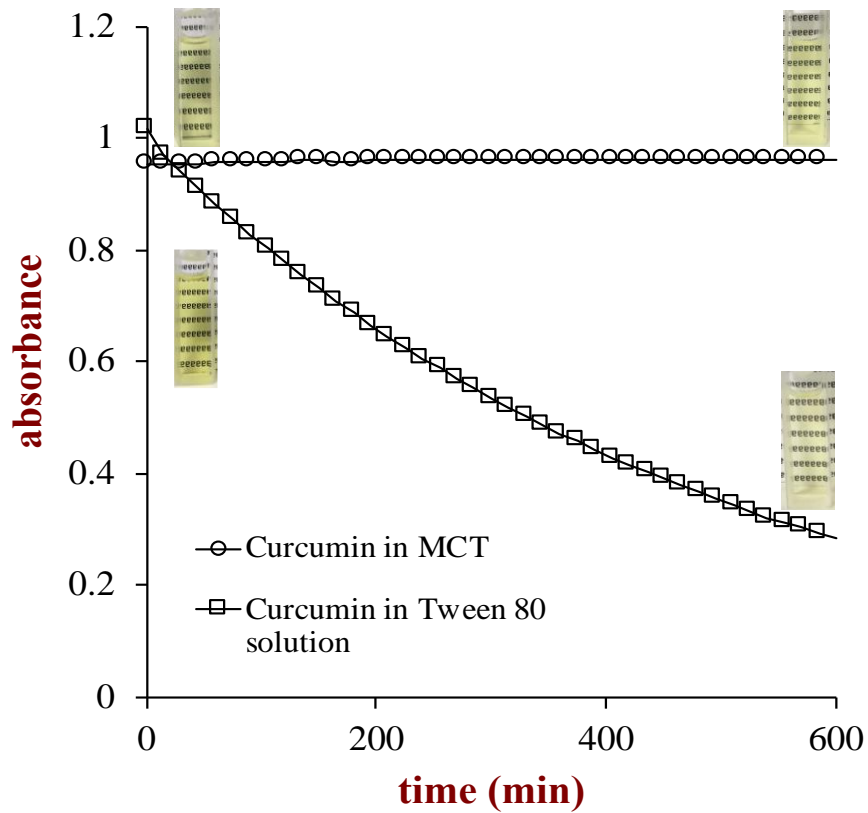


**Figure 3.** Stability of curcumin in MCT oil, and tween 80 solution (1 wt. % tween 80, pH 6.5)

#### 1.2.4. Stage 4: Particle specification and delivery system specification

Once the desired properties of delivery system are identified, it is possible to confirm the particle design and thus the delivery system. There are variety of ingredients which act as building blocks in designing a colloidal particle. These include water, lipids, proteins, biopolymers, surfactants and emulsifiers, minerals, antioxidants, and so on. Selection of the ingredients would depend on many factors such as end-product properties, processing, cost, consumer perception and market trends and more. For example, to develop a clear aqueous beverage containing curcumin, the choice of

ingredients may be restricted to surfactants, proteins, and biopolymers that can interact with curcumin and improve its water solubility. Moreover, it would also be restricted to their amounts as using high concentrations of protein or biopolymers is likely to cause turbidity in the product. In addition, antioxidants could be added to enhance chemical stability of curcumin (Nimiya et al., 2015). To produce a clear beverage with high protein content, thermal processing may be necessary which could affect curcumin stability (Etzel, 2004; LaClair & Etzel, 2010). However, if the product is a cloudy dairy beverage then lipids, and milk protein could be used in fabricating the delivery system. This would be beneficial as oils can solubilize more curcumin and can provide much higher chemical and thermal stability (**Figure 3**). Based on current consumer trend that is shifting towards more sustainable plant-based diet, some manufacturers may want to produce a beverage that is suitable to vegans. This would require using proteins from plant source such as pea, legume, or soy (David Julian McClements & Cansu Ekin Gumus, 2016). If the beverage is to combine delivery of both  $\omega$ -3 fatty acids and curcumin for increased health benefits (Jia et al., 2011), then an oil rich in  $\omega$ -3 fatty acids (such as flaxseed, corn, or fish oil) will have to be included in the delivery system. However, this would require additional strategies to slow down or inhibit lipid oxidation. This could be achieved by using emulsifiers that form thick interfacial membrane at the oil-water interface and provide steric barrier against prooxidant iron ( $Fe_{2+}$ ) (Silvestre, Chaiyasit, Brannan, McClements, & Decker, 2000). Alternatively, oil-water interface could be engineered to produce a positively charged oil droplet that will repel iron from reaching the interface and thereby slow down lipid oxidation (Lesmes, Baudot, & McClements, 2010). Consequently, process of designing a colloidal particle has to be tailored for a specific



application. However, some of the widely studied delivery systems that could be used in developing commercial food products are presented in **Figure 4** and discussed below.

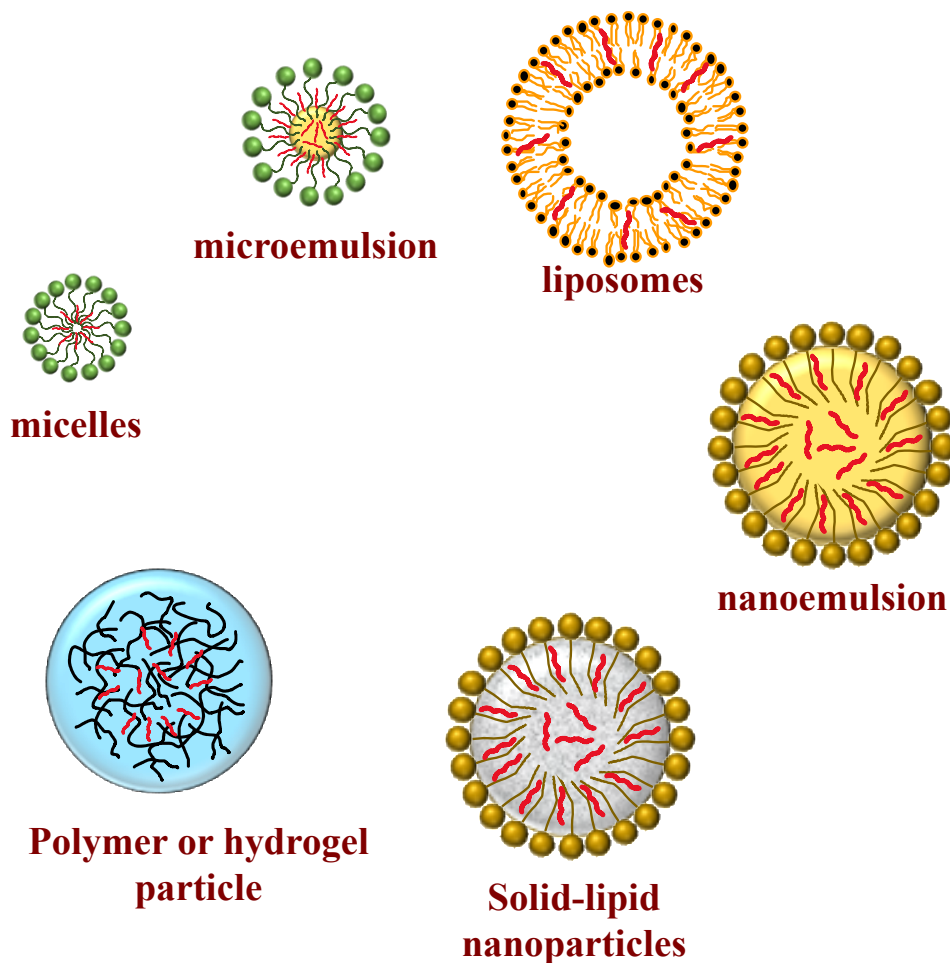


**Figure 4.** Different colloidal system for encapsulation and delivery of curcumin

#### 1.2.4.1 Micelles and microemulsions

Certain surfactants readily form micelles when dispersed in water above their critical micellar concentration. These structures are formed as hydrophilic heads of surfactant molecules interact with each other and also with water, while hydrophobic tails interact with each other. This reduces thermodynamically unfavorable interactions between hydrophilic and hydrophobic regions. Microemulsions are similar to micelles in

structure and are formed when oil (usually 1 wt. % or less) is incorporated. Here, hydrophobic tails of surfactant encapsulate oil and curcumin can be solubilized in hydrophobic regions of both the surfactant and oil.

Numerous studies have been carried out to assess the potential of micelles and microemulsions for encapsulation and delivery of curcumin. For example, non-ionic surfactants (tween 20, and tween 80) were shown to increase the water solubility and stability of curcumin (Mandal, Banerjee, Ghosh, Kuchlyan, & Sarkar, 2013). In a clinical trial, micellar formulation of curcumin and tween 80 was found to increase curcumin bioavailability in human subjects by 88-folds compared to curcumin in its native powdered form (Kocher, Schiborr, Behnam, & Frank, 2015). Indeed, it has been shown that micellar form of curcumin is absorbed more efficiently, and at a faster rate (Yu & Huang, 2011). It was also found that curcumin formed complex with cationic surfactants at high pH and lowered the surface tension. (Kumar, Kaur, Kansal, Chaudhary, & Mehta, 2016; Leung, Colangelo, & Kee, 2008; M. N. Wang, Wu, Tang, Fan, Han, & Wang, 2014). This is because curcumin has negative charge at highly alkaline pH and thus can bind to cationic species. Formation of curcumin-surfactant complex also led to increased stability of curcumin to degradation. It would be interesting to design such studies using cationic surfactants that are more suitable for food applications (Bonnaud, Weiss, & McClements, 2010). Peng and others used sophorolipid (biosurfactants synthesized in yeast fermentation) micelles to encapsulate curcumin and observed bioavailability as high as 3.6-fold compared to that of crystallized form of curcumin (Peng, Li, Zou, Liu, Liu, & McClements, 2018).

Cui et al. (2009) formulated a self-microemulsifying drug delivery system (SMEDDS) with an average particle size of around 20nm that had enhanced curcumin solubility (21 mg/g) and over 90% bioavailability (Cui et al., 2009). Microemulsion preparation consisting of food grade materials namely Capryol 90 (oil), Cremophor RH40 (surfactant), and Transcutol P (co-surfactant) could solubilized curcumin at higher level (32.5 mg/mL) and showed 22.6-fold increase in curcumin bioavailability when compared to that of curcumin suspension (L. D. Hu, Jia, Niu, Jia, Yang, & Jiao, 2012). In an *in-vitro* study, Lin et al. (2014) showed that microemulsion having smaller particle size were more effective against liver cancer cells. This microemulsion was produced entirely from food grade materials such as soybean oil, soy lecithin, and tween 80 with application of simple physical processing including mixing, heating (50 °C) and sonication.

Micelles and microemulsions are thermodynamically stable systems. Being transparent, they are an excellent candidate for delivering curcumin through clear beverages and can be incorporated in liquid products in general. However, considerably large quantities of surfactants required to produce these structures is a challenge in terms of cost and taste. Many of these surfactants are synthetic and therefore have low consumer acceptance. Moreover, recent studies indicate about possible adverse health effects associated with food grade surfactants like polysorbates which are widely used in many commercial products (Chassaing et al., 2015; Weiszhar, Czucz, Revesz, Rosivall, Szebeni, & Rozsnyay, 2012).

#### 1.2.4.2 Liposomes

Liposomes are typically formed from phospholipids molecules which are an important part of cell membranes. Structurally, they are similar to triacylglycerol molecule where one of the fatty acids is replaced by phosphate group. Because of this, phospholipids are amphiphilic in nature and readily form bilayers when dispersed in a suitable solvent such as water. In bilayers, hydrophobic tails interact with each other while polar head groups are in contact with water (Taylor, Davidson, Bruce, & Weiss, 2005). They can be unilamellar or multilamellar depending on the number of bilayer rings formed. Liposomes can be produced using variety of methods such as solvent injection, heating, film evaporation, microfluidization, and more (Maherani, Arab-Tehrany, Mozafari, Gaiani, & Linder, 2011).

Numerous studies show potential of liposomes for curcumin delivery. They can protect curcumin from chemical degradation by solubilizing it in their hydrophobic core (Niu, Wang, Chai, Chen, An, & Shen, 2012). In a study, liposomes made of egg lecithin were shown to provide substantially higher protection against curcumin degradation in serum at physiological pH (Matloob, Mourtas, Klepetsanis, & Antimisiaris, 2014). (Takahashi, Uechi, Takara, Asikin, & Wada, 2009) showed in an in-vivo study that liposomal curcumin had greater bioavailability with higher rate and extent of absorption when compared to curcumin in free form. After 2 h of administration, plasma curcumin concentration in rats was about 5 times more for curcumin encapsulated in liposome than free curcumin. In an *in-vitro* study, cellular uptake of curcumin from liposomes was found to be preferential over curcumin-loaded albumin (Kunwar, Barik, Pandey, & Priyadarsini, 2006). Recently, a simple pH-driven approach was used to load curcumin in

liposomes (Cheng, Peng, Li, Zou, Liu, & Liu, 2017). Curcumin bioaccessibility of liposomes prepared using this method was comparable to conventional thin-film evaporation technique and it was significantly higher than that for ethanol-injection approach. In a study, lecithins with varying phospholipid content and composition were used to load curcumin and it was concluded that composition of phospholipids may have effect on stabilizing curcumin (Peng, Zou, Liu, Liu, & McClements, 2018). Furthermore, not only can liposomes protect curcumin, but also curcumin may improve chemical stability of liposomes. Many phospholipids contain an unsaturated fatty acid which is prone to oxidation. Liposomal curcumin can chelate iron and prevent lipid oxidation which otherwise may lead to structural breakdown and instability (Tonnesen, Smistad, Agren, & Karlsen, 1993).

Important advantage of using liposomes as delivery system is that they can be prepared using natural ingredients. They may be clear (< 50 nm) or cloudy (> 100 nm) in appearance depending on their size. Hence curcumin-loaded liposomes could be added to variety of commercial products. The biggest challenge however is their economical production on industrial level. Moreover, they are likely to be unstable due to factors such as high temperature, and ionic strength (Makino, Yamada, Kimura, Oka, Ohshima, & Kondo, 1991; Niu, Wang, et al., 2012). Such instabilities are even more pronounced at increased curcumin loading since this would probably change the packing in bilayers. Although, biopolymer coatings may be applied to enhance structural stability of liposomes (Karewicz et al., 2013).

### 1.2.4.3 Emulsions and nanoemulsions

Emulsion can be defined as kinetically stable system in which two immiscible components, usually oil and water, remain mixed without phase separation. An emulsifier (a surface-active agent) is needed for this purpose which adsorbs at the oil-water interface and reduces the surface tension between two phases. This prevents droplets from aggregation due to either steric or electrostatic repulsion and provides kinetic stability (McClements & Rao, 2011). The most common emulsifiers used in the food industry are natural and artificial surfactants, proteins, phospholipids, and polysaccharides. Depending on the mean size of the oil droplets, they can be termed as emulsions ( $d \geq 100$  nm) or nanoemulsions ( $d \leq 100$  nm). Oil-in-water emulsions have been extensively studied for curcumin delivery because oil can solubilize curcumin and protect it from chemical degradation (Araiza-Calahorra, Akhtar, & Sarkar, 2018).

Curcumin loaded nanoemulsion was found to slow down lipid oxidation when fortified in milk. This was probably because curcumin could diffuse from nanoemulsion droplet in to milk and chelate iron (Joung, Choi, Kim, Park, Park, & Shin, 2016). Study by Ahmed et al. showed that bioaccessibility of curcumin was higher for medium-chain triglyceride emulsion compared to emulsions fabricated using short and long chain triglycerides (Ahmed et al., 2012). In a recent study, curcumin loaded emulsions were prepared using casein and soy polysaccharide complex. The study demonstrated that simulated gastric fluid could extract only 10% of total released curcumin and rest was released when mixed with simulated intestinal fluid as lipases digested the fat (Xu, Wang, & Yao, 2017). *In vivo* experiment using mice revealed that nanoemulsion formulation had about 11-fold higher bioavailability than micellar curcumin formulation.

This reaffirms effectiveness of oil droplets to protect curcumin from degradation in foods as well as during digestion. Comparative studies to assess the effectiveness of different emulsifiers in fabricating stable curcumin emulsions have also been carried out. It is clear that not all emulsifiers would perform equally in all conditions and they have to be chosen according to the final application. For example, whey proteins could not result in stable emulsion at pH 5.0 as their solubility decreases greatly around isoelectric point, but gum arabic, tween 80, and lecithin formed stable emulsions (M. H. Wu, Yan, Chen, & He, 2017). Some emulsifiers, such as quillaja saponins, may induce degradation which may be due to their chemical nature (M. Kharat, G. D. Zhang, & D. J. McClements, 2018). An organogel-based nanoemulsion was fabricated using span 20- saturated MCT, monostearin, and curcumin as lipid phase and stabilized by tween 20. This nanoemulsion had similar bioaccessibility and improved lipid digestibility when compared to the non-emulsified organogel. It also had significantly greater (about 10x) bioavailability in mice than that of curcumin-water suspension (Yu & Huang, 2012). More reports are present validating that curcumin loaded nanoemulsion have much greater bioaccessibility when compared to crystalline and micellar formulation used in commercial supplements (Zheng, Peng, Zhang, & McClements, 2018).

Emulsions and nanoemulsions have many benefits over other delivery systems. For example, they can be fabricated using food-grade ingredients (oils, and emulsifiers) that are easily available at lower cost. They can be produced on large scale by techniques such as high-pressure homogenization, and microfluidization. Emulsions containing curcumin could also be dried in to powder form and used in many different products as needed (Y. Wang, Lu, Lv, & Bie, 2009). For example, curcumin powder can be used to

disperse in dairy or plant milk, or alternatively curcumin encapsulated protein powders could be reconstituted to beverage. Despite these advantages, emulsion and nanoemulsion have tendency to break down over time as they are thermodynamically unstable. This can happen through various mechanisms such as gravitational separation, flocculation, coalescence, Ostwald ripening, and phase inversion (McClements, 2015b).

#### **1.2.4.4 Solid lipid nanoparticles and nanostructured lipid carriers**

Solid-lipid nanoparticles (SLN) are very similar to oil-in-water nanoemulsions, the only difference being that the dispersed lipid droplets phase is solid. Usually, fats having high melting point are used to formulate SLN. To prepare them, nanoemulsion is first formed using melted fat and emulsifier solution which is usually heated to the same temperature as fat. SLN are formed after cooling the hot nanoemulsion below the melting temperature of fat (Weiss, Decker, McClements, Kristbergsson, Helgason, & Awad, 2008). Curcumin containing SLN are obtained by dissolving curcumin in the fat melt where it can be solubilized in the hydrophobic cores. Curcumin gets locked in the solid interior of SLN and hence diffusion related loss is very negligible in SLN. This is an advantage over using nanoemulsion for curcumin encapsulation.

SLN have been proven to solubilize more curcumin and thus enhance its antioxidant activity (T. R. Wang, Ma, Lei, & Luo, 2016). Also, different loading methods may result in SLN with variable antioxidant activity. This is because treatments like pH adjustment, heating, and sequence of ingredient addition will affect the distribution, location, and total amount of curcumin within SLN (Xue, Wang, Hu, Zhou, & Luo, 2018). In vitro studies have shown that using SLN resulted in prolonged curcumin uptake



by cells when compared to curcumin solution (Sun, Bi, Chan, Sun, Zhang, & Zheng, 2013). This is mainly because curcumin is diffused out of the SLN slowly over a period of time. In a study, food grade SLN were prepared using mixture of glycerol stearate, propylene glycol esters of fatty acids, and palmitic acid as the lipid phase and stabilized by tween 80. Pharmacokinetic experiments showed that plasma concentration of curcumin was about 7-fold higher for SLN than that for free curcumin suspension (Ramalingam, Yoo, & Ko, 2016). (Kakkar, Singh, Singla, & Kaur, 2011) formulated curcumin containing SLN with glyceryl behenate, tween 80, and soy lecithin which were stable during 12-month storage at 4 °C. Curcumin content in SLNs lowered from 92.3% to 82.3% indicating that lipid core was efficient in retaining encapsulated curcumin. Also, study on rats showed that total plasma concentration of curcumin for curcumin-SLN formulation was 41.99 µg/mL while that for free curcumin was only 1.08 µg/mL.

Using SLN to deliver curcumin has many advantages. For example, they can be manufactured on a large scale by techniques like high-pressure homogenization. Their fabrication is possible by use of food grade ingredients. Moreover, instability issues such as coalescence, and Ostwald ripening are usually not seen in SLN as the fat droplet is solid. Also, the bioactive suffers less diffusion related loss and remains trapped inside the solid matrix for a considerable period. However, SLN are likely to have lower bioaccessibility (Aditya et al., 2014). This is because they are digested slowly and depending on particle size and concentration, some of the droplets may be left undigested. Also, they are usually prepared using saturated fats which have been linked to adverse health impacts like cardiovascular disease (Astrup et al., 2011). Consequently, consumer acceptance for high saturated food is currently declining. However, if one

needs to use SLN for curcumin delivery then focus should be on formulating stearic acid based carriers as stearic acid is believed to be neutral against cardiovascular disease risk (L. Wang, Folsom, Eckfeldt, & Investigators, 2003). Furthermore, although their solid interior restricts the bioactive movement, studies have shown that bioactive loss is still seen in SLN because of expulsion. It occurs when crystals transform from less ordered  $\alpha$ -lattice to a highly ordered  $\beta$ -structure (Müller, Radtke, & Wissing, 2002). This process minimizes imperfections between crystals that eventually expels the bioactive out of the core and towards SLN surface.

Expulsion is undesirable especially in case of curcumin, as it will then be more exposed to aqueous environment and degrade at a faster rate. To overcome this challenge, nanostructured lipid carriers (NLC) were developed. NLC have lipid core that cannot form highly ordered crystal structure and hence bioactive remains encapsulated. This can be achieved by using mixture of spatially different lipids, or by using specific fats that form amorphous solid-lipid particle upon cooling, or by mixing solid fats with liquid oils (Müller et al., 2002). For example, curcumin was successfully loaded (entrapment efficiency > 75 %) inside NLC fabricated using glycerol monostearate as solid and oleic acid as liquid oil (Aditya, Shim, Lee, Lee, Im, & Ko, 2013). This study also demonstrated higher cellular uptake of Curcumin-NLCs over free curcumin which resulted in decreased cancer cell viability. Application of NLC in the field of food is relatively new and there is great scope for research in this area (Tamjidi et al., 2013). One of the challenges in mixed type NLC (prepared using combination of solid and liquid fat) could be their stability in partially crystalline state (S. A. Vanapalli, J. Palanuwech, & J. N. Coupland, 2002).

However, this may be overcome by choosing proper fat combination and optimum relative concentration of fats.

#### **1.2.4.5 Biopolymer particles**

A variety of colloidal systems like biopolymer nanoparticles, microgels, hydrogel beads etc. can be fabricated by use of food grade biopolymers like proteins, and polysaccharides, and their combination (Joye & McClements, 2014). Generally, these biopolymers form a 3-dimensional network in which solvent and bioactive can be trapped. For encapsulating curcumin in a hydrophobic biopolymer like zein, it can be dissolved in biopolymer solution directly before particle formation. Whereas, encapsulation in a hydrophilic biopolymer like alginate would require use of oil or surfactants to solubilize curcumin before it can be incorporated inside the particle. Fabrication of biopolymer particles could be achieved by various techniques such as solvent evaporation, injection-gelation, gelation by phase separation, antisolvent precipitation, and emulsion templating methods (Joye et al., 2014). A short list of studies carried out to deliver curcumin through a variety of biopolymer based colloidal particles is presented in **Table 3**.

**Table 3.** Examples of biopolymer-based delivery systems for delivery of curcumin

<b>Biopolymer particle type</b>	<b>Preparation technique</b>	<b>Loading capacity (% w/w)</b>	<b>Encapsulation efficiency (%)</b>	<b>Compared with</b>	<b>Important outcomes</b>	<b>Reference</b>
casein	pH driven solubilization, and lyophilization	7	70	curcumin-DMSO solution	comparable antioxidant activity, and improved antiproliferation activity	(Pan, Luo, Gan, Baek, & Zhong, 2014)
zein-pectin	Electrostatic deposition, Solvent evaporation	9.46	86.8 ± 1.9	-	Small (250 nm) particles, hydrophobic interaction between curcumin and zein	(K. Hu, Huang, Gao, Huang, Xiao, & McClements, 2015)
cationised gelatin-sodium alginate	Vacuum drying	-	69	Free curcumin	Faster and efficient release at pH 5.0 than at pH 7.4, higher cellular uptake	(Sarika & James, 2016)
poly(lactic-co-glycolic acid)	Solvent evaporation	5.75	91.96	Native curcumin	640-fold higher water solubility, 5.6-fold increased bioavailability	(Xie et al., 2011)
dextran sulphate-chitosan	Simple mixing	4.4	74	-	Preferential killing of cancer cells over normal cells	(Anitha, Deepagan, Rani, Menon, Nair, & Jayakumar, 2011)
phosphatidylcholine-maltodextrin	high speed homogenization	0.15	65.29	Free curcumin	increased bioavailability (130x), 23-fold reduction in 50% cell growth inhibition	(Chaurasia, Patel, Chaubey, Kumar, Khan, & Mishra, 2015)

Since many biopolymer-based particles are mainly composed of polysaccharides, and proteins they could be perceived healthier as compared to other delivery systems that contain lipids. Moreover, some biopolymers like pectin, and carrageenan are soluble fibers which do not contribute to calories, but in fact assist in digestion (Topping, 1991). Casein based particles could be readily formed during processing and used in dairy based products. For example, curcumin could be added to milk before pasteurization step and then be used to make yogurt, beverages, and other products. Here curcumin would likely be solubilized and stabilized in hydrophobic cores in casein. However, it is a challenge to scale up techniques like antisolvent precipitation, and injection gelation that are used to fabricate them in small scale laboratories.

For developing plant-based ‘Golden Milk’, use of micelles, and microemulsions, would be least effective. This is because there are not many commercially feasible plant-based available. Saponins (such as from Quillaja) may be the only choice which are approved for food use. However, their plant extracts are unpurified and usually contain many other components some of which may be detrimental to curcumin (M. Kharat, G. Zhang, & D. J. McClements, 2018). Also, micelles and microemulsions are optically transparent and therefore can’t be use in isolation. They will have to be used with some other delivery system which develop milky appearance in the product. Liposomes could be used since they can be fabricated to produce a milky yellow beverage. However, they are less stable during processing and storage, and there would be higher costs associated with ingredients (phospholipids), and large-scale production. Oil-in-water nanoemulsions and biopolymer-based particles could be preferred choices as they can be fabricate using plant-based proteins like soy, pea, lentil, and bean protein (David Julian McClements et

al., 2016). Use of proteins would likely to appeal consumer as it enhances nutritional quality of the product. An oil that is high in MCT could be used to produce such nanoemulsion, for example coconut oil. This is because curcumin has been shown to have higher solubility in MCT and enhanced bioaccessibility for MCT based emulsion (Ahmed et al., 2012). A smaller fraction of protein would be required to prepare curcumin encapsulated nanoemulsion. Rest protein amount may be used to produce curcumin-protein nanoparticles to increase the loading and achieve required curcumin content as well as protein content in the final product (Chen, Li, & Tang, 2015). Use of protein would also impart the desired viscosity to the product when used in proper amount.

### **1.2.5 Stage 5: Process specification**

After identifying a suitable delivery system, it is important to optimize parameters for its preparation at lab scale and subsequently scaling up the process so that commercial need for its use is met. For example, if one needs to incorporate curcumin in a transparent beverage then suitable delivery system would be amongst micelles, microemulsion, liposomes, or biopolymer nanoparticles. There would be specific critical processing parameters associated with production of each of these delivery systems.

Oil-in-water nanoemulsions and curcumin-protein nanoparticles were identified as best suitable delivery systems for developing plant-based 'Golden Milk'. To prepare nanoemulsions, curcumin could be dissolved in oil and then homogenized with aqueous protein solution using high pressure homogenizer or microfluidizer. In this case, many parameters would be needed to optimize such as optimum solubilization temperature,

minimum mixing time and mixing rate, optimum protein concentration and number of passes through homogenizer to obtain nanoemulsion having required droplet size. To prepare curcumin-protein nanoparticles, curcumin has to be solubilized in hydrophobic cores in protein. This could be achieved many ways: 1. simply by mixing powdered curcumin with aqueous protein solution; 2. thermally assisted solubilization of curcumin powder in protein solution; 3. dispersing ethanolic curcumin in protein solution; 4. using pH-driven approach to solubilize and encapsulate curcumin in protein network. To choose one of these solubilization and encapsulation methods, factors like processing time, cost, encapsulation efficiency, loading capacity for each approach have to be considered. It is likely that heat assisted solubilization of powdered curcumin may require most time, energy, and may also lead to curcumin loss at high temperatures. Also, use of organic solvent like ethanol may not be perceived as best technique. On the other hand, pH-driven solubilization is quicker, it can be carried out at room temperature requiring low energy needs, and it can be done using simple equipment (e. g. mixer). Most importantly, curcumin is more soluble and stable at high alkaline pH values ( $\text{pH} > 11$ ), which could result in higher encapsulation efficiency. Thus, pH-driven technique may be the best for encapsulation purpose. Hence to confirm this, several lab experiments should be performed to determine the solubilization time and efficiency, curcumin stability, energy requirements and cost. Finally, to prepare nanoparticles, curcumin incorporated protein solution may be processed into a powder by techniques such as solvent evaporation, vacuum drying, spray drying, and lyophilization. Again, each of these techniques should be evaluated with respect to curcumin stability, processing time, energy requirements and cost of production.

### **1.2.6 Stage 6: Performance testing**

To evaluate and ensure the performance of delivery system an extensive protocol must be established. This would include assessment of physical and chemical stability of both curcumin-containing nanoemulsions and protein nanoparticles. The physical stability is characterized by changes in droplet size and charge. These can be measured by use of static and dynamic light scattering, while droplet charge could be measured by laser Doppler microelectrophoresis technique. An optical microscope could be used to study the morphology, and a rheometer could provide information about viscoelastic behavior. An accelerated physical stability studies could be performed by subjecting emulsion to a centrifugal force and analyzing the extent of separation. Chemical stability could be established by measuring the amount of curcumin in delivery system over a period of time. This could be achieved using one or more of techniques such as spectrophotometer, colorimeter, and HPLC. The effect of environmental factors (pH, storage temperature, ionic concentration, and ingredient interaction) on physical and chemical stability should also be studied.

### **1.2.7 Stage 7: System optimization**

Since fabrication of delivery system is a multi-step process, even a slight variation in any of the process/steps may result in a product that do not match the defined attributes. Hence, each batch of delivery system and product should be analyzed, and results should be recorded to identify the cause of such deviations. This would allow optimization of system that sometimes may be possible by just changing the composition of processing conditions. For example, a product showing presence of curcumin crystals



would indicate its improper solubilization in the oil phase. This may be due to relatively larger curcumin particles in a specific lot produced. This problem could easily be solved by allowing more time or slightly increasing the temperature to achieve complete solubilization. Or sometimes, nanoemulsion may result having relatively larger droplet sizes when homogenizer assembly has undergone considerable wear over months of use. In this case, increasing the number of passes through homogenizer to produce finer nanoemulsion may solve the problem.

### **1.3 Conclusion**

Researchers have grown a great interest in encapsulation of curcumin in delivery systems so that its health benefits could be realized. Each delivery system has its own advantages and shortcomings, and no one system can be used for curcumin delivery though wide range of food products. This article attempted to develop a methodical approach, called ‘Delivery-by-Design’, to design colloidal delivery systems for application in specific products. This tailor-made approach first defines the physicochemical properties and functional characteristics of curcumin and the end-product. This further allows identifying the properties of delivery system that would meet pre-defined requirements of the end-product, and then select one or combination of more delivery system types that would best suit the application. It then takes into account effect of various processes on fabrication of the delivery system and analyze its performance in the end-product, a process that could be optimized throughout the development and production stages. Scientists could use this strategy to effectively design and develop delivery system for curcumin that are aimed at application in specific food products.

## CHAPTER 2

# PHYSICAL AND CHEMICAL STABILITY OF CURCUMIN IN AQUEOUS SOLUTIONS AND EMULSIONS: IMPACT OF PH, TEMPERATURE, AND MOLECULAR ENVIRONMENT

### 2.1 Introduction

Many approaches have been studied for their potential to improve the water dispersibility, chemical stability, and bioavailability of curcumin. Encapsulate of curcumin in delivery systems such as conjugates, molecular complexes, micelles, liposomes, suspensions, hydrogels, and emulsions has been discussed in the first chapter. Advantages and disadvantages of each of these delivery systems were also discussed and 'Delivery-by-Design' (DbD) approach was elaborated which focuses on application of delivery system in a particular food product. In the food industry, oil-in-water emulsions are particularly suitable for the encapsulation of hydrophobic nutraceuticals because they can easily be manufactured using food-grade ingredients and widely used production equipment like high-pressure homogenizers (McClements, 2011). In addition, many food products already exist in the form of oil-in-water emulsions (such as beverages, dressings, soups, sauces, desserts, and yogurts), and so it is relatively easy to incorporate nutraceutical-loaded emulsions into them. Moreover, emulsions can easily be converted into a powdered form by freeze- or spray-drying, which means that encapsulated nutraceuticals can also be incorporated into solid foods (such as cereals, confectionary, and baked goods). For these reasons, the main objective of the current study was to examine the impact of incorporating curcumin into emulsion-based delivery systems on

its water dispersibility and chemical stability. Numerous previous studies have highlighted the potential of emulsion-based delivery systems for improving the stability and bioavailability of curcumin (Aditya, Aditya, Yang, Kim, Park, & Ko, 2015; Vecchione et al., 2016; X. Y. Wang, Jiang, Wang, Huang, Ho, & Huang, 2008; Yan, Kim, Kwak, Yoo, Yong, & Choi, 2011). However, to the author's knowledge, the current study is the first to give a detailed comparison of the impact of storage pH on the physical and chemical stability of pure curcumin in aqueous solutions and emulsions. This information is important because encapsulated curcumin may be incorporated into commercial products with different pH values and because ingested curcumin experiences different pH conditions as it travels through the human gastrointestinal tract.

Most of the previous studies on encapsulated curcumin have used naturally occurring curcumin, which is actually a mixture of three major components: curcumin, demethoxy-curcumin, and bis-demethoxy-curcumin (Tonnesen, Karlsen, Adhikary, & Pandey, 1989). Pure curcumin has different physicochemical and physiological properties from demethoxy- and bis-demethoxy-curcumin (Odaine N. Gordon, Luis, Ashley, Osheroff, & Schneider, 2015; Price & Buescher, 1997), which may affect the design of appropriate delivery systems for this nutraceutical. For this reason, pure curcumin was synthesized in the current study and then used to compare the impact of pH on the physical and chemical stability of curcumin in aqueous solutions and oil-in-water emulsions. The knowledge obtained from this study may facilitate the rational design of emulsion-based delivery systems suitable for utilization in foods, supplements, and pharmaceuticals.

## **2.2 Materials and methods**

Pure curcumin was synthesized and purified in the Department of Food Science at the University of Massachusetts using the method described by Pabon (Pabon, 1964). Medium-chain triglyceride (MCT) oil was purchased from Warner Graham Co. (Cockeysville, MD, USA). Dimethyl sulfoxide (DMSO), sodium hydroxide (NaOH), sodium phosphate anhydrous dibasic, and potassium phosphate monobasic were obtained from Fisher Scientific (Fair Lawn, NJ, USA). Curcumin ( $\geq 65\%$ ), hydrochloric acid (HCl), Tween 20, and Tween 80 were purchased from the Sigma-Aldrich Co. (St. Louis, MO, USA). All solvents and reagents were of analytical grade. Double distilled water from a water purification system (Nanopure Infinity, Barnstead International, Dubuque, IA, USA) was used throughout the experiments.

### **2.2.1 Dissolution and Stability of Curcumin in Aqueous Buffer Solutions**

A stock curcumin solution was prepared by adding a weighed amount of curcumin (65%) or pure curcumin into DMSO and then dissolving it for 2 min using a vortex. This solution was stored at 4 °C and used throughout the experiments. An aliquot of the stock curcumin solution (4 mM) was diluted in a quartz cuvette (path length 1 cm) with phosphate buffer solution (10 mM; 0.25 g/L KH<sub>2</sub>PO<sub>4</sub>, and 1.15 g/L Na<sub>2</sub>HPO<sub>4</sub>). HCl and/or NaOH was added previously to adjust the buffer pH to values ranging from 2.0 to 8.0. Curcumin degradation was determined at 37 °C by measuring the change in absorbance at 433 nm over time using a UV–visible spectrophotometer (Cary 100 UV–vis, Agilent Technologies). In some experiments, the effect of mixing was studied

by agitating the samples continuously to ensure homogeneity using a cross-type stir bar (Fisherbrand) driven by a magnetic stirrer.

### **2.2.2 Turbidity Measurements**

Turbidity measurements were used to monitor the formation of curcumin crystals in aqueous systems. The turbidity (at 600 nm) of freshly prepared curcumin solutions was measured at regular time intervals using a UV–visible spectrophotometer, with or without sample mixing using a stir bar and magnetic stirrer. All samples were made uniform by gentle mixing using a spatula before the turbidity was measured.

### **2.2.3 Oil Solubility of Curcumin**

Excess curcumin was added to a weighed amount of MCT oil; the resulting mixture was then stirred at 60 °C and 1200 rpm for 2 h and sonicated for 20 min to ensure dissolution. This process was repeated again if needed to ensure saturation of the curcumin in the oil phase. The mixtures were then centrifuged at 12,000 rpm (accuSpin Micro 17, Fisher Scientific) for 20 min at room temperature to remove the curcumin crystals. The supernatant was collected and analyzed for curcumin content as described later.

### **2.2.4 Preparation of Curcumin Emulsions**

An aqueous phase was prepared by mixing surfactant (either Tween 20 or Tween 80) in phosphate buffer (10 mM, pH 5.0) at room temperature for at least 2 h. An oil phase was prepared by dissolving curcumin in MCT (1 mg/g MCT) with constant stirring

at 60 °C for 2 h and then sonicating for 20 min. This whole procedure was repeated again if needed to completely dissolve the crystals. A stock emulsion was prepared by homogenizing the oil and aqueous phases together using a high-speed blender for 2 min (M133/1281-0, Biospec Products, Inc., ESGC, Switzerland). The resulting coarse emulsion was then passed through a microfluidizer (M110L, Microfluidics, Newton, MA, USA) at 12,000 psi for five passes. The final composition of the stock emulsion produced was 40% oil phase, 2% Tween 20 or Tween 80, and 58% phosphate buffer by weight. Sample emulsions containing 30% w/w oil and a range of different pH values were then prepared by diluting the stock emulsion with pH-adjusted buffer solutions. The sample emulsions were then incubated at 37 °C throughout the study. Additionally, some samples were maintained at 20 and 55 °C to study the effect of storage temperature.

### **2.2.5 Curcumin Concentration Measurements**

Curcumin quantification was carried out using the simple spectrophotometric method described by Davidov-Pardo et al. (Davidov-Pardo, Gumus, & McClements, 2016). A specific volume of emulsion (100  $\mu$ L) was added to DMSO (5900  $\mu$ L), and the contents were mixed well. The bottom layer was withdrawn after centrifugation (2000 rpm) for 15 min, and the absorbance was measured at 433 nm using a spectrophotometer. Preliminary experiments showed that the absorbance of the resulting mixtures was stable for at least 1 h for all pH values (data not shown). Linear regression ( $r_2 = 0.9993$ ) obtained from curcumin–DMSO standard solutions was used to quantify the amount of curcumin present (Appendix, **Figure S1**).

### **2.2.6 Color Measurements**

The intensity of the yellow color of a sample is a measure of the curcumin stability, as well as the overall appearance. For this reason, changes in the color of the curcumin emulsion were measured using an instrumental colorimeter (ColorFlez EZ, HunterLab, Reston, VA, USA) equipped with a tristimulus absorption filter. A measured volume of curcumin emulsion was transferred into a disposable Petri dish and then analyzed using a pure black plate as the background.

### **2.2.7 Particle Size and Charge Measurements**

The particle size distribution of the emulsions was determined using static light scattering (Mastersizer 2000, Malvern Instruments Ltd., Malvern, Worcestershire, UK), which utilizes measurements of the angular scattering pattern of emulsions. Samples were gently hand-mixed to ensure homogeneity. Phosphate buffer (10 mM) was used as diluent and had the same pH as the sample being measured to avoid multiple scattering effects. Average particle sizes are reported as the surface-weighted mean diameter (d<sub>32</sub>). An electrophoresis instrument was used to measure the  $\zeta$ -potential of the droplets in the emulsions (Zetasizer Nano ZS series, Malvern Instruments Ltd.). Before analysis, emulsions were diluted with phosphate buffer (10 mM) having the same pH as the sample to avoid multiple scattering effects.

### **2.2.8 Microstructure Analysis**

The microstructures of aqueous solutions and emulsions containing curcumin were recorded at various pH values using optical microscopy with a 60 $\times$  oil immersion

objective lens and a 10× eyepiece (Nikon D-Eclipse C1 80i, Nikon, Melville, NY, USA). For this, an aliquot of sample was placed on a microscope slide, covered by a coverslip, and then microstructure images were acquired using image analysis software (NIS-Elements, Nikon, Melville, NY, USA). Polarized light microscopy was carried out using a cross-polarized lens (C1 Digital Eclipse, Nikon, Tokyo, Japan).

### **2.2.9 Statistical Analysis**

Experiments were carried out using two or three freshly prepared samples. The results are reported as averages and standard deviations. The significant differences among treatments were evaluated using the Tukey multiple-comparison test at a significance level of  $p \leq 0.05$  (SPSS ver.19, SPSS Inc., Chicago, IL, USA).

## **2.3 Results and discussion**

### **2.3.1 Physical and Chemical Stabilities of Curcumin in Aqueous Solutions**

Initially, the physical and chemical stabilities of curcumin added to aqueous buffer solutions with different pH values were examined. In the absence of continuous stirring, the absorbance of curcumin buffer solutions decreased over time at all pH values studied, with the rate of decrease depending on pH (**Figure 5A**). Under alkaline conditions ( $\text{pH} \geq 7.0$ ), the solutions remained clear throughout storage, but there was a rapid decrease in absorbance during the first 7 min with calculated degradation rates of 92, 135, and 125  $\text{cm}^{-1} / \text{min}$  at pH 7.0, 7.4, and 8.0, respectively. The degradation rates were calculated as the slope of absorbance versus time in the initial period, when the change in absorbance was approximately linear. This result is in agreement with previous



studies that have reported that curcumin is highly unstable to chemical degradation around physiological pH (Nimiya et al., 2015). It was also noted that when curcumin–DMSO stock solution was first added to the buffers, a distinct red-brown color appeared, but that this initial color rapidly changed. As a result, the alkaline curcumin solutions had slightly higher initial absorbance values than the acid curcumin solutions. A possible explanation for this effect could be the formation of condensation products (such as feruloylmethane) under alkaline conditions, which are yellow in color and therefore increase the overall absorbance (Tonnesen et al., 1985a). Interestingly, a commercial curcumin sample, which actually consisted of a mixture of curcuminoids, appeared to have better stability at pH 7 than the pure curcumin sample (**Figure 5A**). This result is in agreement with previous studies (Odaine N. Gordon et al., 2015) and suggests that the different constituents of curcuminoids have different pH stabilities, which is important to understand during the development of effective delivery systems for this bioactive component.

The decrease in absorbance over time occurred much more slowly for the acidic curcumin solutions than for the alkaline ones in the absence of stirring (**Figure 5A**), which is in agreement with previous studies that have shown that curcumin is more chemically stable under acidic conditions (Tonnesen et al., 1985b; Y. J. Wang et al., 1997). Interestingly, the decrease in absorbance over time for the acidic curcumin solutions was much faster when they were continuously stirring than in the absence of stirring (**Figure 5B**). These results suggest that stirring altered either the physical or chemical stability of the curcumin.

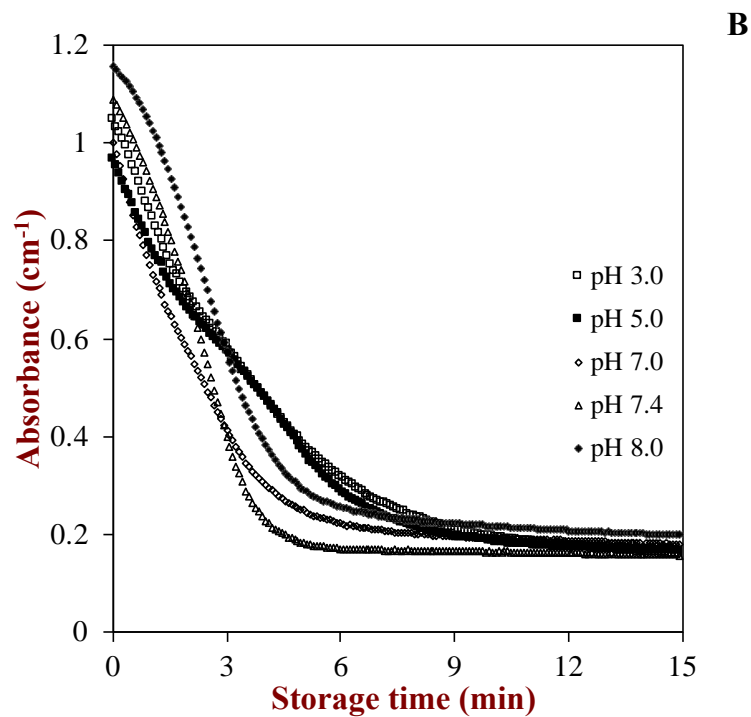
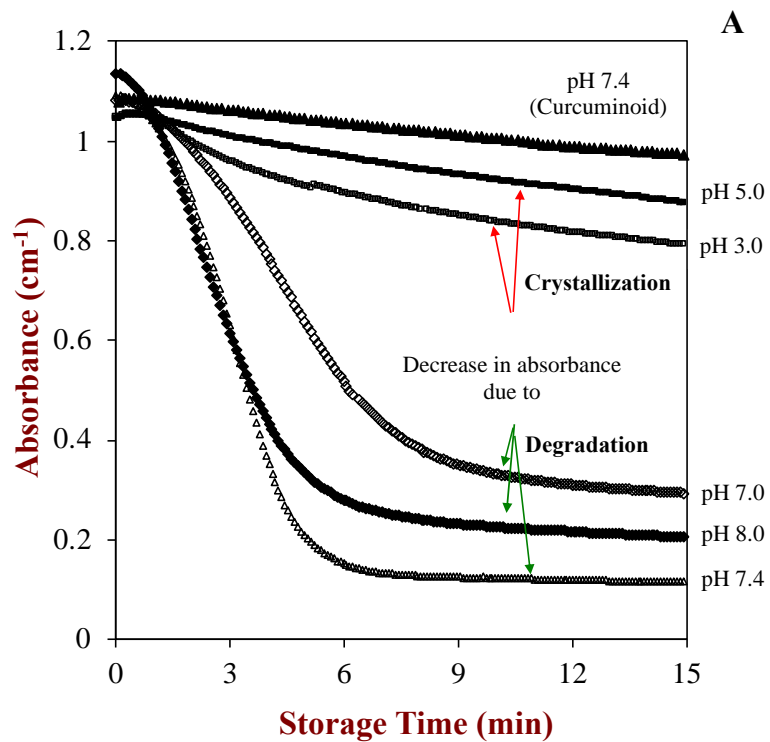


**Figure 5.** Stability of curcumin ( $40 \mu\text{M}$ ) in phosphate buffer solutions ( $10 \text{ mM}$ ) of various pH values when the system was unmixed (A) and mixed (B).

### 2.3.2 Crystallization of Curcumin in Aqueous Solutions

During the spectrophotometric analysis of curcumin stability in aqueous solutions, it was observed that yellow crystals appeared in solution and on the surface of the stir bar. This observation suggested that mixing promoted the nucleation and crystallization of curcumin in solution, which reduced the measured absorbance because some of the curcumin molecules were no longer in the path of the UV–visible light beam used to analyze the samples. It is known that curcumin has a relatively poor solubility in water, especially at lower pH values due to a change in its molecular structure under acidic conditions (Tonnesen et al., 1985b; Tonnesen, Masson, & Loftsson, 2002). The formation of crystals was confirmed using spectrophotometry to measure the turbidity (at 600 nm) of the samples (because curcumin does not absorb light strongly at this wavelength). At this wavelength, a decrease in the intensity of the transmitted light (corresponding to an increase in measured absorbance) is due to light scattering by any crystalline curcumin rather than absorption by the functional groups on curcumin. At acidic pH values (pH <7.0), there was an increase in turbidity over time corresponding to crystal formation (**Figure 6A**). At alkaline pH values (pH  $\geq$ 7.0), there was little change in turbidity over time, which can be attributed to the fact that no visible crystals were seen under these conditions. Optical microscopy analysis is discussed later which indicated that large crystal aggregates were formed under mixing conditions (see **Figure 9C**), but small uniformly dispersed crystals were formed under nonmixing conditions (**Figure 9A**, and **Figure 9B**). This effect would account for the observation that the turbidity of the nonmixed curcumin solutions was greater than that for the mixed solutions (**Figure 6B**) because smaller particles scatter light more effectively, resulting in a higher turbidity.

This tendency for curcumin to crystallize in aqueous solutions might account for the results of some clinical trials in which curcumin was not detected in the blood or urine after ingestion, but was recovered in fecal samples (Sharma et al., 2001).

Overall, these results indicate that curcumin may either chemically degrade (alkaline pH) or crystallize (acidic pH) depending on solution conditions, which limits the utilization of aqueous-based delivery systems for this type of nutraceutical.

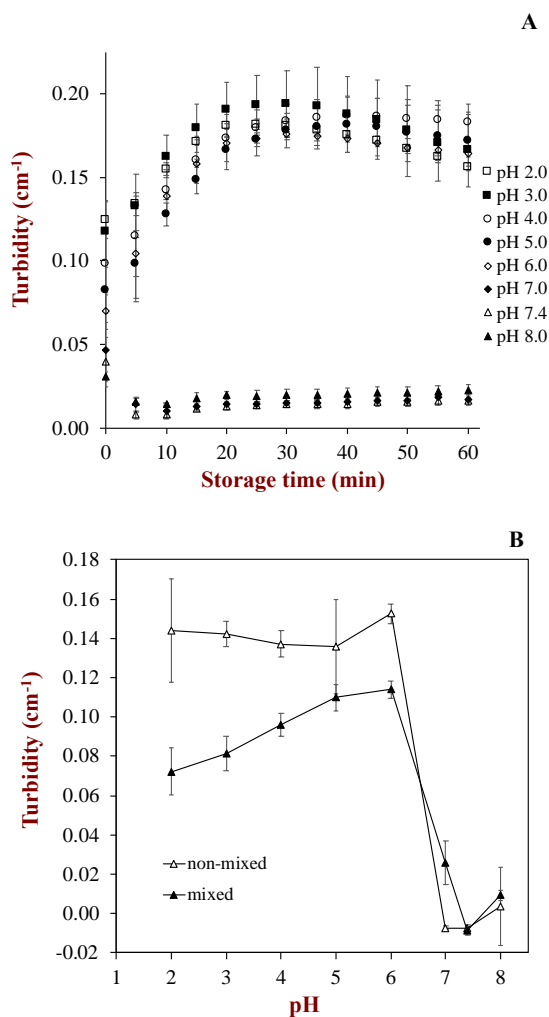


**Figure 6.** Turbidity of aqueous curcumin buffer solutions (40  $\mu\text{M}$ ) measured at 600 nm: (A) effect of pH on turbidity of unmixed samples over a period of 60 min; (B) difference in turbidity values after 15 min as affected by agitation.

### **2.3.3 Oil Solubility of Curcumin**

The maximum amount of hydrophobic bioactive components that can be incorporated into emulsion-based delivery system depends on their solubility in the oil phase.<sup>19</sup> The oil solubility of pure curcumin in MCT was found to be  $2.90 \pm 0.15$  mg/g of oil. This value is appreciably higher than an earlier value (0.26 mg curcumin/g oil) that was determined using a mixture of curcuminoids (Joung et al., 2016). This result highlights the importance of using pure forms of curcumin to better understand the performance of different types of curcuminoids in delivery systems.

### **2.3.4 Chemical Stability of Curcumin in Emulsion Systems**

Initially, oil-in-water emulsions were prepared using MCT as an oil phase and Tween 20 as a surfactant. These emulsions were stable to visible phase separation when stored at room temperature, but they underwent creaming when stored for >24 h at 37 °C. Consequently, this type of surfactant was unsuitable for the long-term storage studies used in this research. Further experiments were therefore carried out using oil-in-water emulsions prepared using Tween 80 as the surfactant because these remained physically stable when stored at 37 °C.

The initial curcumin content in the stock emulsion (40 w/w % MCT, pH 5.0) was around 0.38 mg/mL, which was close to the original amount of 0.39 mg/mL of curcumin added, that is, 1 mg curcumin/g MCT. This result suggested that curcumin was not degraded or lost during the preparation of the emulsions by homogenization.

The stock emulsions were diluted with buffer solutions to create a series of emulsions with the same initial curcumin level (0.285 mg/mL) and oil content (30%

MCT), but different pH values (3.0–8.0). There was an appreciable decrease in the curcumin concentration remaining in the neutral-alkaline emulsions ( $\text{pH} \geq 7.0$ ), but little change in the acidic emulsions ( $\text{pH} < 7$ ) during storage for 30 days (**Figure 7A**).

Interestingly, the alkaline emulsions had appreciably lower curcumin levels than the acidic emulsions on the first day, which implies that curcumin experienced rapid degradation after adjustment of the pH. The impact of pH on the amount of curcumin retained in the emulsions after 31 days of storage is shown in **Figure 7B**. Curcumin was relatively stable (85–95% remaining) in the acidic emulsions, but unstable (53–62% remaining) in the neutral–alkaline emulsions. These results can be explained in terms of pH-induced changes in curcumin structure and physicochemical stability. Curcumin has a hydrophobic backbone consisting of an aliphatic chain with aromatic rings attached on either side. However, both the aliphatic chain (carbonyl) and aromatic rings (hydroxyl and methoxy) have polar groups attached that give the molecule some amphiphilic characteristics. Consequently, one would expect curcumin molecules to adsorb to oil–water interfaces, such as oil droplet surfaces. In the alkaline emulsions, both oxidative and hydrolytic degradation reactions may occur at the oil–water interface, which lead to reaction products such as bicyclopentadione, ferulic acid, and feruloylmethane (O. N. Gordon, Luis, Sintim, & Schneider, 2015; Tonnesen et al., 1985b). Many of these degradation products are relatively hydrophilic and are therefore likely to move into the aqueous phase. To restore the equilibrium, more curcumin molecules would then migrate from the oil phase to the interface, and so the degradation process would continue. At acidic pH, curcumin exists primarily in an enolic structure (Tonnesen et al., 1985b), and therefore the major degradation mechanism is oxidative

rather than hydrolytic. As a result, the curcumin may have been more stable in the emulsions under acidic pH conditions. Moreover, the curcumin was less prone to crystallize in the emulsions than in the aqueous solutions because curcumin has a much higher solubility in oil than in water ( $\text{LogP} = 3.2$ ).

The storage temperature also affected the stability of the encapsulated curcumin (**Figure 7C**). The amount of curcumin remaining after 31 days of storage decreased as the storage temperature of the emulsions increased, particularly for the emulsions stored at pH 7.0. This result suggests that it would be advisable to store curcumin-loaded emulsions at lower temperatures to increase the physicochemical stability of curcumin. In another experiment, the amount of curcumin that remained stable when it was dispersed in bulk MCT for 31 days at 55 °C was measured. In this case, there was no significant change in curcumin concentration compared to the initial value, which indicated that the curcumin was relatively stable to degradation when it was dissolved in pure oil. This result indicates that the molecular environment (oil versus water) has a major impact on the chemical stability of curcumin and suggests that curcumin degradation in emulsions probably occurs at the surfaces of oil droplets rather than in their interiors.

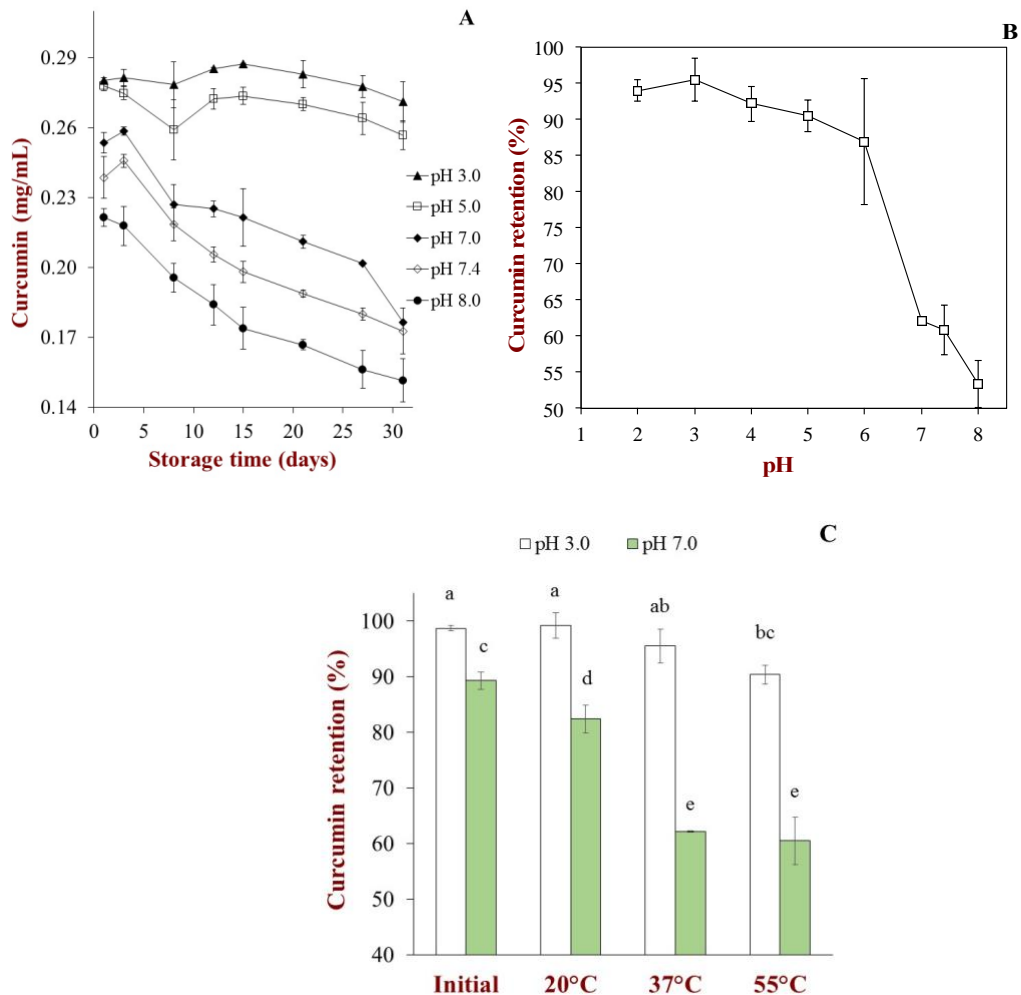


**Figure 7.** Stability of curcumin in oil-in-water emulsions (30 wt % oil) at 37 °C: (A) change in curcumin concentration; (B) curcumin retention in emulsions after 1 month of storage; (C) comparison of residual curcumin in emulsions stored at different pH values and temperatures

### 2.3.5 Changes in Emulsion Appearance during Storage

If emulsion-based delivery systems are going to be used to encapsulate curcumin, then it is important that they remain physically stable throughout storage. For this reason,



we measured changes in the physical properties of the emulsions over time and compared them to aqueous solutions of curcumin.

Unstirred curcumin solutions had a fairly intense yellow color when stored at acidic pH values but exhibited rapid color fading when stored at alkaline pH values (**Figure 8A**). The curcumin crystals were difficult to see in the nonstirred acidic solutions because they were very small and uniformly dispersed throughout the sample. However, large yellow crystals were observed in the stirred acid solutions, which can be attributed to the fact that mixing promoted aggregation of the crystals. Curcumin crystallization resulted in a reduction in the intensity of the yellow color in the acidic solutions. The appearances of emulsions before and after storage at 37 °C for 31 days were measured (**Figure 8B**, and **Figure 8C**). There was no visible creaming or phase separation in any of the samples after storage. Also, no major visual distinction could be made between fresh and stored emulsions, demonstrating that the curcumin in the emulsions was reasonably stable under the storage conditions used. Nevertheless, slight color fading was observed in the pH 7.4 and 8.0 samples compared to the acidic emulsions, highlighting the fact that some degradation had occurred at the higher pH values.

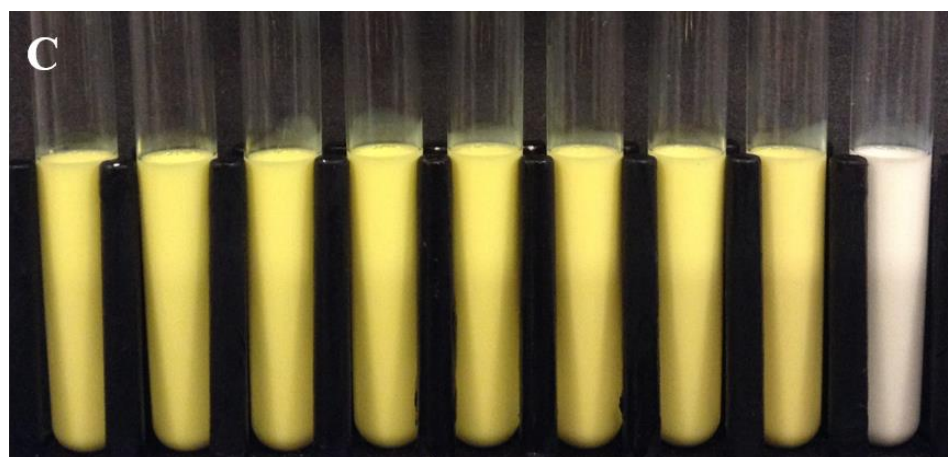
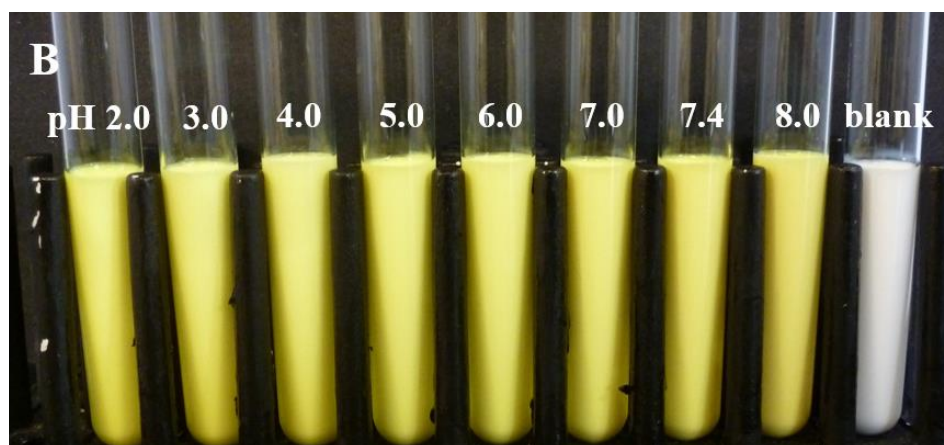
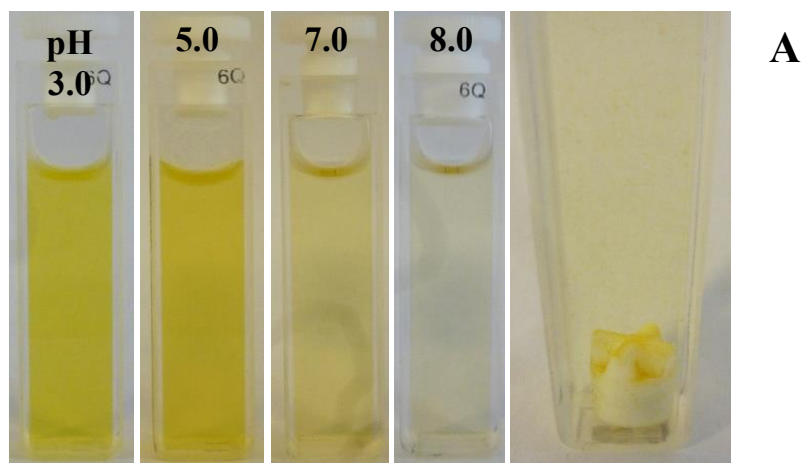


**Figure 8.** Visual appearance of curcumin buffer solution ( $40 \mu\text{M}$ ) incubated at  $37 \text{ }^\circ\text{C}$  for 15 min (A) and MCT-in-water emulsion (30 wt % oil) incubated at  $37 \text{ }^\circ\text{C}$  taken on day 1 (B) and day 31 (C). The labels on day 31 are the same as those on day 1

The observed differences in the visual appearances of the emulsions were supported by instrumental color measurements (see **Table 4** and **Figure S2** in the Appendix). The intensity of the yellow color (positive  $b^*$  value) decreased only slightly for the acidic emulsions during storage, indicating that little chemical degradation of the curcumin occurred. Conversely, there was a steeper decrease in the yellow color of the emulsions stored at the more alkaline pH values, indicating that the curcumin degraded more rapidly under these conditions. The colorimetry measurements therefore support the chemical degradation measurements presented earlier (**Figure 7**). As proposed earlier, this effect can be attributed to hydrolytic degradation of curcumin molecules located at the droplet surfaces under alkaline pH conditions.

**Table 4.** Yellowness ( $b^*$ ), Mean Particle Diameter, and Electrical Characteristics ( $\zeta$ -Potentials) of Emulsions at Days 1 and 31

pH of emulsion	mean particle diameter (nm)		zeta potential (mV)	
	day 1	day 15	day 1	day 15
<b>2.0</b>	301 ± 3	299 ± 2	-0.48 ± 0.17	-0.55 ± 0.30
<b>3.0</b>	295 ± 4	300 ± 1	-1.85 ± 1.13	-1.40 ± 0.31
<b>4.0</b>	296 ± 2	298 ± 3	-1.75 ± 0.64	-1.67 ± 0.23
<b>5.0</b>	298 ± 1	300 ± 1	-1.96 ± 0.14	-2.37 ± 0.16
<b>6.0</b>	299 ± 1	300 ± 1	-2.48 ± 0.14	-2.99 ± 0.20
<b>7.0</b>	299 ± 1	298 ± 3	-2.83 ± 0.06	-3.50 ± 0.48
<b>7.4</b>	299 ± 1	301 ± 1	-3.30 ± 0.08	-4.30 ± 0.13
<b>8.0</b>	299 ± 3	299 ± 1	-5.33 ± 0.49	-6.74 ± 0.38

### 2.3.6 Detection of Curcumin Crystals in Emulsions

As discussed earlier, curcumin crystals formed in some of the aqueous solutions during storage. Optical microscopy was therefore used to determine whether crystals also formed in the curcumin-loaded emulsions during storage. Interestingly, curcumin crystals with dimensions around 10–50  $\mu\text{m}$  were observed in both aqueous solutions and emulsions when stored at pH 3, 5, and 7 (**Figure 9**). In general, the number of crystals present was higher in acidic curcumin solutions than in neutral or basic ones (data not shown), which supported the turbidity experiments (**Figure 6**). The formation of crystals in the aqueous solutions would be expected because the water solubility of curcumin is known to be very low (11 ng/ mL) (O. N. Gordon et al., 2015; Nimiya et al., 2015). The fact that crystals were also observed in the emulsions suggests that the equilibrium solubility of the curcumin in this system was also exceeded. This was unexpected because the curcumin was dissolved in the oil phase (MCT) used to prepare the emulsions at a level (1 mg/g oil) below the experimentally determined equilibrium solubility (2.9 mg/g oil). A possible reason for this phenomenon is that the chemical degradation of curcumin led to the formation of reaction products that had a lower solubility than that of the parent molecule, thereby leading to crystal formation (McClements, 2012).

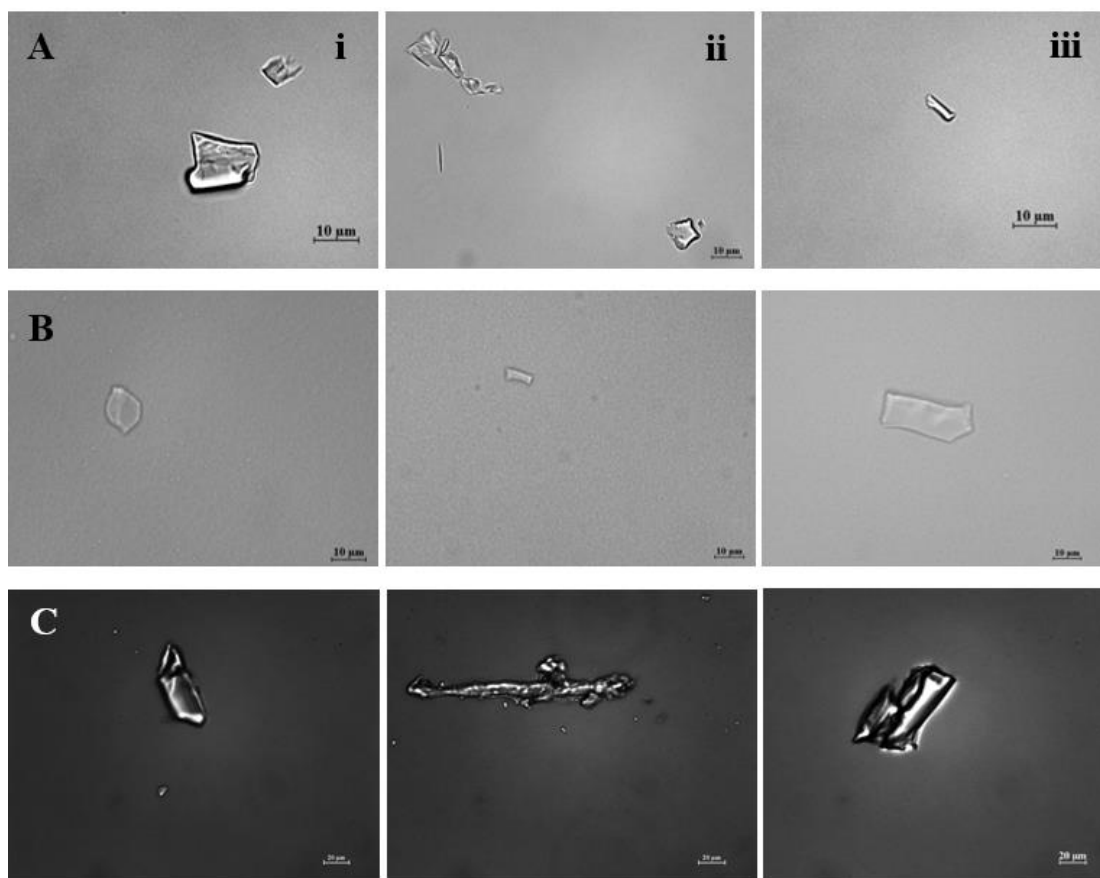


**Figure 9.** Micrographs showing curcumin crystals in (A) unmixed aqueous buffers (scale bar = 10  $\mu\text{m}$ ), (B) emulsions (scale bar = 10  $\mu\text{m}$ ), and (C) mixed aqueous buffers (images taken using cross-polarizer, scale bar = 20  $\mu\text{m}$ ; (i–iii) pH 3.0, 5.0, and 7.0, respectively)

### 2.3.7 Physical Properties of Emulsions during Storage

Immediately after preparation, the curcumin-loaded emulsions had fairly similar mean droplet diameters ( $d_{32} \approx 298 \pm 2 \text{ nm}$ ) and monomodal particle size distributions (see **Figure S3** in the Appendix). Moreover, there was no significant change in particle size over a period of 31 days (**Table 4**). This suggests that the emulsions had relatively good kinetic stability over a wide range of pH values. The mean particle sizes of both the curcumin-loaded and curcumin-free emulsions (pH 5.0) were similar. Hence, it can be concluded that the presence of curcumin in the oil phase did not influence the size of the

droplets produced during homogenization. Similarly, for a specific pH, there was no significant change in the electrical properties ( $\zeta$ -potential) of the lipid droplets over 31 days. The  $\zeta$ -potential on the surfactant-coated oil droplets was close to zero across the entire pH range studied, which suggests that the emulsions were mainly stabilized by steric rather than electrostatic repulsion. This would be expected for oil droplets coated by a nonionic surfactant such as Tween 80, because this type of surfactant has hydrophilic polymer groups (polyoxyethylene) that protrude into the aqueous phase. Overall, this study has highlighted the important role that pH plays on the physical and chemical stability of curcumin in aqueous solutions and emulsions. Under acidic conditions, curcumin has a tendency to form small crystals that may aggregate when the sample is stirred. Under alkaline conditions, curcumin tends to chemically degrade through an autoxidation process. The encapsulation of curcumin within oil droplets appears to improve its physicochemical stability, which may be an advantage for the design of effective emulsion-based delivery systems. These delivery systems could be used to facilitate the incorporation of curcumin into functional foods, supplements, and pharmaceuticals designed to improve human health and well-being. In future studies, it would be useful to examine the stability of curcumin under conditions found in commercial products and to assess its stability and release from the emulsion-based delivery systems under gastrointestinal conditions.

**CHAPTER 3**

**STABILITY OF CURCUMIN IN OIL-IN-WATER EMULSIONS: IMPACT OF  
EMULSIFIER TYPE AND CONCENTRATION ON CHEMICAL  
DEGRADATION**

**3.1. Introduction**

The previous study showed that degradation of curcumin in MCT-in-water emulsions was pH dependent with about 62% curcumin retention after 1 month when emulsions were stored at 37 °C . The ability of an emulsion to act as a good oral delivery system for curcumin depends on its composition and structure (Araiza-Calahorra et al., 2018). Consequently, it is important to optimize these parameters in order to develop effective delivery systems that can be utilized in a range of food and other products. The purpose of the current study was to examine the impact of emulsifier type on the formation and stability of curcumin-loaded oil-in-water emulsions. A variety of synthetic and natural emulsifiers are available for application in food products (Hartel & Hasenhuettl, 2013). However, there is growing interest in the use of natural emulsifiers in the food industry due to consumer concerns about health, environmental, and sustainability issues (D.J. McClements & C.E. Gumus, 2016). In this study, we therefore compared the efficacy of three natural emulsifiers (sodium caseinate, gum arabic, and quillaja saponins) at forming and stabilizing curcumin-loaded emulsions with a commonly used synthetic surfactant (Tween 80). A highly pure form of curcumin, which was synthesized and purified in our laboratories, was used in this study to facilitate the interpretation of the results, rather than a complex mixture of curcuminoids.

## **3.2. Materials and methods**

### **3.2.1. Materials**

Synthesis and purification of curcumin was carried out in the Department of Food Science at the University of Massachusetts using a method reported previously (Pabon, 1964). Medium chain triglyceride (MCT) oil was obtained from Warner Graham Co. (Cockeysville, MD), which was reported to mainly consist of caprylic (58.1 %), and capric (41 %) acids. Dimethyl sulfoxide (DMSO), sodium hydroxide (NaOH), sodium phosphate anhydrous dibasic, and potassium phosphate monobasic were obtained from Fisher Scientific (Fair Lawn, NJ). Sodium azide, hydrochloric acid (HCl), gum arabic (GA), and Tween 80 (T80), were purchased from the Sigma-Aldrich Company (St. Louis, MO). Sodium salt of casein (NaC) was product from MP Biomedicals (Solon, OH). Foamation® QB Dry (SAP), a spray dried purified aqueous Quillaja saponaria extract, was obtained from Ingredion Inc. (Westchester, IL). The manufacturer reported that this ingredient had a saponin content between 10-30 wt. %, with the remainder being mainly maltodextrin and fish gelatin (as processing aids). All solvents and reagents were of analytical grade. Double distilled water from a water purification system (Nanopure Infinity, Barnstaeas International, Dubuque, IA) was used throughout the experiments.

### **3.2.2. Determination of emulsifier surface load**

First, an aqueous phase was prepared by mixing emulsifier (NaC, T80, SAP, or GA) in phosphate buffer (10 mM, pH 7.0) until a clear solution was obtained. For the GA, the solution was then centrifuged twice at 36,000×g for 1 h (Thermo Scientific, Waltham, MA) prior to utilization to remove a small amount of insoluble fraction. To



prepare stock emulsions, both MCT oil and aqueous phase were mixed together for 2 min using a high-speed blender (M133/1281-0, Biospec Products, Inc., ESGC, Switzerland). The resulting coarse emulsion was then passed through a single-channel microfluidizer (M110L, Microfluidics, Newton, MA) at an operating pressure of 12,000 psi for 5 passes. The emulsifier-to-oil (E:O) ratio in the final emulsions ranged from 0.01 to 2.00. All operations were carried out at ambient temperature (~25 °C).

### **3.2.3. Preparation of curcumin-loaded emulsions**

To prepare curcumin-loaded emulsions, an oil phase was prepared by dissolving powdered curcumin into MCT oil at a level of 1 mg curcumin per gram of MCT oil. The resulting mixture was heated to 60 °C and stirred at 1200 rpm for 2 h, and then sonicated for 20 mins. This process was repeated if needed to ensure complete solubilization of curcumin in the oil phase. Emulsions were then prepared using the process described in the previous section. After preparation, sodium azide solution was added as an antimicrobial agent, and the emulsions were adjusted to either pH 3 or 7 using HCl and/or NaOH (0.01, 0.1, or 1N). Finally, the emulsions were diluted with phosphate buffer of the appropriate pH to obtain the final emulsions. The final emulsions contained 9.0 wt. % MCT oil, 0.02 wt. % sodium azide, and had emulsifier concentrations of 0.5, 0.6, 0.8, and 10.0 wt. % for caseinate, Tween 80, saponin, and gum arabic, respectively. These emulsifier levels were selected because they represent the values where the oil droplets surfaces were fully saturated with emulsifier, and small droplets were obtained (see Section 3.3.1. Impact of emulsifier type on emulsion formation).

To study if excess emulsifier affected curcumin stability, another set of emulsions was prepared that contained twice the amount of emulsifier in the aqueous phase. These emulsions therefore had emulsifier concentrations of 1.0, 1.2, and 1.6 wt% for the systems stabilized with caseinate, Tween 80, and saponin, respectively. For the emulsions prepared with excess gum arabic, an emulsifier concentration of 15 wt% was used because higher values led to emulsion instability. Blank emulsions were prepared having the same composition as the corresponding test emulsion, but where the oil phase only contained MCT without added curcumin. All sample and blank emulsions were stored in temperature-controlled rooms (37 or 55 °C), and samples were collected periodically for analysis.

#### **3.2.4. Curcumin concentration measurements**

Curcumin quantification was carried out using a spectrophotometric method described earlier (Davidov-Pardo et al., 2016). An aliquot of emulsion was added to DMSO and then the system was mixed well using a vortex. The bottom layer was withdrawn after centrifugation (2000 rpm for 15 min), and then the absorbance was measured at a wavelength of 433 nm using a UV-visible spectrophotometer (Cary 100 UV-Vis, Agilent Technologies). Preliminary experiments showed that the absorbance of the resulting mixtures was stable for at least 1 h at all pH values (data not shown) indicating the stability of the curcumin in the emulsion-solvent mixture. A blank measurement was included for each sample and was prepared using a blank emulsion having the same composition as the test emulsion but containing no curcumin. A linear

calibration curve ( $r_2 = 0.99$ ) was obtained using curcumin-DMSO standard solutions, and was used for curcumin quantification.

### **3.2.5. Color measurements**

The intensity of the yellow color of curcumin-loaded emulsions provides an indication of the curcumin stability. Therefore, changes in the color of the curcumin emulsions were analyzed using an instrumental colorimeter (ColorFlez EZ, HunterLab, Reston, VA) equipped with a tristimulus absorption filter. An aliquot of curcumin emulsion was placed into a transparent disposable petri dish. An illuminant/observer combination of D65/10 was used by the instrument. The  $L^*a^*b^*$  measurements were recorded using a black cup as a background.

### **3.2.6. Particle size and charge measurements**

The mean particle size and particle size distribution of the emulsions was determined using a static light scattering instrument (Mastersizer 2000, Malvern Instruments Ltd., Malvern, Worcestershire, UK), which utilizes measurements of the angular scattering pattern from small droplets. The refractive indices of aqueous and oil phases were set to 1.33, and 1.44, respectively and the absorption of each phase was set as 0. Blank measurement was taken using phosphate buffer (10 mM) having the same pH as the sample to be measured. Emulsion samples were gently mixed by inverting the container several times to ensure homogeneity and then added to buffer to achieve a light obscuration value of about 4.5. Mean particle sizes are reported as the surface-weighted mean diameter ( $D_{32}$ ).

An electrophoresis instrument was used to measure the  $\zeta$ -potential of the emulsion droplets (Zetasizer Nano ZS series, Malvern Instruments Ltd. Worcestershire, UK). This instrument measures the movement of charged particles under a well-defined applied electric field using a light scattering device. For analysis, samples were diluted with phosphate buffer (10 mM) with the same pH as the sample to avoid multiple scattering effects.

### **3.2.7. Microstructure analysis**

An optical microscope equipped with a 60 $\times$  oil immersion objective lens and 10 $\times$  eyepiece (Nikon D-Eclipse C1 80i, Nikon, Melville, NY, USA) was used to record the microstructures of emulsions containing curcumin. For the analyses, an aliquot of sample was centered on a microscope slide, covered by a glass slip, and then microstructure images were captured using image analysis software (NIS-Elements, Nikon, Melville, NY).

### **3.2.8. Statistical analysis**

Experiments were carried out in 2 replicates. In each replicate, measurements for at least two freshly prepared samples were obtained. The mean and the standard deviations were calculated using Microsoft Excel 2016 package. The significant differences among treatments were evaluated using the Tukey multiple-comparison test at a significance level of  $p \leq 0.05$  (SPSS ver.19, SPSS Inc., Chicago, IL, USA).

### 3.3. Results and Discussions

#### 3.3.1. Impact of emulsifier type on emulsion formation

Emulsifiers vary in their ability to form and stabilize the lipid droplets in oil-in-water emulsions depending on their molecular and physicochemical characteristics (McClements, 2015b). The impact of emulsifier type on emulsion formation was therefore evaluated by plotting the mean particle diameter ( $D_{32}$ ) as a function of emulsifier concentration under fixed homogenization conditions (**Figure 10**). For all emulsifiers,  $D_{32}$  initially decreased with increasing emulsifier concentration because there was more emulsifier present to cover the surfaces of all the small oil droplets generated inside the homogenizer. However,  $D_{32}$  reached a fairly constant value at higher emulsifier concentrations because the droplet size was then limited by the ability of the homogenizer to further disrupt the small oil droplets. This is because the Laplace pressure, which opposes droplet disruption, increases as the droplet diameter ( $D$ ) decreases and the oil-water interfacial tension ( $\gamma$ ) increases:  $\Delta P = 4\gamma/D$  (McClements, 2015b). Consequently, it gets harder and harder to break up the droplets as their size decreases during homogenization.

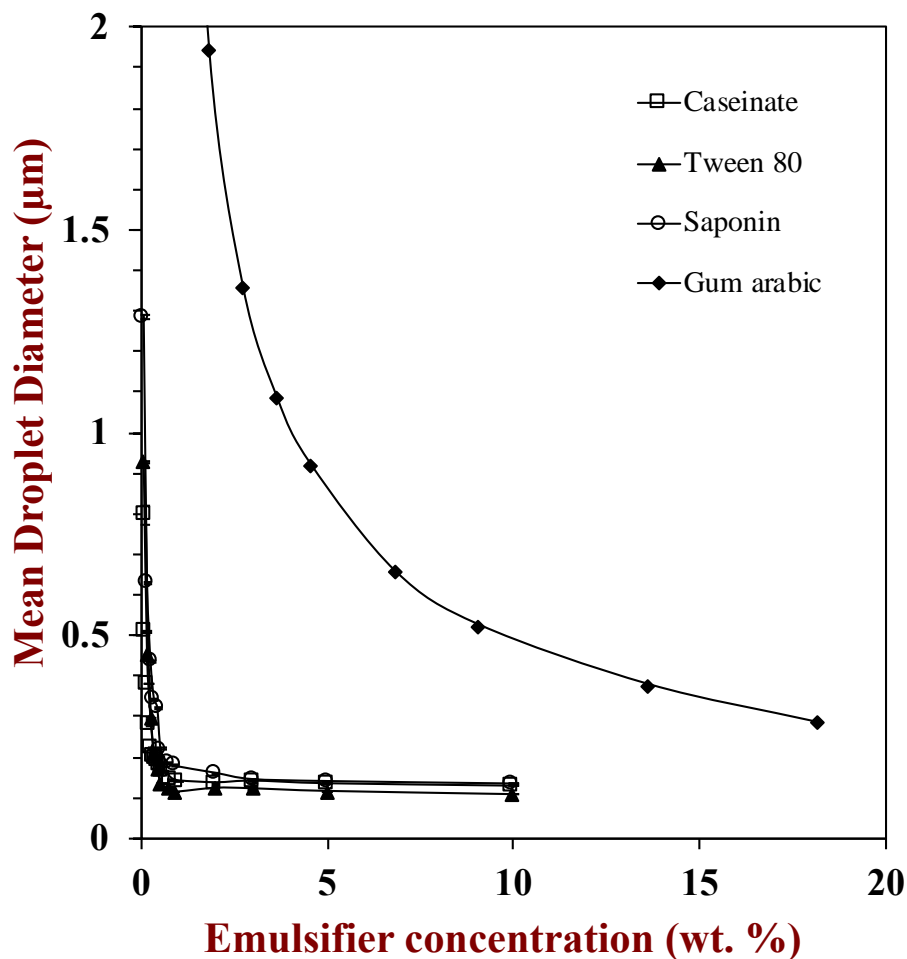


**Figure 10.** Effect of emulsifier type and concentration on the mean droplet diameter ( $D_{32}$ ) of MCT oil-in-water emulsions produced using a high-pressure homogenizer (microfluidizer).

The change in  $D_{32}$  with emulsifier concentration depended on emulsifier type (Figure 10). For the emulsions stabilized by caseinate, Tween 80, and saponin the mean droplet diameter decreased steeply with increasing emulsifier concentration, and then reached a relatively constant value above 1 wt% emulsifier. Nevertheless, there were some slight differences in the  $D_{32}$  versus emulsifier profiles for these three emulsifiers. For instance, at a fixed emulsifier concentration of 1 wt%, the mean droplet diameters

were 0.14, 0.11, and 0.18  $\mu\text{m}$  for caseinate, Tween 80, and saponin, respectively. This suggests that the non-ionic surfactant was most effective at forming small droplets during homogenization. The emulsions stabilized by gum arabic behaved quite differently from those stabilized by the other emulsifier types. For gum arabic, the mean droplet diameter was much larger than in the other emulsions when used at an equivalent emulsifier level and it did not reach a constant value even at the highest emulsifier level used (17.5%). The differences between the emulsifiers can be attributed to two main effects. First, the relatively large gum arabic molecules may adsorb to the droplet surfaces more slowly than the other emulsifiers, which leads to some droplet coalescence inside the homogenizer (Chanamai & McClements, 2001). Second, the gum arabic molecules have a higher surface load than the other emulsifiers, and therefore a greater amount is required to cover the surfaces of the oil droplets formed in the homogenizer (Bai, Huan, Gu, & McClements, 2016).

The performance of an emulsifier during emulsion formation can be quantified by its *surface load* ( $\Gamma$ ), which is the mass of emulsifier per unit surface area:

$$\Gamma = \frac{D_{32}C_s}{6\varphi} \quad (1)$$

Here,  $C_s$  is the concentration of emulsifier in the emulsion ( $\text{kg}/\text{m}^3$ ),  $\Gamma$  is the surface load of the emulsifier at saturation ( $\text{kg}/\text{m}^2$ ),  $\varphi$  is the dispersed phase volume fraction (dimensionless), and  $D_{32}$  is the surface-weighted mean droplet diameter (m) (McClements, 2007). This equation assumes that all of the emulsifier is adsorbed to the

droplet surfaces at low emulsifier concentrations (emulsifier-limited regime). This assumption is likely to be valid for the surfactant and protein but may not be valid for the gum Arabic because it contains a mixture of many different biopolymers with different surface activities. The surface load of the emulsifiers was calculated from this equation and from knowledge of the oil droplet concentration ( $\phi=0.091$ ), emulsifier concentration (0.1–17.5%, or 1–175 kg/m<sup>3</sup>), and the measured mean droplet diameters ( $D_{32}$ ). First, Equation 1 was rearranged to give:

$$D_{32} = 6\Gamma\phi\left(\frac{1}{C_s}\right) \quad (2)$$

Then, the surface load was calculated from the slope ( $6\Gamma\phi$ ) of a plot of  $D_{32}$  versus the reciprocal of the emulsifier concentration ( $1/C_s$ ). Only the data points in the region where the droplet diameter fell steeply with increasing emulsifier concentration were used in these calculations, *i.e.*, where the droplet size was limited by the emulsifier concentration rather than by the ability of the homogenizer to disrupt the droplets.

The calculated surface loads of the caseinate, Tween 80, saponin, and gum arabic were 1.5, 1.6, 2.0, and 55.3 mg/m<sup>2</sup>, respectively. The much higher surface load for gum arabic than for the other three emulsifiers is probably because of its unique molecular structure. It has an amphiphilic polypeptide chain that anchors it to the oil-water interface, and a much larger hydrophilic polysaccharide chain that protrudes into the surrounding aqueous phase (Dickinson, 2003). Consequently, a much larger mass of this emulsifier is required to saturate the droplet surfaces than for the smaller protein and



surfactant emulsifiers used, which would be expected to form thinner and denser interfacial layers. Our results are in agreement with those of previous studies that have also compared the interfacial properties of different types of emulsifiers (Bai et al., 2016; Bos & van Vliet, 2001; Chazelas, Razafindralambo, Dumont de Chassart, & Paquot, 1995; Euston & Hirst, 2000). In summary, our results show that a much higher concentration of gum arabic is required to stabilize the emulsions than for the other three emulsifiers, which may have important practical consequences for commercial applications.

In the following experiments, emulsions were prepared using two different emulsifier levels. Emulsions prepared using a *critical level* had just enough emulsifier to saturate the droplet surfaces, while those prepared at an *excess level* had twice the critical level, so there would be some free emulsifier present in the aqueous phase surrounding the droplets. These experiments were carried out because food manufacturers often want to minimize the level of emulsifier used in their products to reduce costs. On the other hand, non-adsorbed emulsifiers may be able to improve the physical and chemical stability of emulsions (Gumus, Decker, & McClements, 2017).

Experimentally, the critical level was defined as the emulsifier concentration where a linear line drawn from the region where  $D_{32}$  decreased with increasing  $C_s$  intersected with another linear line extrapolated from the region where  $D_{32}$  was independent of  $C_s$ . The critical levels were found to be 0.5, 0.6, and 0.8 wt% for caseinate, Tween 80, and saponins, respectively. The critical value could not be determined for gum arabic using this approach because the mean droplet diameter kept decreasing with increasing emulsifier concentration (**Figure 10**). In this case, the critical

value was arbitrarily taken to be 10 wt% gum arabic, and the excess value was taken to be 15 wt%, because higher levels led to some emulsion instability, probably due to depletion flocculation (Chanamai et al., 2001).

### **3.3.2. Impact of emulsifier on color fading of curcumin-loaded emulsions**

The chemical degradation of curcumin leads to a reduction in the intensity of its orange-yellow color (Heger et al., 2014; Kharat et al., 2017). For this reason, visual observations and instrumental colorimetry measurements were carried out to determine the impact of storage temperature, pH, emulsifier type, and emulsifier level on the stability of encapsulated curcumin to degradation in the emulsions.

#### **3.3.2.1. Preliminary experiments**

Initially, curcumin-loaded oil-in-water emulsions were prepared from the four different emulsifiers and stored at pH 3 and 7 at 37 °C. All of the initial emulsions had a bright yellow color (**Figure 11**), and there were no obvious differences in their appearance when the emulsifier concentration was varied (not shown). The only exception was the caseinate-stabilized emulsion that was adjusted from pH 7 to pH 3, which exhibited extensive droplet aggregation and creaming (not shown). This effect can be attributed to the fact that irreversible flocculation of the caseinate-coated oil droplets occurred when the pH passed through the isoelectric point of the adsorbed proteins (Jourdain, Leser, Schmitt, Michel, & Dickinson, 2008). For this reason, this emulsion was not used in the color fading experiments. After 15 days storage at 37 °C, none of the emulsions exhibited any obvious changes in their visual appearance when held at pH 3,

but the emulsions stabilized by Tween 80 and saponins exhibited a small amount of creaming when held at pH 7. The visual observations were supported by instrumental colorimetry measurements, which showed that there was little change in the tristimulus color coordinates of the emulsions when they were stored at 37 °C at pH 3 or 7 (**Figure S4. A and B** in Appendix). Indeed, after 15 days storage the magnitude of the changes in the  $L^*$ ,  $a^*$ , and  $b^*$  values of the emulsions were less than 2.5, 7, and 7.5, respectively.

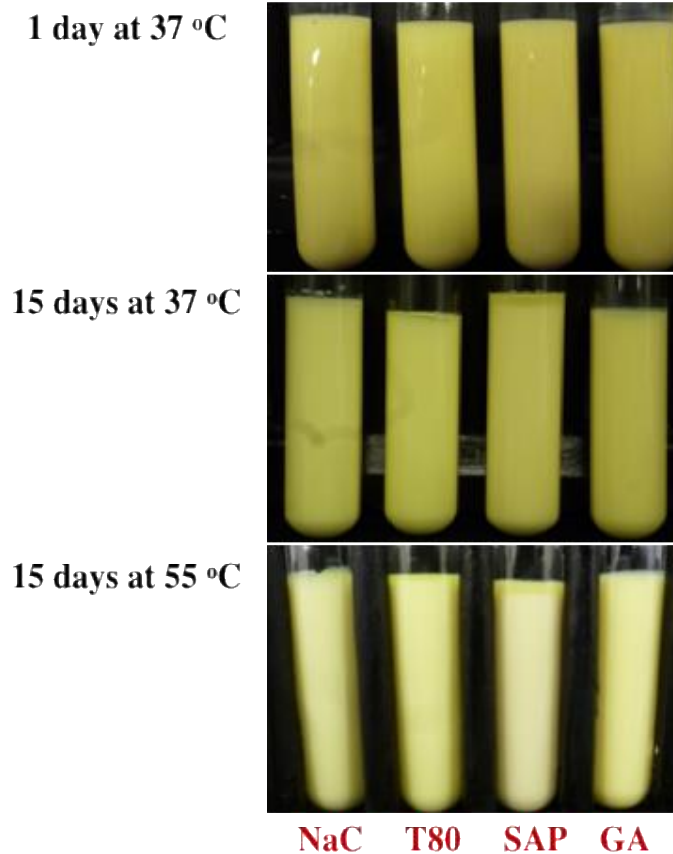


**Figure 11.** Photographs of curcumin-loaded oil-in-water emulsions prepared at the critical emulsifier concentration when stored under different conditions (pH 7.0). Emulsions were stabilized by sodium caseinate (NaC), Tween 80 (T80), quillaja saponins (SAP) or gum

Because our preliminary experiments showed that there was little color fading in the emulsions when they were stored at 37 °C, further experiments were carried out using a higher storage temperature and neutral pH since these conditions have been shown to accelerate curcumin degradation in previous studies (Heger et al., 2014; Kharat et al., 2017). After 15 days storage at 55 °C and pH 7, all the emulsions exhibited noticeable color fading indicating that appreciable chemical degradation of the encapsulated curcumin occurred (**Figure 11**). For this reason, this higher storage temperature was used for the remainder of the studies.

### **3.3.2.2. Color stability**

Further insights into color fading were obtained using instrumental colorimetry measurements of the curcumin-loaded emulsions. Changes in the tristimulus color coordinates ( $L^*a^*b^*$ ) of the emulsions were measured throughout storage at 55 °C for 15 days at pH 7 (**Figure 12**). Under these storage conditions, there was a relatively fast change in the color coordinates of the emulsions over time. Only the kinetic results for the emulsions containing an excess level of each emulsifier type are shown, since the emulsions containing the critical level of corresponding emulsifier behaved very similarly, as seen by the overall changes in the  $b^*$ -values after 15 days storage (**Figure 13**). The color differences between emulsions containing critical and excess emulsifier levels can be mainly attributed to the color contributed by the emulsifiers themselves. For instance, the sodium caseinate, Tween 80, quillaja saponin, and gum arabic solutions used to prepare the emulsions were hazy white, clear, clear brown, and clear light brown, respectively.

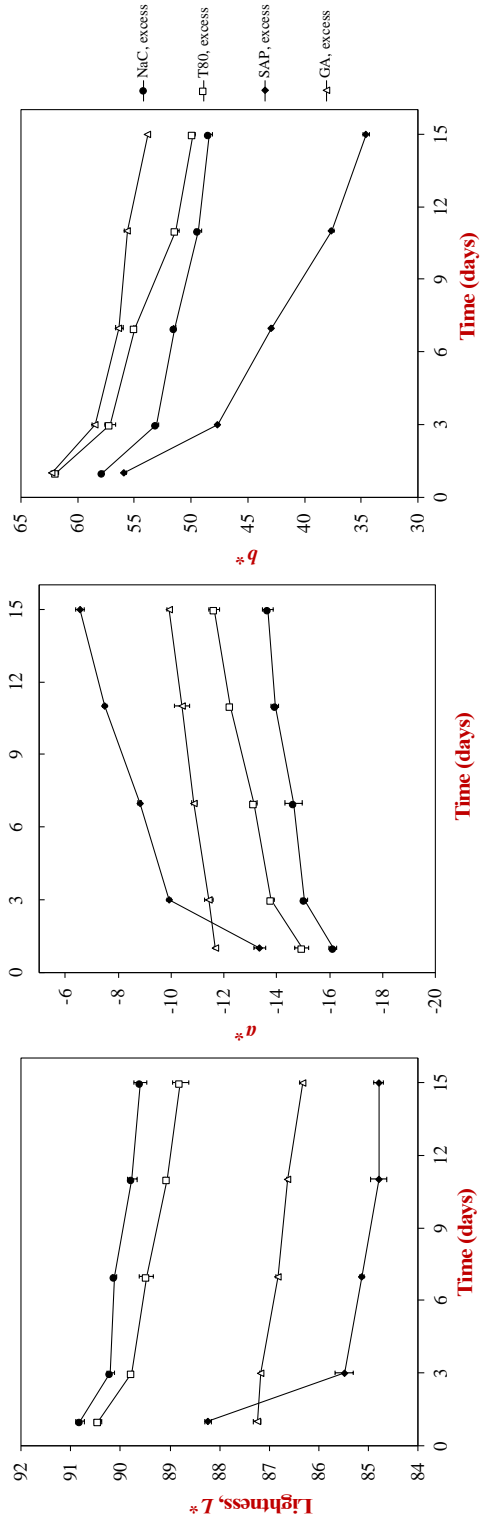


**Figure 12.** Change in tristimulus color coordinates ( $L^*$ ,  $a^*$ ,  $b^*$ ) of curcumin-loaded oil-in-water emulsions during storage at pH 7 and 55 °C.

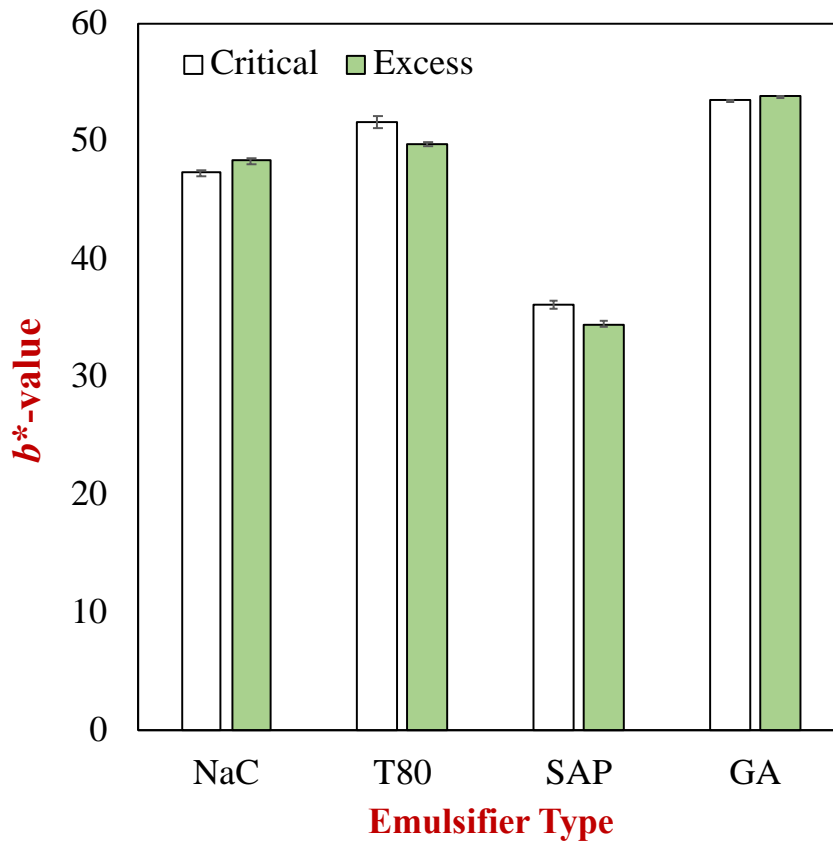


**Figure 13.** Impact of emulsifier type and concentration on the yellowness ( $b^*$ -values) of emulsions stored at pH 7 and 55 °C for 15 days.

There was a gradual decrease in the lightness ( $L^*$ ) of all the emulsions during storage, except in those stabilized by saponins, which showed a sudden decrease from Day 1 to 3 followed by a more gradual decrease afterwards. This effect may have been due to some chemical change in the saponins themselves, *e.g.*, a browning reaction. All the emulsions initially had slightly negative  $a^*$ -values and strongly positive- $b^*$  values, indicating that they initially had a slightly green/strongly yellow color. The  $a^*$ -values became slightly less negative during storage, which suggests that the emulsions became less green. Similarly, the  $b^*$ -values became less positive during storage, which suggests

that the emulsions became less yellow. This type of behavior is consistent with color fading caused by curcumin degradation (Y. J. Wang et al., 1997).

There were pronounced differences in the rate and extent of color fading in the different emulsions indicating that emulsifier type played an important role in curcumin degradation (**Figure 12** and **Figure 13**). Since the emulsions appeared predominantly yellow to the eye, the  $b^*$ -values were used as a convenient measure of color fading. The rate of color fading ( $b^*$  units / day) in the emulsions followed the order: saponins (1.52) >> Tween 80 (0.86)  $\approx$  caseinate (0.67)  $\approx$  gum arabic (0.60). These results suggest that the curcumin was least stable to color fading when trapped inside of lipid droplets coated by the saponins. This effect may be due to the fact that saponins contain conjugated double bonds, which have previously been reported to promote lipid peroxidation in microsomal membranes (Babu, Sarkar, Ghosh, Saha, Sukul, & Bhattacharya, 1997). These authors suggested that the conjugated unsaturated system in the saponins generated free radicals that accelerated peroxidation. Indeed, free radicals are known to be potent hydrogen abstractors that can initiate curcumin auto-oxidation (O. N. Gordon et al., 2015).

### **3.3.3. Impact of emulsifier on chemical stability of curcumin in emulsion systems**

Additional information about the impact of emulsifier type and concentration on the stability of curcumin to chemical degradation was obtained by measuring the amount remaining during storage. As expected from the color fading measurements, there was only a slight decrease in the level of curcumin remaining in the emulsions stored at 37 °C for 15 days at both pH 3 and 7 (**Figure 14**). Indeed, there was > 90% curcumin retention

in all of the emulsions after storage, with the exception of the ones stabilized by gum arabic at pH 7 where there was around 80% curcumin retention. The retention of curcumin was fairly similar or slightly higher for the emulsions stored at pH 3 than at pH 7.

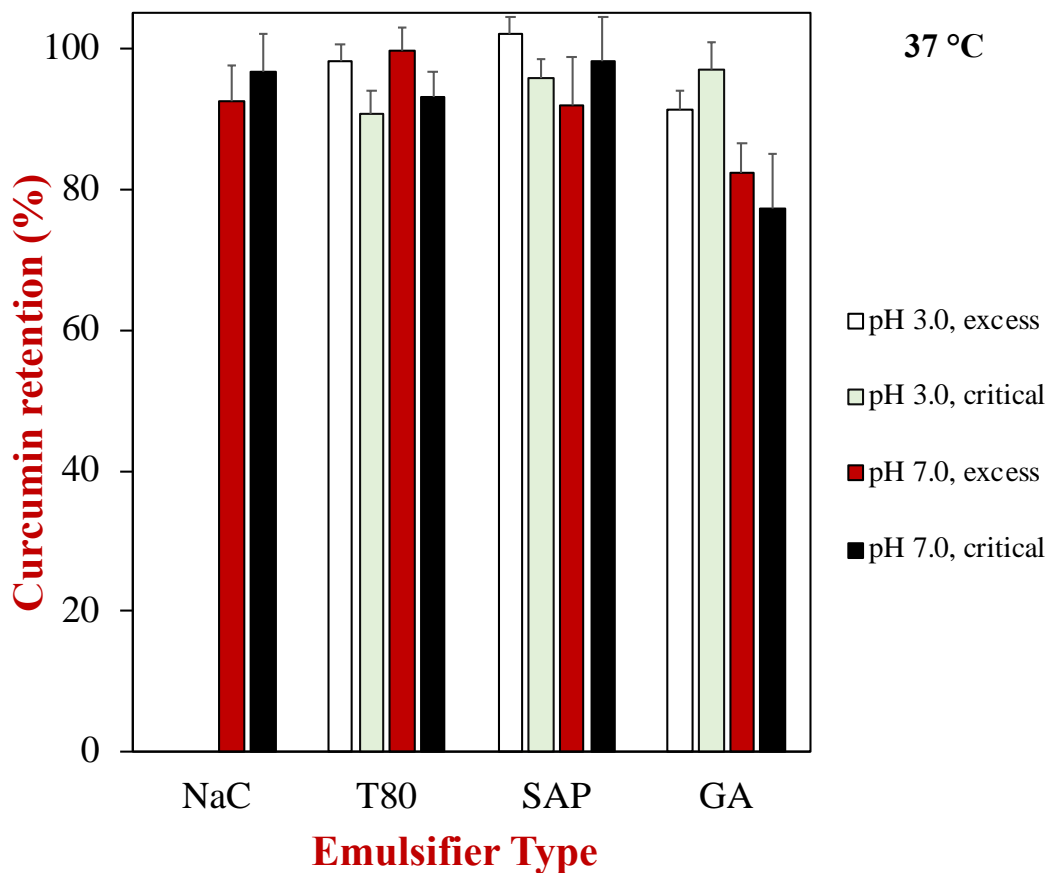


**Figure 14.** Impact of emulsifier type and concentration on curcumin retention in emulsions stored at pH 3 and 7 at 37 °C for 15 days

The rate of curcumin degradation was therefore accelerated by storing the emulsions under neutral conditions (pH 7) at a higher temperature (55 °C) so as to more clearly establish the differences between the emulsifiers. As expected, the rate and extent of curcumin degradation was much higher at the elevated temperature (**Figure 15** and



**Figure 16).** There was a steady decrease in the amount of curcumin remaining in the emulsions throughout storage, with the most rapid decrease occurring in the emulsions stabilized by the saponins. These results are therefore in good agreement with the color fading measurements at 55 °C, which showed that the color of the emulsions stabilized by the saponins faded more rapidly than for the emulsions stabilized by the other three emulsifiers (**Figure 12** and in appendix **Figure S5. A**). Again, the emulsifier level in the emulsions had little impact on the extent of curcumin degradation after 15 days of storage (**Figure 16**), which is in agreement with the color fading measurements (**Figure 13**). **Figure S5. A** also suggests that colorimetric analysis may provide an indication of curcumin content in emulsions and therefore can be used in rapid quality control and quality assurance analysis of commercial products.

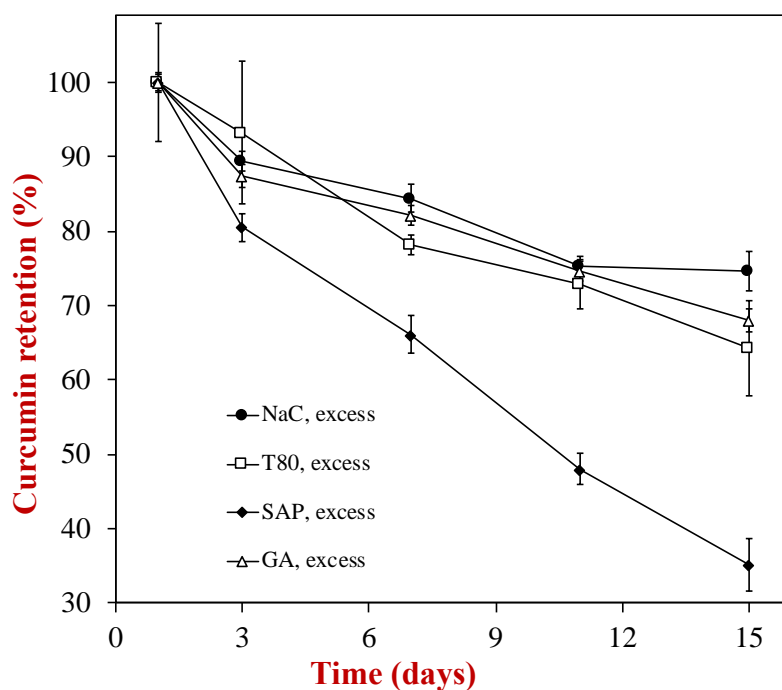


**Figure 15.** Impact of emulsifier type on curcumin retention in emulsions during storage at pH 7 and 55 °C

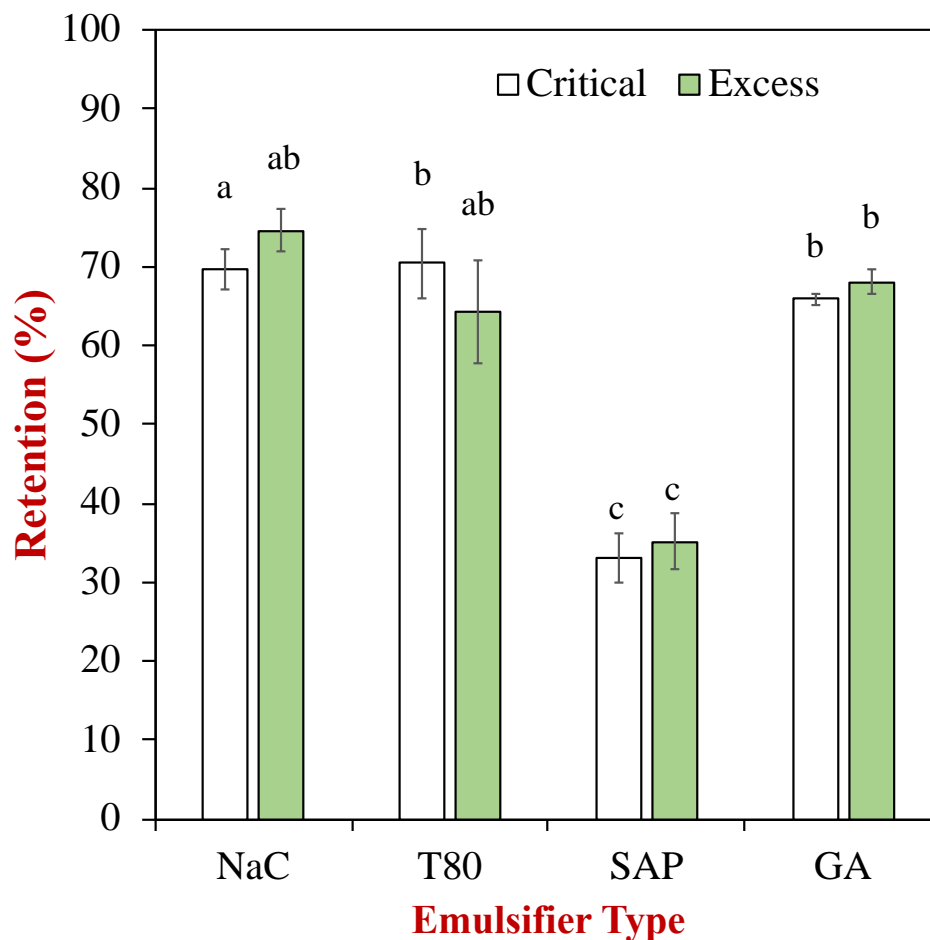


**Figure 16.** Impact of emulsifier type and concentration on curcumin retention in emulsions stored at pH 7 and 55 °C.

In summary, these measurements suggest that the saponins are the least effective emulsifier at inhibiting curcumin degradation in the emulsions, while the other three emulsifiers behave fairly similarly.

### 3.3.4. Impact of emulsifier on physical stability of curcumin-loaded emulsions

The curcumin-loaded emulsions had similar mean droplet diameters and particle size distributions as the corresponding curcumin-free emulsions, which suggested that the

presence of curcumin did not interfere with the homogenization process (data not shown). As mentioned earlier, the emulsions stabilized by caseinate, Tween 80, or saponins contained droplets that were considerably smaller than those in the emulsions stabilized by gum arabic (**Table 5**). In general, the emulsions prepared using excess emulsifier levels had similar or only slightly smaller mean particle diameters than those prepared using critical emulsifier levels. This might be expected since most of the excess emulsifier will remain in the aqueous phase. The impact of the pH of the emulsions on the mean particle diameter depended on the nature of the emulsifier used. For Tween 80 and gum arabic, the particle size did not depend strongly on pH. For sodium caseinate, the emulsions underwent irreversible flocculation when the pH was adjusted from 7 to 3 because they passed through the isoelectric point (pI 4.6) of the protein-coated droplets. For this reason, these emulsions were not tested in other experiments. For the saponin, the mean particle diameter was much smaller at pH 7 ( $D_{32} = 0.20 \mu\text{m}$ ) than at pH 3 ( $0.54 \mu\text{m}$ ). This effect can be attributed to protonation of the carboxylic groups on the saponins, which reduced the negative charge on the droplets (**Table 5**) thereby reducing the electrostatic repulsion between them. Interestingly, in the presence of excess emulsifier the increase in mean particle diameter when the saponin-stabilized emulsions were adjusted from pH 7 ( $D_{32} = 0.20 \mu\text{m}$ ) to pH 3 ( $0.35 \mu\text{m}$ ) was considerably smaller. It is possible that the reduction in droplet charge allowed more saponin molecules to adsorb to the oil droplet surfaces, which partially protected them from aggregation at lower pH values.

**Table 5.** Mean droplet diameter (D32) and electrical characteristics ( $\zeta$ -potentials) of curcumin emulsions at Day 1 and Day 15 (37 °C)

Emulsifier type, concentration, and pH			Mean droplet diameter ( $\mu\text{m}$ )		$\zeta$ -potential (mV)	
			Day 1	Day 15	Day 1	Day 15
<b>NaC</b>	Excess	7.0	0.18 $\pm$ 0.00	0.19 $\pm$ 0.00	-42.4 $\pm$ 1.0	-41.4 $\pm$ 1.2
	Critical	7.0	0.18 $\pm$ 0.00	0.18 $\pm$ 0.01	-48.7 $\pm$ 1.1	-46.1 $\pm$ 1.6
<b>T80</b>	Excess	3.0	0.13 $\pm$ 0.00	0.13 $\pm$ 0.00	-2.3 $\pm$ 0.3	-2.5 $\pm$ 0.6
		7.0	0.13 $\pm$ 0.00	0.13 $\pm$ 0.00	-9.3 $\pm$ 0.5	-9.4 $\pm$ 0.4
	Critical	3.0	0.14 $\pm$ 0.01	0.19 $\pm$ 0.02	-2.2 $\pm$ 0.3	-1.6 $\pm$ 0.2
		7.0	0.13 $\pm$ 0.00	0.15 $\pm$ 0.00	-9.2 $\pm$ 0.7	-9.6 $\pm$ 0.7
<b>SAP</b>	Excess	3.0	0.35 $\pm$ 0.01	0.35 $\pm$ 0.01	-12.8 $\pm$ 1.0	-14.5 $\pm$ 0.8
		7.0	0.20 $\pm$ 0.00	0.21 $\pm$ 0.01	-65.3 $\pm$ 2.4	-64.1 $\pm$ 1.3
	Critical	3.0	0.54 $\pm$ 0.06	0.56 $\pm$ 0.07	-11.8 $\pm$ 1.5	-13.0 $\pm$ 0.7
		7.0	0.20 $\pm$ 0.00	0.24 $\pm$ 0.01	-57.3 $\pm$ 1.4	-60.7 $\pm$ 1.4
<b>GA</b>	Excess	3.0	0.38 $\pm$ 0.02	0.39 $\pm$ 0.02	-13.7 $\pm$ 0.3	-14.3 $\pm$ 0.9
		7.0	0.37 $\pm$ 0.02	0.39 $\pm$ 0.02	-31.7 $\pm$ 0.6	-31.1 $\pm$ 0.9
	Critical	3.0	0.38 $\pm$ 0.02	0.39 $\pm$ 0.02	-13.8 $\pm$ 0.9	-14.5 $\pm$ 0.8
		7.0	0.37 $\pm$ 0.02	0.38 $\pm$ 0.02	-31.8 $\pm$ 0.7	-31.6 $\pm$ 0.8

There was an appreciable increase in the mean particle diameter in all of the emulsions stored at pH 7 at 55 °C for 15 days, which suggested that the elevated storage temperature promoted droplet aggregation (Appendix **Figure S6**). This may have been because the droplets moved around more rapidly and collided with each other more

frequently at higher temperatures because of the greater thermal energy and reduced viscosity of the system. In addition, partial dehydration of the polar groups of the adsorbed emulsifier molecules at elevated temperatures may also have reduced the repulsive interactions between the droplets.

Changes in the droplet size of the emulsions were also confirmed by optical microscopy experiments (**Figure 17**). After preparation (Day 1), all the emulsions contained relatively small droplets that were evenly dispersed throughout the system. After 15 days of storage, the emulsions containing excess emulsifier had a distinctly different appearance to those containing the critical level of emulsifier. In particular, there appeared to be more individual large oil droplets in the emulsions containing the lower emulsifier concentration, which suggested that some droplet coalescence had occurred. This effect was particularly evidenced in the emulsions prepared from Tween 80, which indicated that this emulsion was the least stable to coalescence during storage at higher temperatures. Oil-in-water emulsions stabilized by non-ionic surfactants are known to be unstable to droplet coalescence at higher temperatures due to partial dehydration of the surfactant head group (Kabalnov & Wennerstrom, 1996). Additionally, the ester linkage between the hydrophilic head group and hydrophobic tail group in Tween 80 is prone to hydrolysis at low pH values (Bates, Nightingale, & Dixon, 1973), which may cause loss of emulsifier properties and hence instability in the emulsion.

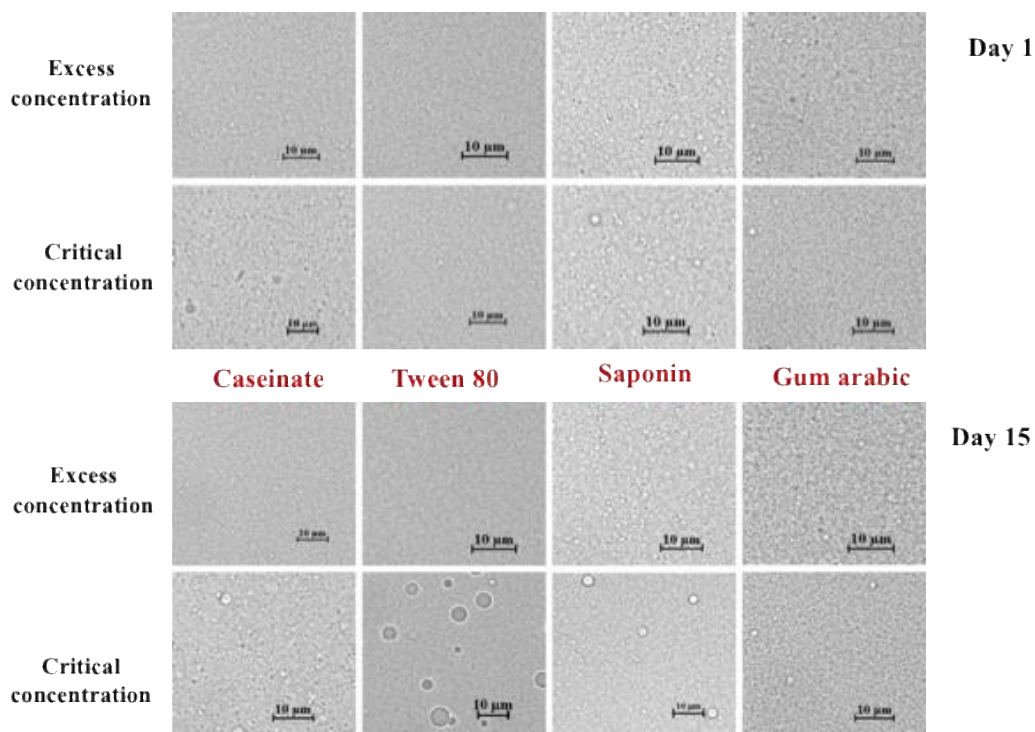


**Figure 17.** Micrographs of curcumin-loaded emulsions after storage at pH 7 and 55 °C at Day 1 and 15.

### 3.3.5. Electrical characteristics of emulsion droplets

Further insights into the impact of emulsifier type and concentration on the properties of the emulsions was obtained by measuring their electrical characteristics. The  $\zeta$ -potential of all the emulsifier-coated oil droplets was negatively charged, but the magnitude of the charge depended strongly on emulsifier type and pH (**Table 5**). At pH 7, the caseinate, saponin, and gum arabic stabilized emulsions had relatively high negative charges of -48.7, -57.3, and -31.8 mV, respectively. For the caseinate-coated droplets, this is because the protein is well above its isoelectric point ( $pI = 4.6$ ) and so there are more anionic carboxyl groups ( $-\text{COO}^-$ ) than cationic amino groups ( $-\text{NH}_3^+$ ). For the saponin-coated, the carboxyl groups in the glucuronic acid residues are almost fully charged at pH 7:  $-\text{COO}^-$ ,  $pK_a = 3.25$ . Similarly, for the gum arabic-coated droplets the

carboxyl groups on the hydrophilic carbohydrate chains are also almost fully charged at neutral pH:  $\text{-COO}^-$ ,  $pK_a = 3.5$  (Renard, Lavenant-Gourgeon, Ralet, & Sanchez, 2006).

The slight negative charge on the Tween 80-coated droplets can be attributed to the presence of some anionic impurities (*e.g.* free fatty acids) in the commercial surfactant product. Adjusting the system to pH 3 resulted in an appreciable lowering in the magnitude of the negative charge in all the emulsions, which can be attributed to partial protonation of the carboxylic acid groups ( $\text{-COOH}$ ). There was no substantial change in the electrical characteristics of the droplets after 15 days storage at either 37 or 55 °C, which suggests there was little change in the electrical properties of the interface.

### **3.4. Conclusions**

This study has shown that the type and amount of emulsifier used to coat the lipid droplets in a curcumin-loaded oil-in-water emulsion impacts the rate and extent of curcumin degradation. This may be important for developing emulsion-based delivery systems for curcumin that can be used in commercial food, supplement, or pharmaceutical products. Ideally, an emulsion should remain both physically and chemically stable within a commercial product prior to ingestion. Sodium caseinate was able to make emulsions that had small droplet sizes, good physical stability to creaming (at neutral pH), and good chemical stability to curcumin degradation during storage. This natural emulsifier may therefore be particularly suitable for forming emulsion-based delivery systems from label-friendly ingredients. On the other hand, the emulsions prepared using saponin had relatively poor stability to curcumin degradation and color fading, which suggested that this was not a good emulsifier to use for this kind of

product. In future studies, it will be important to establish the impact of emulsifier type on the gastrointestinal fate of the curcumin, *e.g.*, its bioaccessibility, transformation, and absorption. In addition, it will be important to determine whether the emulsifier-coated oil droplets remain stable under the environmental stresses that they experience in commercial products, such as chilling, freezing, pasteurization, sterilization, or dehydration.



## CHAPTER 4

### STABILITY OF CURCUMIN-ENRICHED OIL-IN-WATER EMULSIONS: ROLE OF INTERFACIAL SURFACE AREA

#### 4.1. Introduction

In previous chapters, it was found that curcumin degradation occurs mostly due to the presence of aqueous phase in the oil-in-water emulsion. Curcumin is a relatively hydrophobic molecule ( $\log P = 3.29$ ) and so it is primarily located within the oil phase of oil-in-water emulsions. Nevertheless, a small fraction of the curcumin is also present within the aqueous phase, where it is more susceptible to chemical degradation (Kharat & McClements, 2019). We hypothesized that the rate of curcumin degradation in oil-in-water emulsions would increase as their droplet size decreases, because the exchange of curcumin molecules between the oil and water phases would occur more rapidly for smaller droplets. As a result, more of the curcumin would be exposed to the water phase where it would chemically degrade more rapidly. In the pharmaceutical industry, studies of the chemical stability of a hydrolytically susceptible hydrophobic drug (phenyl salicylate) showed that their degradation depended on droplet size (Krickau, Mueller, & Thomsen, 2007). In this case, the transfer of phenyl salicylate from the oil phase to the water phase occurred more rapidly when the droplet size decreased (surface area increased), which resulted in greater degradation. In the present study, we therefore studied the effect of droplet size on the chemical stability of curcumin in oil-in-water emulsions. The information obtained should facilitate the rational design of more effective curcumin delivery systems for application in the food industry.

## 4.2 Materials and methods

### 4.2.1 Materials

Sodium hydroxide (NaOH), sodium phosphate anhydrous dibasic (Na<sub>2</sub>HPO<sub>4</sub>), sodium phosphate anhydrous monobasic (NaH<sub>2</sub>PO<sub>4</sub>), and dimethyl sulfoxide (DMSO) were obtained from Fisher Scientific (Fair Lawn, NJ). Quillaja saponins (QS) (Q-Naturale 200®) having an actual saponin content of this ingredient was between 10-30 wt. % was a gift from Ingredion Inc. (Westchester, IL). Medium chain triglycerides (MCT) was secured from Warner Graham Co. (Cockeysville, MD) mainly consisting of caprylic (58.1 %), and capric (41 %) acids. Synthesized curcumin (purity > 97%) was obtained from TCI Chemical Company (Portland, OR). Hydrochloric acid (HCl) was purchased from the Sigma-Aldrich Company (St. Louis, MO). The chemical reagents and solvents used in this study were all of analytical grade. A water purification system (Nanopure Infinity, Barnstaeas International, Dubuque, IA) was used to prepare the double distilled water utilized in our experiments.

### 4.2.2. Preparation of curcumin-loaded emulsions

Powdered curcumin was dispersed in MCT oil at 75 °C and then stirred at 1200 rpm for 2h, followed by sonication (20 mins) to obtain an oil phase containing 1 mg curcumin/g oil phase. To prepare the aqueous phase, filtered liquid QS extract was dispersed into phosphate buffer solution (5 mM, pH 7.0). Four different emulsions were then prepared by blending the oil and aqueous phases together using different homogenizing equipment **Table 6.** to produce a range of different droplet sizes (and hence surface areas). A large emulsion was prepared using a simple high-shear handheld

blender. This emulsion was then further processed using different approaches to obtain the medium, small, and very small emulsions. The final composition of all the emulsions was as follows: 9.99 wt. % MCT oil, 0.01 wt. % curcumin, 1 wt. % QS liquid extract, and 89 wt. % phosphate buffer solution (pH 7.0, 5 mM).

**Table 6.** Different emulsion types, and their preparation

<b>Emulsion droplet type</b>	<b>Equipment used</b>	<b>Parameters</b>
Large	Hand-held blender (M133/1281-0, Biospec Products, Inc., ESGC, Switzerland)	Low speed setting processed for 2 min
Medium	Ultrasonicator (model 500, Sonic Disembrator, Fisher Scientific, Pittsburgh, PA)	Frequency = 20 kHz amplitude = 20 %, duty cycle = 1 s processed for 2 min
Small	Air-driven microfluidizer (M110L, Microfluidics, Newton, MA)	Air pressure= 4 kpsi 1 pass
Very small	Air-driven microfluidizer (M110L, Microfluidics, Newton, MA)	Air pressure= 12 kpsi 3 passes

Note: In case of emulsions containing medium, small, and very small droplets, a coarse emulsion was first prepared and then it was further processed to obtain the corresponding emulsion.

#### 4.2.3 Appearance

A digital camera was used to record the overall appearance of the emulsions. The optical properties of the emulsions were also quantified using a dual-beam spectrophotometer (ColorFlex® EZ, HunterLab, Reston, VA). The sample was illuminated by a xenon lamp emitting artificial daylight (400-700 nm). An aliquot (10 mL) of curcumin-enriched emulsion was placed in a clear petri dish and illuminated using simulated daylight conditions (D65/10) with a black cup used as a background. The

intensity of the reflected light was measured and converted to CIE  $L^*a^*b^*$  values. The degradation of curcumin was monitored by determining the  $b^*$  value, which provides a quantitative measure of the intensity of the yellowness of the emulsion.

#### **4.2.4 Curcumin concentration measurements**

Curcumin quantification was done spectrophotometrically as described in previous chapter with slight modification. Briefly, about 0.3 mL of curcumin emulsion was mixed with acidified DMSO (5.7 mL) solution and vortexed. About 1 mL of hexane was then added to emulsion-DMSO mixture and vortexed. Contents were then centrifuged ( $500 \times g$  for 15 min) and the lower layer, which contained the curcumin, was collected. The absorbance of this solution was measured at 433 nm using a UV-visible spectrophotometer (Cary 100 UV-Vis, Agilent Technologies).

#### **4.2.5. Particle characterization**

Emulsion droplets were characterized by measuring their particle size distribution and mean diameter using a static light scattering device (Mastersizer 3000, Malvern Instruments Ltd., Malvern, Worcestershire, UK). The electrical characteristics of the oil droplets ( $\zeta$ -potential) was determined using an electrophoresis technique (Zetasizer Nano ZS series, Malvern Instruments Ltd.). Samples were diluted with phosphate buffer (10 mM, pH 7.0) to avoid multiple light scattering events and to ensure accurate measurements.

#### **4.2.6. Particle morphology**

The morphology of the emulsions was studied using a fluorescence microscope at a magnification of 600× (Nikon D-Eclipse C1 80i, Nikon, Melville, NY, USA). A small amount (~ 6 µL) of sample was put on a glass microscope slide and then covered using a glass slip. A laser attachment was used to excite the emulsion sample at 488 nm and images were recorded and analyzed using the instrument software (NIS-Elements, Nikon, Melville, NY). Large and medium emulsions were observed under a 20× objective lens through a 10× eyepiece, while small and very small emulsions were observed using an oil immersion objective lens (60×). Curcumin produced green fluorescence when excited with the monochromatic laser light, which provided details about its distribution and emulsion microstructure.

#### **4.2.7. Statistical analysis**

Experiments were carried out using two replicates and each replicate was measured twice. The mean and standard deviations were then calculated from these four values using Microsoft Excel. Significant differences among treatments were evaluated using the Tukey multiple-comparison test at a significance level of  $p \leq 0.05$  (SPSS ver.19, SPSS Inc., Chicago, IL, USA).

### **4.3 Results and discussions**

#### **4.3.1. Emulsion droplet characteristics**

Initially, we characterized the properties of the oil droplets in the curcumin-loaded emulsions prepared using the different homogenization approaches (**Table 7** and **Figure**

**18).** As expected, the emulsion prepared using only a hand-held blender contained the largest droplets, while the emulsion prepared using multiple passes through the microfluidizer at high pressure contained the smallest droplets. The mean diameters ( $d_{32}$ ) of the droplets in the large, medium, small, and very small emulsions were  $20.9 \pm 0.8 \mu\text{m}$ ,  $2.53 \pm 0.19 \mu\text{m}$ ,  $0.26 \pm 0.01 \mu\text{m}$  and  $0.083 \pm 0.015 \mu\text{m}$ , respectively. The emulsions produced using the blender (large) and the sonicator (medium) had bimodal distributions, whereas the ones produced by the microfluidizer (small and very small) had monomodal distributions (**Figure 18**). The specific surface area ( $A_s$ ) of the oil droplets in the emulsions, which is the oil-water interfacial area per unit mass of oil ( $\text{m}^2 \text{kg}^{-1}$ ), was calculated using the following expression:  $A_s = 6/(\rho_0 d_{32})$ , where  $\rho_0$  is the density of the oil phase ( $940 \text{ kg m}^{-3}$ ) and  $d_{32}$  is the surface-weighted mean droplet diameter (m) (McClements, 2007). The calculated  $A_s$  values were approximately 300, 2,500, 24,000, and 80,000  $\text{m}^2 \text{kg}^{-1}$  for the large, medium, small, and very small emulsions, respectively (**Table 7**). There was no significant change in the surface-weighted mean droplet diameter of the emulsions after the completion of study, with the exception of the small emulsion where there was a slight increase (**Figure S7** in Appendix). This suggested that the majority of the droplets in the emulsions were resistant to aggregation during storage. On the other hand, there was an appreciable increase in the volume-weighted mean diameter ( $d_{43}$ ) of the emulsions after storage, which can be attributed to the fact that some of the droplets aggregated. The  $d_{43}$  value is highly sensitive to the presence of a few large particles in an emulsion, so if there is even a little droplet aggregation during storage, then there will be an appreciable increase in  $d_{43}$ . (McClements, 2015a)

Initially, the  $\zeta$ -potentials for the emulsions containing large, medium, small, and very small droplets were all strongly negative:  $-72.3 \pm 4.4$ ,  $-76.9 \pm 1.7$ ,  $-62.0 \pm 1.5$ , and  $-48.3 \pm 1.4$  mV, respectively (**Figure 19**). The lipid droplets were coated by saponins, which would be expected to have a strong negative charge at pH 7.0 due to the presence of deprotonated glucuronic acid groups ( $pK_a = 3.25$ ). In general, the magnitude of the  $\zeta$ -potential decreased with decreasing droplet size, which may have been due to changes in droplet surface chemistry or due to a measurement artefact associated with limitations in the mathematical model used to analyze the electrophoresis data.(McClements, 2015a)

After 17 days storage at 55 °C, the  $\zeta$ -potential on the emulsion droplets changed, but in no consistent manner. For instance, the negative charge decreased in the large and medium emulsions but increased in the small and very small emulsions. The physicochemical origin of these effects is currently unknown. It could be due to changes in the surface chemistry of the lipid droplets, *e.g.*, due to the generation of charged reaction species caused by the chemical degradation of the curcumin or saponin. Alternatively, it could be due to changes in the adsorption/desorption of charged species at the oil-water interface during storage.

**Table 7.** Emulsion droplet characteristics after emulsion preparation (Day 0)

Emulsion droplet type	Mean droplet size, D <sub>32</sub> (μm)	Specific surface area (m <sup>2</sup> kg <sup>-1</sup> )	
		measured	rounded-off
Large	20.917 ± 0.751	304 ± 11	300
Medium	2.525 ± 0.187	2526 ± 187	2500
Small	0.261 ± 0.007	24313 ± 645	24000
Very small	0.083 ± 0.015	78085 ± 13137	80000

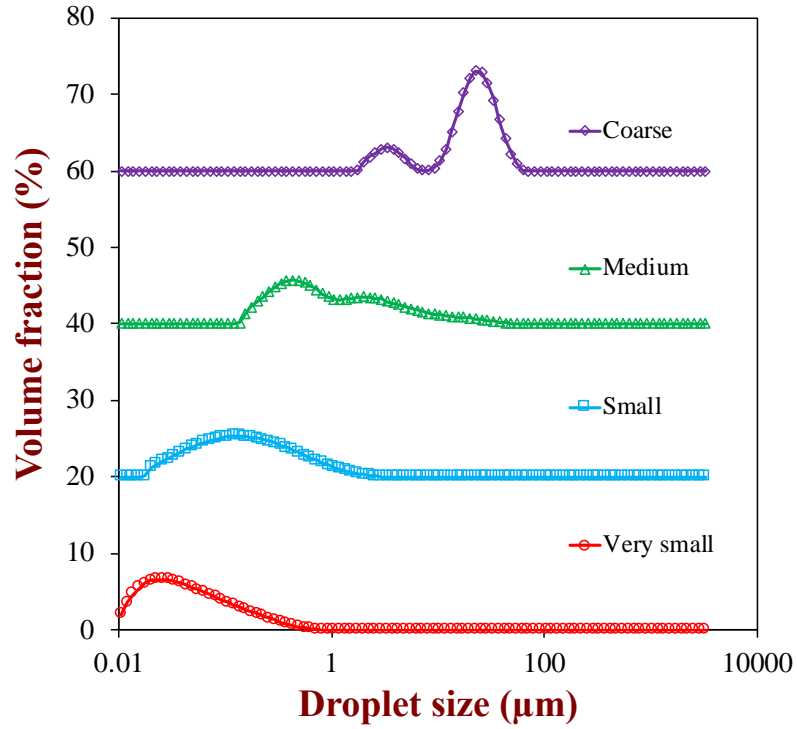


**Figure 18.** Droplet size distribution of different emulsion types

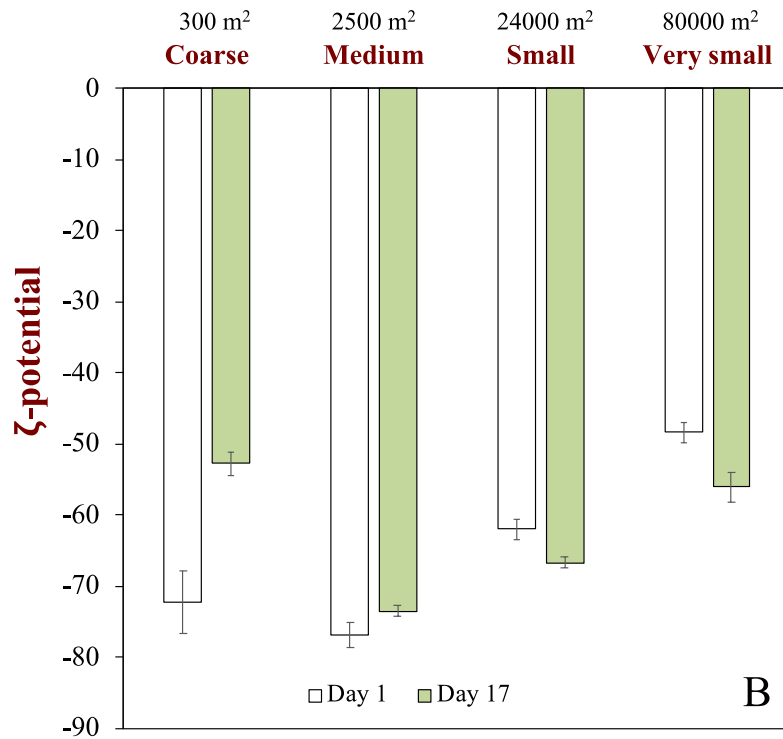


**Figure 19.** Change in the electrical characteristics of droplets before and after storage



### 4.3.2. Microstructure analysis

**Figure 20** shows changes in the microstructure of the emulsions during storage monitored by confocal microscopy. The microscopy images were consistent with the light scattering analysis of particle size, with the dimensions of the individual oil droplets in the emulsions decreasing in the order: large > medium > small > very small. Green fluorescence staining confirmed that most of the curcumin was encapsulated inside the oil droplets. Initially, the individual droplets in the small and very small emulsions were too little to be seen directly in the microscopy images. At the end of storage, however, some relatively large individual droplets were observed in these emulsions, suggesting that some droplet coalescence had occurred. Coalescence may have been promoted because droplet-droplet collisions are more frequent at the relatively high temperature used in the storage study (55 °C) due to the decrease in aqueous phase viscosity. Moreover, the headgroups of the surfactant molecules may have become partially dehydrated at elevated temperatures, which would have allowed the droplets to come closer together. (McClements, 2015a) It should be noted that a thin layer of free oil was observed at the top of the small and very small emulsions after prolonged storage, which is also indicative of droplet coalescence and oiling off.

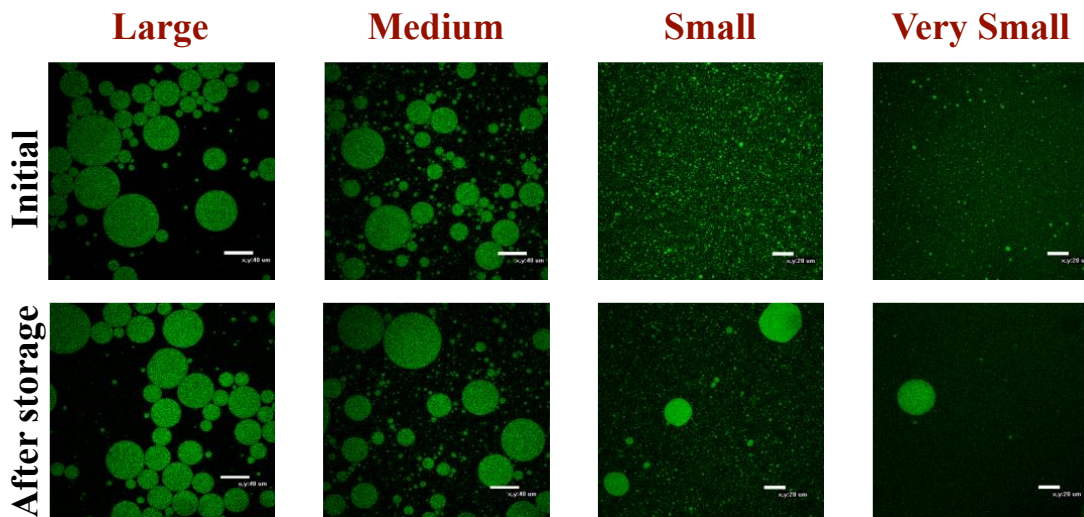


**Figure 20.** Micrographs of curcumin-loaded emulsions having different specific surface area taken at Day 0 (Initial) and Day 17 (After storage, pH 7, 55 °C). Scale bars represent 20  $\mu\text{m}$ .

#### 4.3.3. Impact of droplet size on emulsion appearance.

Initially, all the curcumin-loaded emulsions had a milky yellow appearance after preparation (**Figure 21**). However, the large emulsion was less turbid than the others, which can be attributed to the reduced light scattering associated with larger droplets.(McClements, 2015a) The emulsions containing small and very small droplets were relatively stable to gravitational separation (creaming) during storage because of the weak gravitational forces acting upon the droplets. Conversely, rapid gravitational separation was observed in the emulsions containing medium and large droplets because the creaming velocity increases with the square of the droplet size.(McClements, 2007) After 3 days storage, the oil droplets in the large emulsions had moved to the top of the test tubes forming a bright yellow cream layer above a clear serum layer, which had a

slightly yellow appearance. The slight yellow tinge of the serum layer suggested that a small fraction of the curcumin was solubilized in the water phase, which is consistent with the theoretical partitioning calculations discussed later. Interestingly, the intensity of the yellow color in the serum layer decreased over time, which is indicative of rapid chemical degradation of solubilized curcumin.

There was also a distinct yellow cream layer formed at the top of the emulsions containing the medium droplets after 3 days storage, but in this case the serum layer had a more turbid yellow appearance. This effect can be attributed to the fact that the medium emulsion contained a population of relatively small droplets ( $d < 1 \mu\text{m}$ ) that only creamed slowly (**Figure 18** and **Figure 20**). Interestingly, the yellow color of the serum layer faded much more quickly than that of the cream layer. This visual observation suggested that curcumin was more susceptible to degradation in smaller oil droplets than in larger ones, which was confirmed in the experiments described later.

As mentioned earlier, the emulsions containing the small and very small droplets were much more stable to gravitational separation because of the weaker gravitational forces acting upon the droplets. However, visual observation of these samples indicated that the rate of color fading was much faster than in the emulsions containing the large droplets. Indeed, the emulsions with the very small droplets appeared almost white after 17 days storage (**Figure 21**), suggesting that considerable curcumin degradation had occurred.

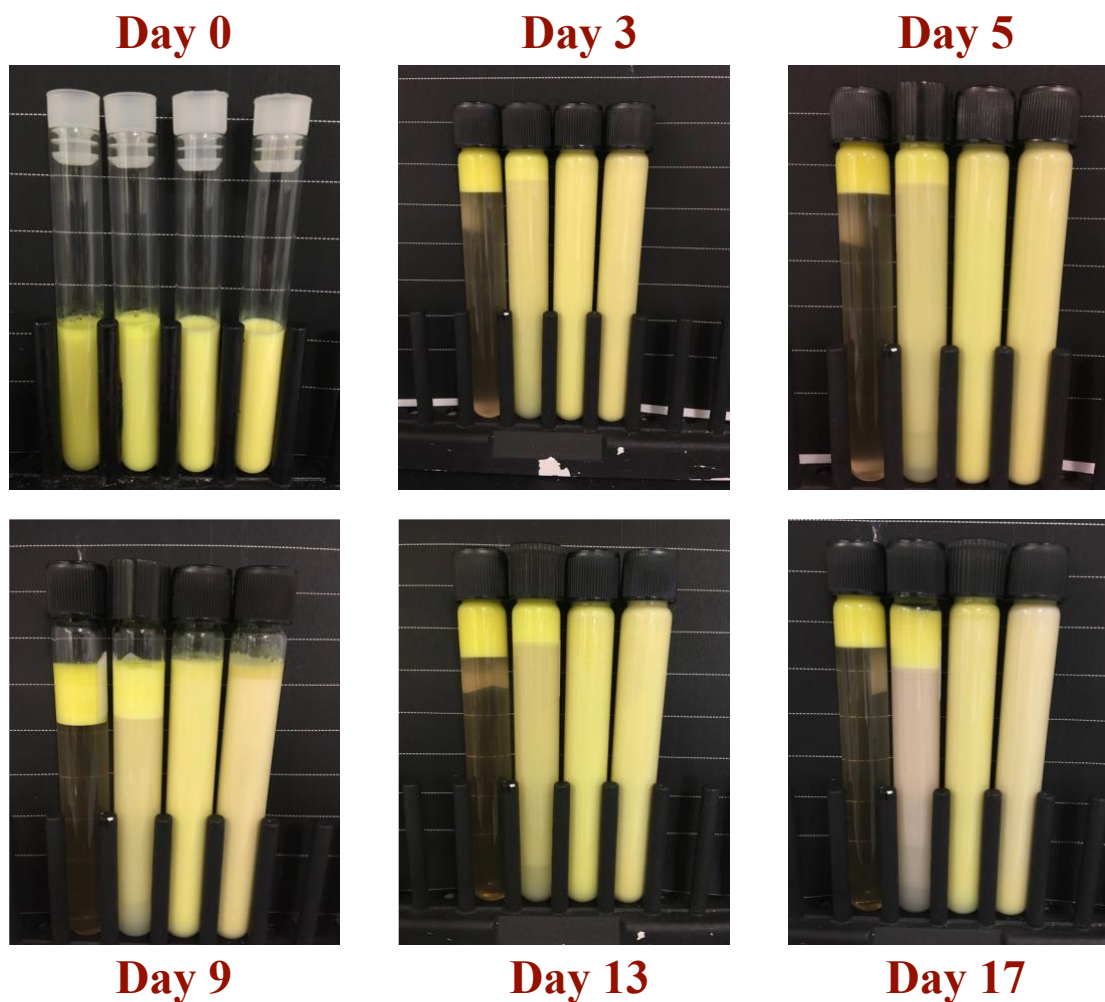


**Figure 21.** Photographs of curcumin-loaded oil-in-water emulsions with different specific surface area of droplets (300, 2500, 2400, 80000 m<sup>2</sup>, left to right) during storage (55 °C). Emulsions composition: oil 10 wt.%, curcumin 0.01 wt.%, Quillaja saponin extract 1 wt.%, and rest phosphate buffer (pH 7.0, 5 mM)

#### 4.3.4. Impact of droplet size on color fading

A more quantitative analysis of the impact of droplet size on the rate of color fading was obtained using an instrumental colorimeter. In this case, the emulsions were gently agitated prior to analysis to ensure they were homogeneous. Initially, the yellowness ( $b^*$ ) of all the emulsions was relatively high, and all samples had fairly

similar  $b^*$  values, with the exception of the large emulsion for which the  $b^*$  value was slightly lower (**Figure 22A**). This latter effect is mainly because the droplets in this emulsion are much larger ( $\sim 20 \mu\text{m}$ ) than the wavelength of visible light (400-700 nm) leading to a reduced light scattering intensity. (Chantrapornchai, Clydesdale, & McClements, 1998) The  $b^*$  value of all the emulsions decreased during storage, which is indicative of color fading. This decrease was fairly gradual in the large, medium, and small emulsions but relatively rapid in the very small emulsions (especially during the first 3 days), which agrees with the visual observations.

The rate of color fading was clearly dependent on the lipid droplet size. An estimation of this effect was obtained by calculating the *yellowness retention*, which was defined as the percentage of instrumental yellowness ( $b^*$ ) remaining after 17 days storage compared to the initial value. There was only a slight decrease in the yellowness retention of the large and medium emulsions after storage, a more pronounced decrease in the small emulsions, but a much more dramatic decrease in the very small emulsions (**Figure 22B**). The loss in yellowness after storage increased in the following order:  $13.8 \pm 0.2 \%$  (large) <  $14.7 \pm 0.2 \%$  (medium) <  $20.0 \pm 0.5 \%$  (small) <<  $43.9 \pm 2.8 \%$  (very small). Since the yellow color of the emulsions was due to the presence of curcumin, these results suggest that curcumin degradation occurred more rapidly as the droplet size decreased (surface area increased). For this reason, the concentration of curcumin remaining in the emulsions during storage was quantified using a spectrophotometric method.

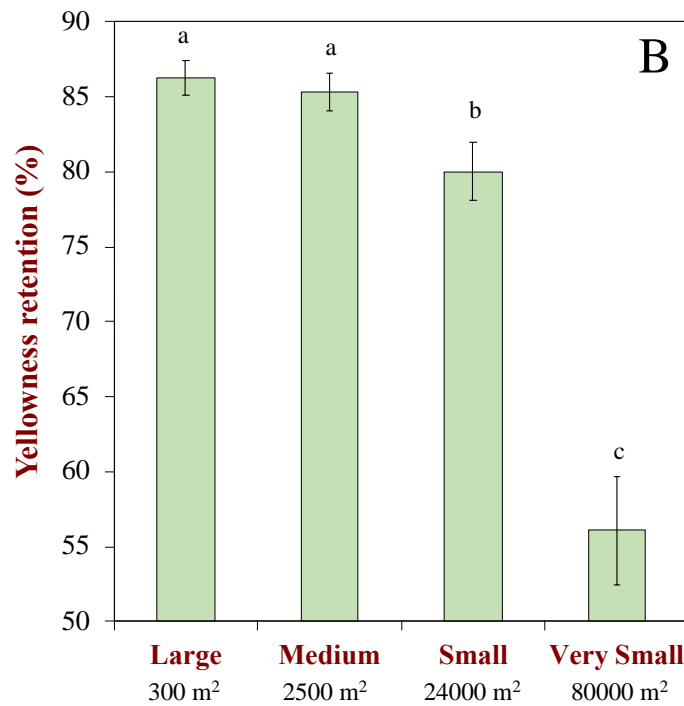
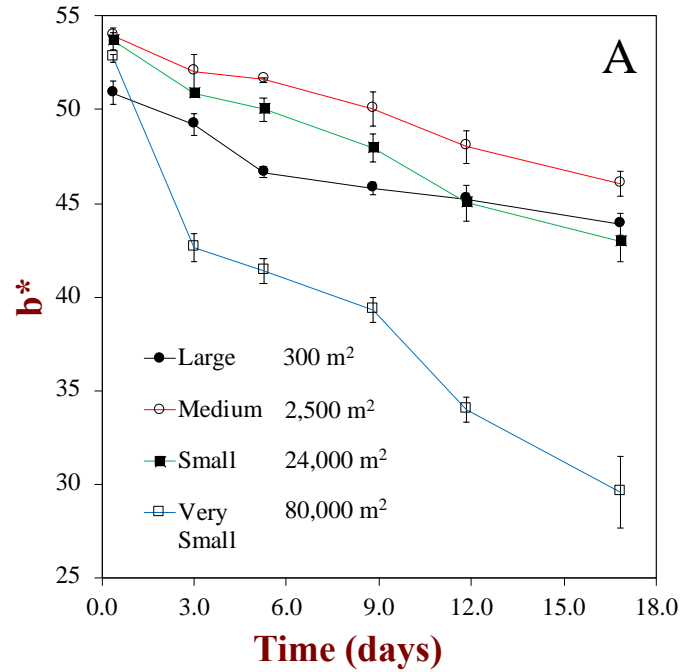


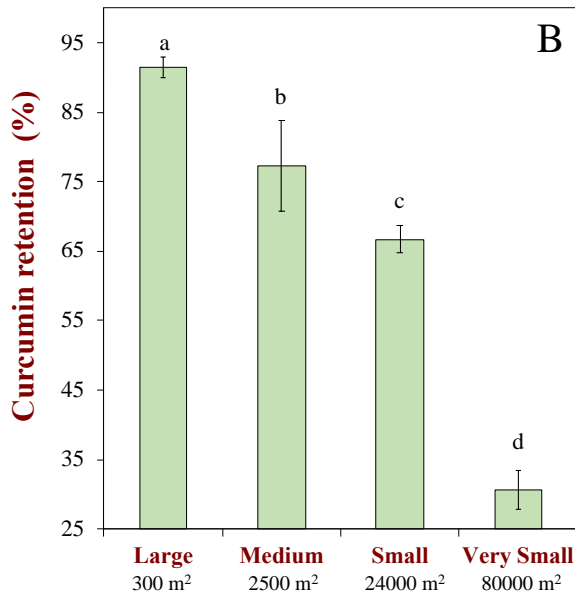
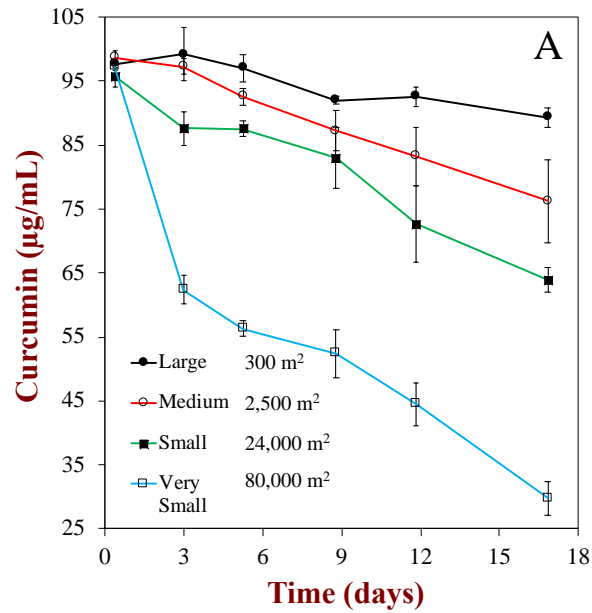
**Figure 22.** Impact of specific surface area of droplets on change (A) and retention (B) in tristimulus color coordinate ( $b^*$ ) of curcumin-loaded oil-in-water emulsions during storage at pH 7 and 55 °C.

#### 4.3.5. Impact of droplet size on chemical stability of curcumin

Previous studies have shown that the stability of curcumin encapsulated within oil-in-water emulsions is controlled by many physicochemical factors, including pH, temperature, emulsifier type, and emulsifier concentration (Kharat et al., 2017; Mahesh Kharat et al., 2018). In this series of experiments, we focused on the impact of droplet size on the chemical stability of the encapsulated curcumin. As mentioned earlier, as the droplet size decreases, the specific surface area of the oil droplets increases, which would be expected to impact the transfer rate of curcumin in and out of the droplets, and therefore its chemical stability.

As shown in **Figure 23A**, the curcumin concentration in all the freshly prepared emulsions was close to 100  $\mu\text{g/mL}$ , which was the amount added initially. The curcumin concentration in the large, medium, and small emulsions decreased gradually with time, whereas that in the very small emulsions decreased rapidly during the first 3 days but then decreased more gradually afterwards. These results are therefore consistent with the instrumental colorimetry measurements discussed earlier. In general, the curcumin degradation rate increased as the droplet size decreased (surface area increased). For instance, the curcumin remaining at the end of the storage period decreased in the following order:  $91.4 \pm 1.5 \%$ ,  $77.3 \pm 6.6 \%$ ,  $66.7 \pm 1.9 \%$ , and  $30.6 \pm 2.8 \%$  for the large, medium, small, and very small emulsions, respectively (**Figure 23B**). In designing and manufacturing a commercial product which is aimed at delivering curcumin, it would be important to control the droplet size (hence surface area) characteristics in order to ensure the functional characteristics of the product as well as to maintain the product stability. The final amount of curcumin present in a product could be determined by calculating the

curcumin degradation rate. As shown in **Figure 23C**, curcumin degraded at a much higher rate of  $4.1 \pm 0.2 \mu\text{g mL}^{-1} \text{ day}^{-1}$  at an  $A_s = 300 \text{ m}^2 \text{ kg}^{-1}$  for very small emulsions compared to a rate of  $0.5 \pm 0.1 \text{ mL}^{-1} \text{ day}^{-1}$  in large emulsions having  $A_s = 80,000 \text{ m}^2 \text{ kg}^{-1}$ . This is important to know to from commercial viewpoint because one can optimize the product performance by selecting a suitable droplet size.





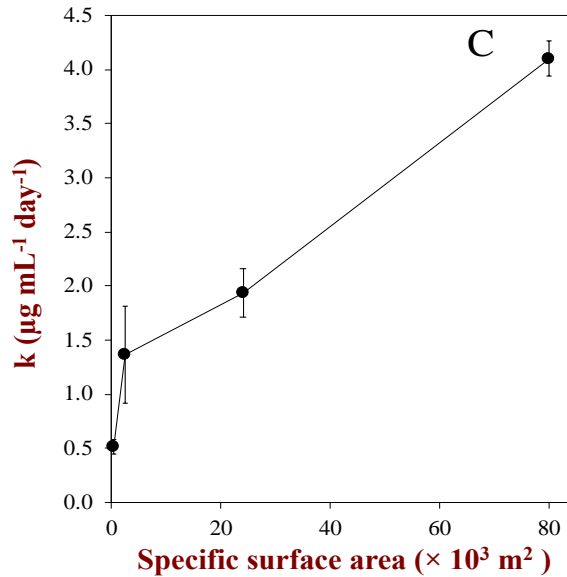


**Figure 23.** Impact of specific surface area of droplets on change (A) and retention (B) in curcumin concentration, and (C) rate of curcumin degradation,  $k$ , in oil-in-water emulsions during storage at pH 7 and 55 °

It is important to note that many of the droplets in the large and medium emulsions moved to the top of the samples during storage. As a result, these droplets were packed into a dense cream layer where they were mainly surrounded by other oil droplets. This phenomenon may have further reduced the exposure of the oil phase to the surrounding water phase, thereby further slowing down the exchange of curcumin molecules between the oil and water phases. In contrast, the droplets in the small and very small emulsions remained dispersed throughout the aqueous phase during storage and so were always surrounded by water.

Our results are consistent with an earlier study on excipient emulsions. (Zou, Zheng, Liu, Liu, Xiao, & McClements, 2015) This study showed that the solubilization of powdered curcumin within the oil phase of an emulsion increased as the droplet size decreased. However, the chemical stability of the curcumin tended to decrease as the

droplet size was reduced. In our study, the curcumin was added to the oil phase before preparing the emulsions but the impact of droplet size on curcumin stability followed a similar trend.

**Physicochemical origin of curcumin degradation.** Our results clearly show that the chemical stability of curcumin decreases as the oil droplet size decreases, which can be partly attributed to the increase in surface area of oil exposed to the surrounding aqueous phase. In this section, we provide some insights into the physicochemical origin of this phenomenon. The distribution of curcumin between the oil and water phases of an oil-in-water emulsion is important because curcumin is known to be more stable to chemical degradation when it is surrounded by oil than by water (Kharat et al., 2017). Based on a mass balance calculation, the fraction of curcumin in the oil phase of an oil-in-water emulsion is given by:

$$\Theta = \left(1 + \frac{(1-\phi)}{K\phi}\right)^{-1} \quad (1)$$

Here,  $\phi$  is the disperse phase volume fraction (oil droplet concentration) and  $K$  is the equilibrium oil-water partition coefficient ( $K = 10^{\log P}$ ). Curcumin is a relatively hydrophobic molecule with a  $\log P$  value of around 3.29 (chemspider.com), while the emulsion used in this study had an oil concentration of 10 wt% ( $\phi \approx 0.1$ ). Inserting these values into the above equation shows that about 99.5% of the curcumin should be present inside the oil droplets while only 0.5% should be present in the surrounding water phase. Based on previous studies, one would expect the small fraction of curcumin in the water phase to chemically degrade much faster than the large fraction of curcumin within the oil phase.(Kharat et al., 2017)

It should be noted, however, that curcumin molecules continuously exchange between the interior and exterior of the oil droplets due to their Brownian motion. Consequently, all of the curcumin molecules in the system will eventually be exposed to the water phase. However, the rate of curcumin exchange between the oil and water phases increases as the oil droplet size decreases because of the increase in the specific surface area of the oil-water interface ( $A_s \propto 1/d$ ). As a result, one would expect the curcumin to degrade more rapidly in an emulsion containing smaller droplets because the curcumin molecules are exposed to the water phase more quickly.

We could not find a theoretical model that deals with this specific problem, but we can obtain an indication of the impact of droplet size on the mass transport of bioactive molecules from the theories developed to model drug release from colloidal particles. The release of curcumin from a spherical particle under similar conditions can then be described by the Crank model (McClements, 2015a):

$$\frac{M(t)}{M(0)} = 1 - \exp\left[-\frac{4.8D\pi^2t}{Ka^2}\right] \quad (2)$$

Here,  $D$  is the translational diffusion coefficient of the curcumin through the oil phase. The diffusion coefficient can be calculated from the Stokes-Einstein equation:

$$D = \frac{k_B T}{6\pi\eta r} \quad (3)$$

Here,  $k_B$  is Boltzmann's constant ( $1.38 \times 10^{-23}$  J K<sup>-1</sup>),  $T$  is the absolute temperature (328 K),  $\eta$  is the viscosity of the oil phase, and  $r$  is the radius of hydration of the curcumin molecule. The viscosity of the MCT oil (assumed to be similar to that of coconut oil) at 55 °C has been reported to be 16 mPa s, while the radius of hydration of curcumin has been reported to be 0.690 nm. (Patsahan, Ilnytskyi, & Pizio, 2017) This

leads to a diffusion coefficient of  $2.2 \times 10^{-11} \text{ m}^2\text{s}^{-1}$  for curcumin in the interior of the oil droplets. Predictions made using the Crank equation show that the rate of transfer of the curcumin molecules from inside the oil droplets to the surrounding water phase (or *vice versa*) increases as the droplet size decreases (**Figure 24**). This phenomenon would therefore account for the fact that the curcumin degrades more rapidly in the smaller droplets – there is a faster exchange of curcumin molecules between the oil phase (where it is relatively stable to degradation) to the water phase (where it is relatively unstable) as described in **Figure 25**.

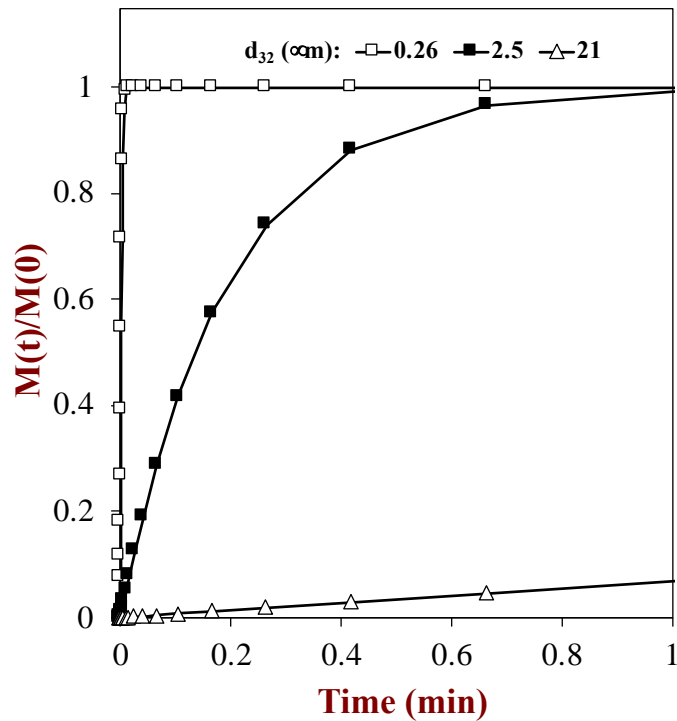


**Figure 24.** Effect of droplet size on the release profiles of curcumin from a spherical oil droplet as derived from the Crank model.

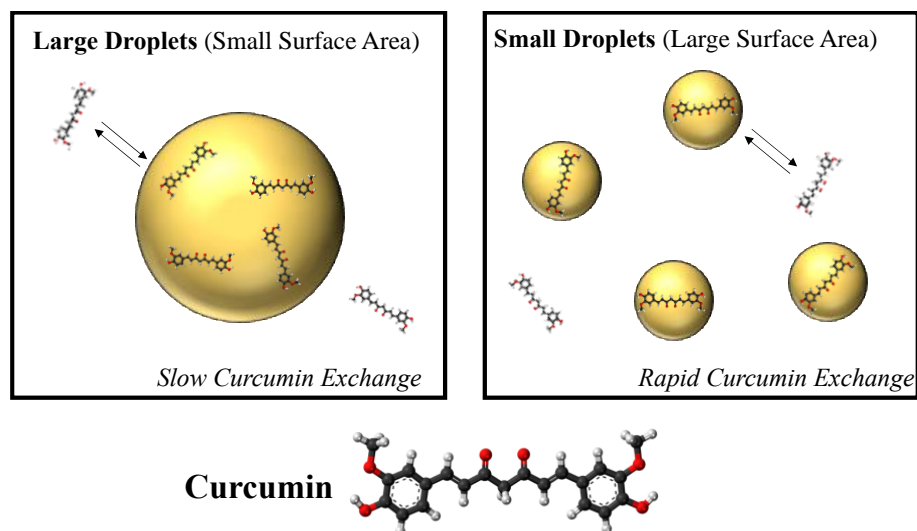


**Figure 25.** Hydrophobic curcumin is distributed between the oil and water phases according to its LogP value (3.29). The rate of exchange is faster in emulsions with smaller droplet, leading to faster degradation since each curcumin molecule spends more time in the water

#### 4.4 Conclusions

In summary, in this study we have shown that the size of the oil droplets in emulsion-based delivery systems plays a critical role in determining the chemical stability of encapsulated curcumin. This knowledge is important for formulating functional food and beverage products that can keep the curcumin in a bioactive form during storage. Ideally, the size of the oil droplets in the emulsion should be relatively large to protect the curcumin, but this may cause a reduction in the creaming stability and bioaccessibility. The problem with droplet creaming may be overcome by adding thickening agents to inhibit the upward movement of the large droplets. In commercial products with relatively low viscosities, such as beverages, it is important to utilize relatively small oil droplets to inhibit creaming. In these products, it is therefore

important to utilize alternative strategies to retard curcumin degradation during storage. For instance, curcumin degradation can be inhibited by storing at a low temperature, ensuring the product has a mildly acidic pH, adding antioxidants, solidifying the lipid phase, or controlling the interfacial properties using emulsifier technology.

## CHAPTER 5

### ENHANCEMENT OF CHEMICAL STABILITY OF CURCUMIN-ENRICHED OIL-IN-WATER EMULSIONS: IMPACT OF ANTIOXIDANT TYPE AND CONCENTRATION

#### 5.1. Introduction

In previous chapters, we found that curcumin is susceptible to degradation in emulsions, especially those stabilized with natural quillaja saponins. As the use of such natural emulsifiers is greatly increasing in commercial products, it is important to optimize emulsion properties to ensure good curcumin stability in foods and beverages. Antioxidants have been proven to be effective in protecting curcumin against chemical degradation in aqueous solutions (Nimiya et al., 2015). In the present study, the efficacy of various antioxidants in protecting curcumin from degradation in emulsions was compared. The impact of antioxidant polarity was investigated by using water-soluble (ascorbic acid and Trolox), amphiphilic (ascorbic acid 6-palmitate), and oil-soluble ( $\alpha$ -tocopherol) antioxidants (**Table 8**). As curcumin is known to degrade at a higher rate in aqueous solutions, we hypothesized that water-soluble antioxidants would be better at protecting it than oil-soluble ones.

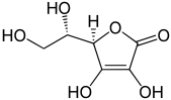
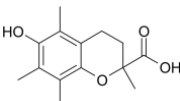
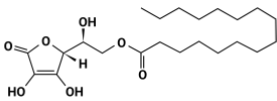
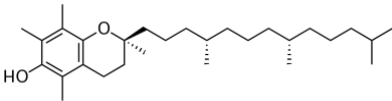
#### 5.2 Materials and methods

##### 5.2.1 Materials

Sodium hydroxide (NaOH), sodium phosphate anhydrous dibasic (Na<sub>2</sub>HPO<sub>4</sub>), sodium phosphate anhydrous monobasic (NaH<sub>2</sub>PO<sub>4</sub>), and dimethyl sulfoxide (DMSO)

were obtained from Fisher Scientific (Fair Lawn, NJ). Quillaja saponins (QS) (Q-Naturale 200®) having an actual saponin content of this ingredient was between 10-30 wt. % was a gift from Ingredion Inc. (Westchester, IL). Medium chain triglycerides (MCT) was secured from Warner Graham Co. (Cockeysville, MD) mainly consisting of caprylic (58.1 %), and capric (41 %) acids. Synthesized curcumin (purity > 97%) was obtained from TCI Chemical Company (Portland, OR). Hydrochloric acid (HCl), and all antioxidants including ascorbic acid (≥ 98%), ascorbic acid 6-palmitate (≥ 98%), α-tocopherol (≥ 96%), and 6-hydroxy-2,5,7,8-tetramethylchroman-2-carboxylic acid (or Trolox, 97%) were purchased from the Sigma-Aldrich Company (St. Louis, MO). The chemical reagents and solvents used in this study were all of analytical grade. A water purification system (Nanopure Infinity, Barnstaeas International, Dubuque, IA) was used to prepare the double distilled water utilized in our experiments.

**Table 8.** Molecular structure and partition coefficients of antioxidants used in this study

Antioxidant	Molecular Structure	log P*
ascorbic acid		-0.2
trolox		1.3
ascorbic acid 6-palmitate		6.0
α-tocopherol		10.7

\*obtained from <http://www.chemspider.com/>



### 5.2.2. Preparation of curcumin-loaded emulsions

An oil phase containing 1 mg of curcumin per gram of oil was produced by stirring a mixture of powdered curcumin and MCT at 75 °C at 1200 rpm for 3h, and then sonicating for 20 mins. If required, mixing and sonication were carried out for longer to make sure that all the curcumin was fully dissolved. For oil-soluble antioxidants (ascorbic acid 6-palmitate, or  $\alpha$ -tocopherol), the final oil phase was prepared by mixing the antioxidants with the curcumin-enriched MCT oil and then heating again (if required) to make sure all components were dissolved. An aqueous phase was made by dispersing liquid QS extract into the phosphate buffer (5mM, pH 7.0). Water soluble antioxidants were also dissolved in the buffer. An emulsion pre-mix was obtained by mixing oil and aqueous phases using a high-shear mixer for 2 min (M133/1281-0, Biospec Products, Inc., ESGC, Switzerland). The emulsion pre-mix was then homogenized further by passing it three-times through a microfluidizer (M110L, Microfluidics, Newton, MA) using a pressure of 12,000 psi. The emulsions resulting from this procedure contained 10 wt. % MCT oil, 1 wt. % QS liquid extract, 0.01 wt. % curcumin, 600  $\mu$ M antioxidants, and the rest was comprised of phosphate buffer (pH 7.0, 5 mM). This antioxidant concentration was selected based on a few factors including their typical concentrations in foods, their permitted levels in foods, and their solubility characteristics (Aguilar et al., 2015; Bele, Matea, Raducu, Miresan, & Negrea, 2013).

In one study, the effect of antioxidant concentration was examined by using ascorbic acid dissolved at various levels in the aqueous phase (15, 50, 100, 300, and 600  $\mu$ M), with the concentration of the other ingredients remaining the same as described above. A control emulsion was prepared that did not contain antioxidant. For the control

and all antioxidant emulsions, a corresponding blank emulsion was also prepared that contained no curcumin. All emulsions were stored in a temperature-controlled incubator (55 °C, quiescent conditions) to accelerate degradation, and samples were periodically collected for analysis.

### **5.2.3 Appearance**

Emulsion appearance was recorded using a digital camera, while instrumental optical properties were quantified using colorimetry (ColorFlex® EZ, HunterLab, Reston, VA). In this dual-beam spectrophotometer, sample is illuminated by artificial daylight (400-700 nm) flashes using a xenon lamp. Curcumin-enriched emulsion was poured into a transparent petri dish, and a black cup was utilized as a background. The sample was then illuminated and observed using simulated daylight conditions (D65/10). The intensity of the reflected light was measured and converted to CIE  $L^*a^*b^*$  values. Curcumin degradation in the emulsions was monitored by determining the  $b^*$  value, which provides a measure of the intensity of the yellow color.

### **5.2.4 Curcumin concentration measurements**

Curcumin quantification was done as described previously. A portion of emulsion (0.3 mL) was mixed with acidified DMSO (5.7 mL) solution and the resulting mixture was vortexed. A small volume of hexane (1 mL) was then added and the contents were mixed to solubilize the curcumin within this organic solvent. This mixture was then centrifuged ( $500 \times g$  for 15 min) and the lower layer, which contained the curcumin, was collected. The absorbance of this solution was measured at 433 nm using a UV-visible

spectrophotometer (Cary 100 UV-Vis, Agilent Technologies). The final absorbance was obtained after comparing with the corresponding blank measurement. A linear calibration curve ( $r_2 = 0.99$ ) was prepared using DMSO solutions of known curcumin concentration. The concentration of curcumin extracted from the samples was then determined by comparing the measured absorbance to the calibration curve.

#### **5.2.5. Particle characterization**

The droplet size characteristics were determined by static light scattering (Mastersizer 3000, Malvern Instruments Ltd., Malvern, Worcestershire, UK). The droplet charge characteristics ( $\zeta$ -potential) were determined using electrophoresis (Zetasizer Nano ZS series, Malvern Instruments Ltd.). Samples were diluted with phosphate buffer (10 mM, same pH as original sample) to obtain a light scattering signal in an appropriate range for measurement.

#### **5.2.6. Particle morphology**

Emulsion morphology was studied using a fluorescence microscope at a magnification of 600 $\times$  (Nikon D-Eclipse C1 80i, Nikon, Melville, NY, USA). For the analyses, a small volume of sample was centered on a microscope slide and then covered using a glass slip. Samples were excited at 488 nm using a laser and images were recorded and analyzed using the instrument software (NIS-Elements, Nikon, Melville, NY). The microscopy images provided information about emulsion microstructure and curcumin distribution (since curcumin naturally fluoresces under the conditions used).

### **5.2.7. Statistical analysis**

Experiments were carried out using two replicates, with two measurements being made on each replicate (leading to four total measurements). The mean and standard deviations were calculated using Microsoft Excel. Significant differences among treatments were evaluated using the Tukey multiple-comparison test at a significance level of  $p \leq 0.05$  (SPSS ver.19, SPSS Inc., Chicago, IL, USA).

## **5.3 Results and discussions**

### **5.3.1. Impact of Antioxidants on appearance of curcumin loaded emulsions**

Curcumin-enriched emulsions had a milky, bright yellow appearance (**Figure 26**). All emulsions looked alike after preparation and it was not possible to visually differentiate the control and antioxidant-containing emulsions. The majority of the antioxidants used in this study were colorless and hence did not change the optical characteristics of the emulsions. The  $\alpha$ -tocopherol, however, had a reddish-brown color in its pure form, but it did not significantly affect the color of the curcumin emulsions because it was used in such a highly diluted form (600  $\mu\text{M}$ ). Visually, the intensity of the yellowness of all the emulsions faded after storage. Fading was especially prevalent in the control and  $\alpha$ -tocopherol-containing emulsions when compared to those containing the other antioxidants. It was difficult, however, to draw a visual difference within these groups.

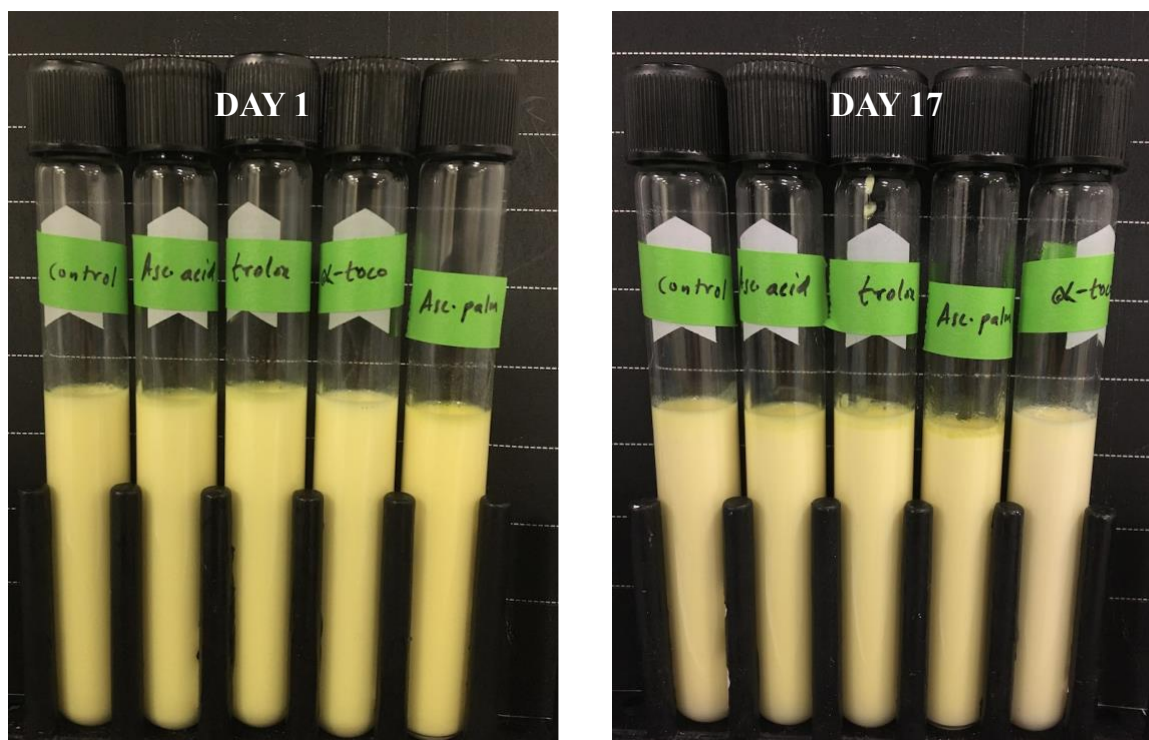


**Figure 26.** Photographs of curcumin-loaded oil-in-water emulsions incorporated with different antioxidants. Emulsions composition: oil 10 wt.%, curcumin 0.01 wt.%, Quillaja saponin extract 1 wt.%, antioxidants (600  $\mu$ M), and rest phosphate buffer (pH 7.0, 5 mM).

The instrumental analysis of color revealed minute differences in color characteristics. As shown in **Figure 27. A**, the yellowness ( $b^*$ ) of all emulsions was quantitatively similar except for the ascorbyl palmitate emulsion for which the  $b^*$  value was slightly lower. When stored at 55 °C, the drop in yellowness followed a higher rate during the initial period and it became slower eventually later in the storage. The visual analysis was confirmed by colorimetry study which showed that color fading in the  $\alpha$ -tocopherol emulsion was the highest followed by the control. Emulsions containing ascorbic acid, Trolox, and ascorbyl palmitate incurred lower  $b^*$  reduction at the end of storage (**Figure 27. B**) with retention of 89.5, 89.8, and 88.9% respectively. While the

extent of yellowness retention in the control and  $\alpha$ -tocopherol emulsion was 76.7 and 72.7% respectively. As color coordinates measured in this analysis result due to exposure to light in a wide visible spectrum range (400-700 nm), lowering in  $b^*$  value could only suggest possible degradation of curcumin in emulsions. To specifically quantify the amount of curcumin lost during storage, a spectrophotometric analysis was done as explained below.

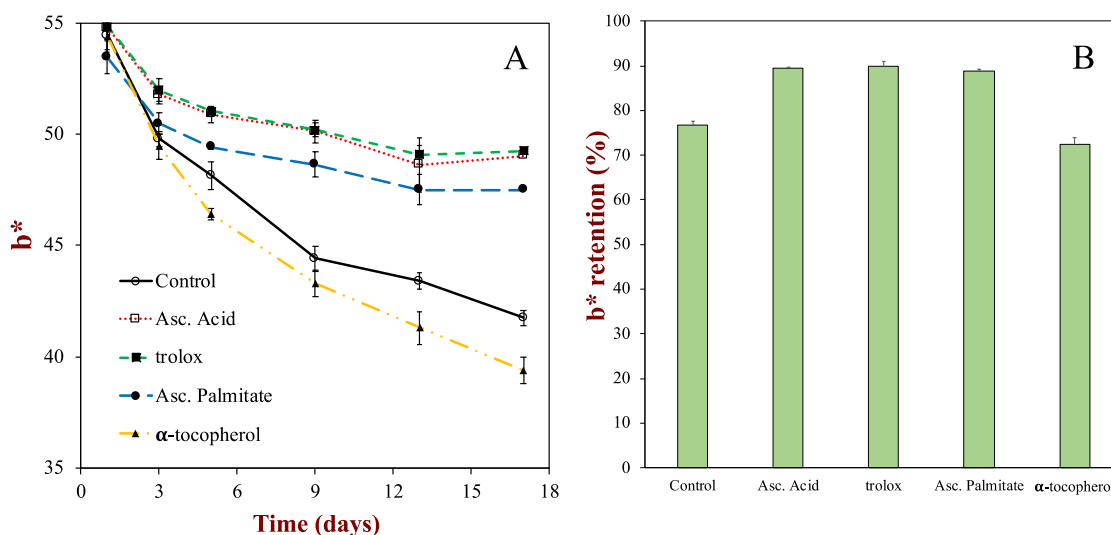


**Figure 27.** Impact of antioxidant type on change (A) and retention (B) in tristimulus color coordinate ( $b^*$ ) of curcumin-loaded oil-in-water emulsions during storage at pH 7 and 55 °C. Antioxidant concentration, 600  $\mu$ M.

### 5.3.2. Impact of antioxidant type on chemical stability of curcumin

Previously, the degradation of emulsified curcumin has been found to depend on the type of emulsifier used to coat the curcumin-loaded oil droplets. For instance, quillaja saponin-stabilized emulsions exhibited a greater curcumin loss than caseinate-, Tween 80-, or gum arabic-stabilized ones (Mahesh Kharat et al., 2018). This was attributed to several factors including the ability of the saponins to promote peroxidation reactions, as well as the presence of impurities (like metal ions) that could enhance the oxidative or

hydrolytic degradation of curcumin. The food industry, however, has been promoting the use of natural emulsifiers in commercial foods. It is, therefore, important to find strategies to mitigate curcumin degradation when it is used with natural emulsifiers that may promote curcumin degradation. Redox active antioxidants have been shown to inhibit the breakdown of curcumin dispersed within aqueous solutions (Nimiya et al., 2015).

Since curcumin can be distributed amongst oil, water, and interfacial domains in emulsions, we studied the effect of water soluble (ascorbic acid, and Trolox), oil soluble ( $\alpha$ -tocopherol), and amphiphilic (ascorbyl palmitate) antioxidants. It was found that water soluble antioxidants were more effective in protecting curcumin from degradation than interfacial or oil soluble antioxidants (**Figure 28. A**). At the start, all the emulsions contained a fairly similar amount of curcumin: 100  $\mu\text{g}$  curcumin/mL of emulsion, except the ascorbyl palmitate one which contained 96  $\mu\text{g}$  curcumin/ mL of emulsion. According to colorimetric analysis, curcumin degradation occurred rapidly within the control and  $\alpha$ -tocopherol-containing emulsions during the first few days of storage but then degraded slower during the remainder of storage. On the other hand, ascorbic acid-, Trolox-, and ascorbyl palmitate-containing emulsions followed a slower curcumin loss in the later stages of storage. This result clearly highlights the importance of antioxidant location on their efficacy to protect curcumin from degradation.

Previous studies have shown that curcumin is highly resistant to degradation when dissolved in oil, but degrades relatively quickly when dissolved in aqueous solutions, especially under neutral or alkaline conditions (Kharat et al., 2019). This result suggests that curcumin degradation mainly occurs in the aqueous phase of oil-in-water

emulsions. It should be noted that even though curcumin is a relatively hydrophobic molecule ( $\text{Log}P \approx 3$ ), a fraction of it will be located within the aqueous phase of an oil-in-water emulsion. Moreover, curcumin molecules close to the surfaces of the lipid droplets will also be in proximity to the surrounding aqueous phase. The curcumin molecules surrounded by, or close to, water molecules may therefore be more susceptible to degradation. This phenomenon would explain why higher amounts of curcumin (82.2 and 82.6%) remained in the emulsions containing ascorbic acid and Trolox, because these two antioxidants were mainly located within the aqueous phase and could therefore protect the curcumin more effectively (**Figure 28. B**).

Ascorbyl palmitate is a surface-active antioxidant because it contains a hydrophobic palmitate group that prefers being surrounded by oil phase and a hydrophilic ascorbate group that prefers to be surrounded by aqueous phase. The antioxidant group on ascorbate palmitate is similar to that of ascorbic acid, and therefore it might be expected to exhibit a similar antioxidant activity if it is located in the region where oxidation occurs. Curcumin retention in the ascorbyl palmitate-containing emulsions was around 79.5%, which was only slightly lower than that of the water-soluble antioxidant-containing emulsions (**Figure 28. B**). This result suggests that curcumin degradation may have occurred within the aqueous phase, but close to the oil droplet interface, which is consistent with studies that have shown that degradation occurs more quickly in emulsions with a higher surface area (Zou et al., 2015).



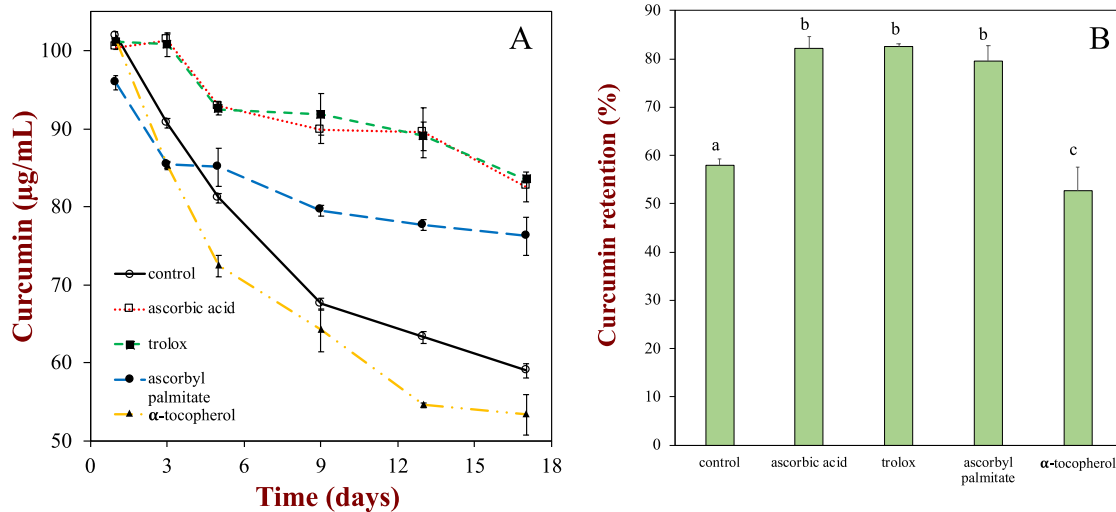


**Figure 28.** Impact of antioxidant type on change (A) and retention (B) in curcumin concentration of oil-in-water emulsions during storage at pH 7 and 55 °C. Antioxidant concentration, 600  $\mu\text{M}$

Oxidative degradation of curcumin is considered to have some similarities to lipid oxidation, where hydrogen is first abstracted from the phenolic group to form a phenolic radical before oxygen addition (O. N. Gordon et al., 2015; Nimiya et al., 2015). Studies have shown that  $\alpha$ -tocopherol can act as a prooxidant, especially when used without co-antioxidants (Kontush, Finckh, Karten, Kohlschutter, & Beisiegel, 1996). Under such conditions, singlet-oxygen can oxidize tocopherol to a tocopheroxyl radical that can then abstract hydrogen from the phenolic group in curcumin and promote its degradation (Combs & McClung, 2017). Additionally, hydrophobic  $\alpha$ -tocopherol molecules are primarily located within the oil droplets where curcumin is already relatively stable to chemical degradation, and hence it is not very effective as an antioxidant in this kind of system.

### 5.3.3. Impact of antioxidant concentration on chemical stability of curcumin

After studying the effectiveness of various antioxidants, we also considered the effect of antioxidant concentration on the degradation of curcumin. We decided to carry out this experiment using ascorbic acid as it is naturally found in many foods, and it is generally recognized as safe (GRAS) by the USDA for addition in numerous food and beverage products. The amount of curcumin used was about 100 µg/mL of emulsion at the start of the experiment. In all emulsions, there was a rapid loss of curcumin during the initial storage period, followed by a more gradual loss at later times (**Figure 29. A**). The rate of curcumin degradation decreased as the ascorbic acid concentration in the emulsions increased. As shown in **Figure 29. B**, curcumin retention at the end of the experiment decreased in the order: AA, 600 µM (82.2%) ~ AA, 300 µM (82.1%) > AA, 100 µM (71.1%) ~ AA, 50 µM (71.4%) > AA, 15 µM (64.3%) > control (57.9%). Previous *in vitro* studies have reported that ascorbic acid was effective at protecting curcumin from degradation in aqueous solutions (Nimiya et al., 2015). Presumably, increasing the antioxidant concentration enhances its protective effects by scavenging more free radicals that initiate curcumin degradation or by donating more protons to the curcumin radical to regenerate curcumin. This effect, however, reached a plateau after which adding more antioxidant did not increase curcumin retention. For instance, the final curcumin concentration in emulsions with 300 and 600 µM ascorbic acid was  $83.0 \pm 0.6$  µg/ mL and  $82.6 \pm 1.9$  µg/ mL, respectively.

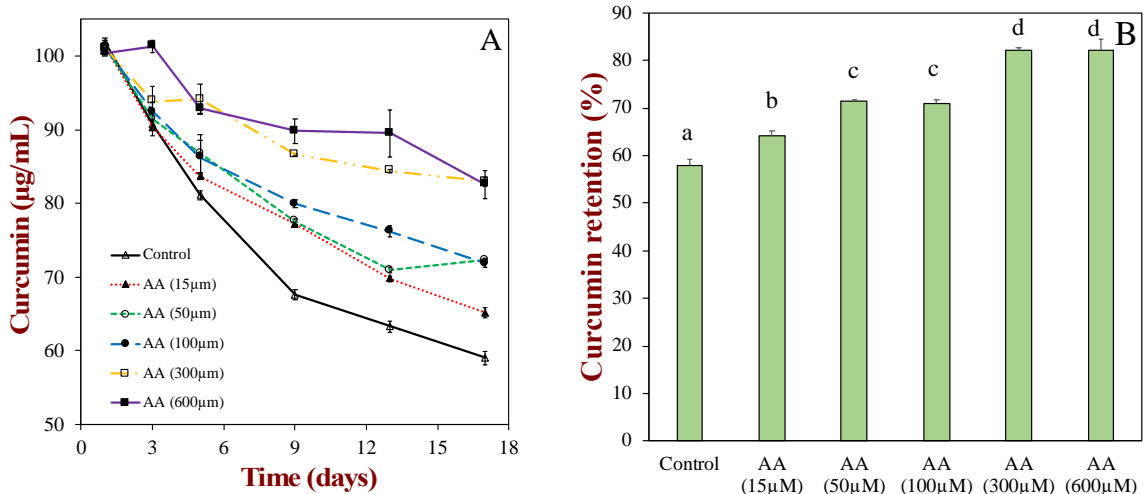


**Figure 29.** Impact of antioxidant concentration on curcumin concentration (A) and retention (B) in oil-in-water emulsions during storage at pH 7 and 55 °C.

### 5.3.4. Impact of antioxidant addition on physical stability of curcumin-loaded emulsion

The particle size characteristics of the curcumin-enriched emulsions were similar to those of the corresponding blank emulsions, indicating that the incorporation of curcumin into the oil phase did not influence droplet formation during homogenization (data not shown). As shown in **Figure 30. A**, the droplets were relatively smaller (~ 0.1 µm) in the control emulsion, as well as in all antioxidant-containing emulsions. This suggests that quillaja saponins, which is as a natural plant-based emulsifier, has comparable performance to synthetic polysorbates and animal-based milk proteins (Uluata, McClements, & Decker, 2015). The mean droplet diameter of the ascorbic acid- and Trolox-containing emulsions was slightly less than the others. This suggests that these water-soluble surfactants may have been able to enhance droplet disruption during homogenization or prevent droplet flocculation after homogenization. For instance, the presence of more ions in the solution may have decreased the thickness of the interfacial

double layer. As a result, it was easier for negatively charged saponins to approach and adsorb onto the oil-water interface (W. J. Wu, Hu, Guo, Yan, Chen, & Cheng, 2015). Earlier reports have suggested similar results where addition of salts enhanced the adsorption of anionic surfactants (Rao & He, 2006). Moreover, a strong negative charge was generated at the interface at pH 7.0 due to the adsorbed anionic saponin molecules ( $pK_a \sim 3.25$ ), which may have kept the oil droplets from aggregating (**Figure 30. B**).

The  $\zeta$ -potentials for the control, ascorbic acid, Trolox, ascorbyl palmitate, and  $\alpha$ -tocopherol emulsions were:  $-48.2 \pm 3.2$ ,  $-48.7 \pm 2.2$ ,  $-49.6 \pm 2.9$ ,  $-55.7 \pm 2.3$ , and  $-49.3 \pm 2.5$  mV, respectively. The significantly higher negative charge for the emulsion containing ascorbyl palmitate is consistent with its adsorption to the droplet surfaces in the form of an ascorbate ion. After 17 days of storage at 55 °C, the surface-weighted droplet diameter did not change significantly except for the emulsions containing the water-soluble antioxidants. The surface potential of the oil droplets become more strongly negative after storage, which may have been due to the formation of some surface-active reaction products.

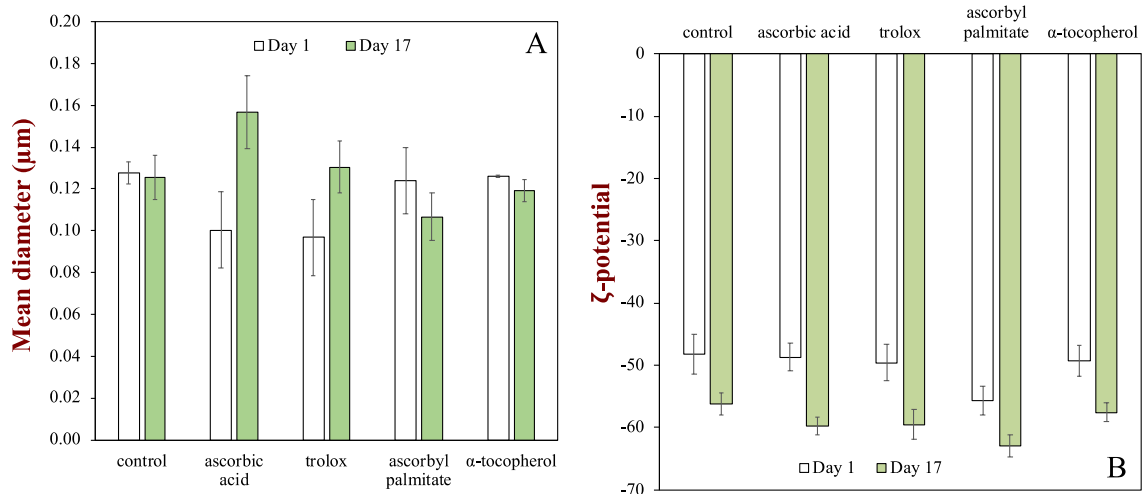


**Figure 30.** Effect of antioxidant type (A) and ascorbic acid concentration (B) on the mean droplet diameter ( $D_{32}$ ) of MCT oil-in-water emulsions produced using a high-pressure homogenizer (microfluidizer).

### 5.3.5. Microstructure analysis

Changes in the emulsion droplet microstructure during storage were also monitored using confocal microscopy (**Figure 31**). All emulsions consisted of small oil droplets uniformly distributed throughout the images. Green fluorescence staining confirmed that most of the curcumin was encapsulated inside the oil droplets. At the end of storage, bigger droplets were observed in all the emulsions confirming the occurrence of coalescence. Coalescence may have been promoted because droplet-droplet collisions are more frequent at higher storage temperatures (55 °C) due to the decrease in viscosity. The intensity of the green color was lower in the control and ascorbyl palmitate-emulsions after storage, which suggests there was less curcumin present, thereby agreeing with the spectrophotometric studies (**Figure 28**).

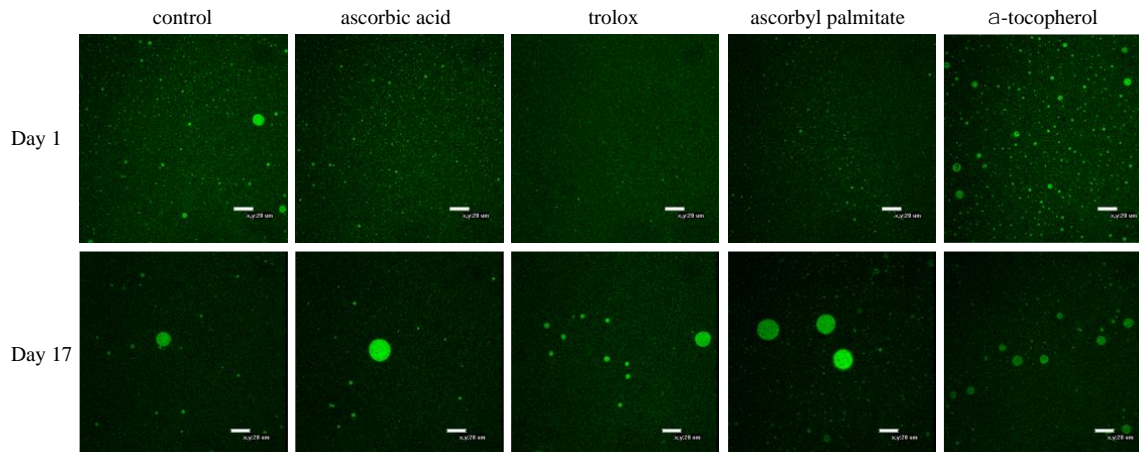


**Figure 31.** Micrographs of curcumin-loaded emulsions added without and with different antioxidants at Day 1 and Day 17 (pH 7, 55 °C). Scale bars represent 20  $\mu\text{m}$ .

## 5.4 Conclusions

In summary, this study showed that antioxidants can be utilized to improve the chemical stability of curcumin in oil-in-water emulsions. The type and amount of antioxidant used impacted the rate and extent of curcumin degradation. This information may be helpful for developing emulsion-based delivery systems for curcumin that could be used in foods, supplements, or pharmaceutical products. Water-soluble antioxidants, ascorbic acid and Trolox, were highly effective as they could suppress oxidative degradation of curcumin in the aqueous phase. Ascorbic acid may be the best choice for commercial applications because it is already naturally present in many foods or can be added as a label-friendly ingredient. Furthermore, our study showed that an antioxidant concentration of 300  $\mu\text{M}$  or more may be required for maximum curcumin stabilization. On the other hand, oil soluble  $\alpha$ -tocopherol was the least effective in protecting curcumin and hence its utilization may not be beneficial.

**CHAPTER 6**

**FABRICATION AND CHARACTERIZATION OF NANOSTRUCTURED LIPID  
CARRIERS (NLC) USING A PLANT-BASED EMULSIFIER: QUILLAJA  
SAPONINS**

**6.1. Introduction**

In past chapters, we studied use of nanoemulsions to encapsulate and stabilize curcumin. Nanoemulsions can be used to deliver both hydrophilic (water-soluble) and hydrophobic (oil-soluble) bioactives by dispersing them in either the continuous or dispersed phases, respectively. Their rheological properties can be manipulated by changing their composition (fat content, salts, thickeners) and microstructure (droplet size). Also, their optical properties can be manipulated from clear to opaque by controlling the droplet size and concentration. Nanoemulsions also tend to have good long-term stability because the small droplet size reduces the tendency for gravitational separation and aggregation to occur. The small size of the lipid droplets in nanoemulsions can be used to increase the oral bioavailability of encapsulated hydrophobic bioactives (McClements & Xiao, 2012; Silva, Cerqueira, & Vicente, 2012). Another advantage of nanoemulsions is that they can be produced economically on a large scale using conventional processing methods such as high-pressure homogenization and microfluidization. Moreover, nanoemulsions can be simply incorporated into a broad range of foods, including beverages, creamers, sauces, dressings, and desserts.

Despite their various advantages, there are some drawbacks to using nanoemulsions for encapsulation and delivery of bioactive agents. In particular, their

small size, high specific surface area, and fluid interior make it difficult to protect encapsulated components from chemical degradation induced by components within the surrounding aqueous phase or to control their release profile (**Figure 32**) (McClements, Decker, & Weiss, 2007). For example,  $\beta$ -carotene and curcumin were shown to undergo chemical degradation in nanoemulsions during storage (Mahesh Kharat et al., 2018; Yuan, Gao, Zhao, & Mao, 2008). In principle, some of these disadvantages can be overcome by crystallizing the lipid phase inside the droplets to create SLNs (Thrandur Helgason, Salminen, Kristbergsson, McClements, & Weiss, 2015; Salminen et al., 2019). SLNs have a similar structure to nanoemulsions but the lipid particles are completely solidified at ambient temperature (Salminen, Gommel, Leuenberger, & Weiss, 2016; Santos, Ribeiro, & Santana, 2019). It has been hypothesized that crystallization of the lipid phase would increase the stability of the lipid droplets to coalescence, enhance the stability of the encapsulated bioactives to chemical degradation, and lead to slower release profiles (McClements, 2005; Salminen et al., 2016).

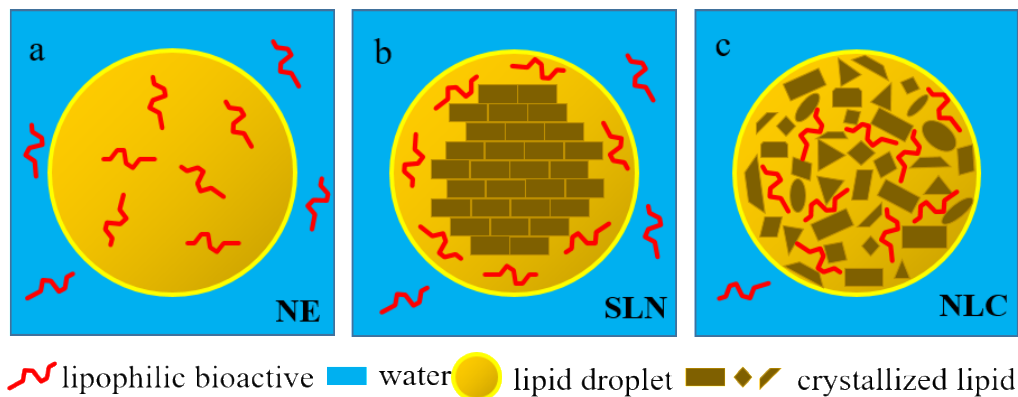


**Figure 32.** Potential loss of bioactive agents by simple diffusion from liquid oil droplets in nanoemulsions (a) or expulsion from homogeneous crystal matrices in solid lipid nanoparticles (b). Potential entrapment of bioactives in heterogeneous crystal matrix in nanostructured lipid carriers (c). Modified from (Müller et al., 2002)



In practice, however, these beneficial attributes of SLNs may not be realized (Weiss et al., 2008). When the oil droplets in a hot nanoemulsion are cooled during the formation of a SLN, the lipid phase can form a highly regular crystalline phase that can cause the lipid nanoparticles to change their morphology from spherical to irregular. As a result, there is an increase in the surface area of the lipid nanoparticles, which can promote extensive aggregation because some hydrophobic patches are exposed (T. Helgason, Awad, Kristbergsson, McClements, & Weiss, 2009). Moreover, the highly ordered structure of the crystals within the solidified lipid nanoparticles can promote the expulsion of the bioactives (Das, Ng, & Tan, 2012), which makes them more prone to chemical degradation (Qian, Decker, Xiao, & McClements, 2013). Changes in particle morphology and bioactive expulsion are often a result of a polymorphic transition of the lipid phase, from the less ordered  $\alpha$ -form, to the more ordered  $\beta$ -form (Mehnert & Mäder, 2001; Salminen et al., 2016).

Another kind of colloidal delivery system, nanostructured lipid carriers (NLCs), was developed by the pharmaceutical industry to overcome the shortcomings of both nanoemulsions and SLNs (Santos et al., 2019). NLCs are formulated from fats that have a broad melting range, which leads to the formation of a solidified lipid phase containing imperfections (**Figure 32**) (Muller, Radtke, & Wissing, 2002). The more irregular packing of the lipid molecules prevents particle morphology changes and bioactive expulsion. Thus, NLCs are able to overcome some of the disadvantages of nanoemulsions and SLNs (Müller et al., 2002). For example, it has been shown that the degradation of  $\beta$ -carotene was only about 47.3% in NLCs but 94.8% in nanoemulsions (Zhang, Hayes, Chen, & Zhong, 2013). Another recent study also showed that NLCs could be used to

effectively encapsulate and protect  $\beta$ -carotene (Pezeshki et al., 2019). In another study, it was found that the bioaccessibility of encapsulated quercetin in NLCs (52.7%) was only slightly lower than that in nanoemulsions (58.4%), but considerably higher than that in SLNs (39.7%) (Aditya et al., 2014). Food-grade NLCs have also been developed to encapsulate various other hydrophobic nutraceuticals and vitamins (Babazadeh, Ghanbarzadeh, & Hamishehkar, 2016; Karimi, Ghanbarzadeh, Hamishehkar, Mehramuz, & Kafil, 2018; Mohammadi, Pezeshki, Abbasi, Ghanbarzadeh, & Hamishehkar, 2017; Seo, Lee, Chun, Park, Lee, & Kim, 2019). Recently, the fabrication, characterization, and application of NLCs in foods has been reviewed (Tamjidi et al., 2013).

The objective of the current research was to examine the feasibility of formulating food-grade NLCs using hydrogenated vegetable oil as a lipid phase and quillaja saponin as a natural emulsifier (Reichert, Salminen, & Weiss, 2019). Unlike partially hydrogenated oils (PHOs), fully hydrogenated oils contain a negligible amount of trans fats. Moreover, since they are comprised of a range of fatty acids with different melting points, we hypothesize that they are excellent candidates to fabricate stable NLCs that could replace delivery systems fabricated from PHOs. These NLCs may therefore be useful for application in functional foods and beverages.

## **6.2 Materials and methods**

### **6.2.1 Materials**

Fully hydrogenated oils (coconut, HCO; cottonseed, HCtO; palm, HPO; palm-kernel, HPKO; and soybean, HSO) were a gift from Cargill (Charlotte, NC). The major fatty acids present in HSO, which was used to assemble the NLCs, were: C<sub>16:0</sub>, 11.9%;

C<sub>18:0</sub>, 85.8%; C<sub>18:1</sub>, 0.4%; and C<sub>20:0</sub>, 0.6%. Sodium hydroxide (NaOH), sodium phosphate anhydrous dibasic, and sodium phosphate monobasic were obtained from Fisher Scientific (Fair Lawn, NJ). Hydrochloric acid (HCl) was purchased from the Sigma-Aldrich Company (St. Louis, MO). Q-Naturale 200® (QN), an extract from *Quillaja Saponaria*, was obtained from Ingredion Inc. (Westchester, IL). The manufacturer reported that this ingredient had a saponin content between 10- and 30 wt. %. All solvents and reagents were of analytical grade. Deionized water obtained from a water purification system (Nanopure Infinity, Barnstaeas International, Dubuque, IA) was used for all the experiments.

### **6.2.2. Differential scanning calorimetry (DSC)**

The thermal behavior of the various fats was characterized using DSC (Q100, TA Instruments, New Castle, DE). A small amount (~ 5 mg) of sample was weighed in an aluminum pan and then sealed hermetically with an aluminum lid. A hermetically sealed empty pan was used as a reference. The heating and cooling rate employed were both 10 °C/min. The onset temperatures of crystallization and melting of the fat phase were determined using the instrument software (TA Universal Analysis 2000).

### **6.2.3 Preparation of NLC**

Quillaja saponin (emulsifier) was filtered through Whatman 41 paper to remove any insoluble matter. An aqueous phase was then prepared by mixing the filtered saponin with phosphate buffer (10 mM, pH 7.0) and then heating to 75 °C with continuous stirring (75 rpm). The oil phase consisted of completely hydrogenated soybean oil (30 wt. %)

which was melted prior to use. The samples were maintained at a hot temperature throughout the homogenization process to avoid fat phase crystallization. First, a coarse emulsion was prepared by adding the heated aqueous phase to the heated melted fat phase and then blending for 2 min using a hand-held mixer (M133/1281-0, Biospec Products, Inc., ESGC, Switzerland). The sample was maintained at 75 °C during mixing to avoid fat crystallization. The hot coarse emulsion (75 °C) was then passed through a single-channel microfluidizer (M110.L, Microfluidics, Newton, MA) under a pressure of 12,000 psi to obtain a nanoemulsion. The internal surfaces of the microfluidizer were brought to the required temperature by passing hot water through the instrument before introducing the coarse emulsion. The temperature of the hot nanoemulsion leaving the microfluidizer was around 63 °C, which was still well above the crystallization point of the emulsified oil phase. Finally, the NLCs were obtained by cooling the hot nanoemulsion.

The hot microfluidization process was optimized by examining the impact of a number of the operating parameters on nanoemulsion formation:

1. *Effect of number of passes*: The nanoemulsion obtained after the first pass was reheated to 75 °C and then passed through the microfluidizer again.
2. *Effect of cooling rate and stirring*: The hot nanoemulsion obtained after one pass was cooled to 10 °C with varying cooling rates: fast (10 °C/min, using an ice bath), moderate (5 °C/min, using a water bath), and slow (1 °C/min, first by natural air-cooling and then using cold water). The effect of stirring was examined by applying no stirring or stirring (75 rpm) conditions to the nanoemulsions during the cooling process.

3. *Effect of emulsifier concentration*: This was studied to find the optimum emulsifier concentration to form relatively small and stable lipid nanoparticles during microfluidization. NLCs were therefore prepared with a fixed HSO content (30 wt %) and varying Quillaja saponin content (3, 6, 9, and 12 wt. %). The remainder of the system consisted of phosphate buffer (67, 64, 61, and 58 wt. % respectively).

#### **6.2.4 Droplet size and charge measurements**

The mean particle size and particle size distribution of the NLCs was obtained using a laser diffraction instrument (Mastersizer 3000, Malvern Instruments Ltd., Malvern, Worcestershire, UK). The refractive indices of the aqueous and lipid phases used in data interpretation were 1.33, and 1.60, respectively and the absorption coefficient was assumed to be 0.001. Phosphate buffer (10 mM, pH 7.0) was used as a dispersant to avoid multiple scattering effects. NLC samples were thoroughly mixed by inverting the container a few times and then added to the buffer solution to achieve a laser obscuration value of around 4.5. The particle size was reported as the volume-weighted mean diameter ( $D_{43}$ ) as well as Sauter mean diameter ( $D_{32}$ ).

The  $\zeta$ -potential of the particles in a colloidal dispersion provides an indication of their electrical surface potential. The  $\zeta$ -potential of the particles in the NLC suspensions was measured using a laser Doppler micro-electrophoresis technique (Zetasizer Nano ZS series, Malvern Instruments Ltd. Worcestershire, UK). Samples were diluted (2000 $\times$ ) with phosphate buffer (10 mM, pH 7.0) to avoid multiple scattering.

### 6.2.5. Thermal analysis of NLC and estimation of solid fat content

The melting and crystallization of the emulsified lipid particles within the NLC suspensions was studied using the DSC method (described in section 5.2.2. ). The solid fat content (SFC) *versus* temperature profile of the NLCs was calculated from the relative area under the heat flow *versus* temperature profile. The SFC in the lipid phase ( $\phi$ ) was calculated as a function of temperature (T) using the following expression:

$$\phi(T) = \frac{\int_{T_1}^T Q(T)dT}{\int_{T_1}^{T_2} Q(T)dT}$$

Here,  $Q(T)$  is the heat released at temperature  $T$  as a result of the phase transition, and  $T_1$  and  $T_2$  are the temperatures at which crystallization begins and ends respectively (McClements, Dungan, German, Simoneau, & Kinsella, 1993).

### 6.2.6. Turbidity measurements

The turbidity of a colloidal dispersion depends on the refractive index of the particles and can therefore be used to provide information about changes in the physical state of lipid nanoparticles: solid fat has a higher refractive index than liquid oil. To study this, a quartz cuvette containing diluted NLC (6% QN) sample was heated in a cell holder, and the turbidity (at 600 nm) was recorded using a spectrophotometer (Cary 100 UV–Vis, Agilent Technologies) during heating and cooling cycles carried out at a rate of 10 °C min<sup>-1</sup>.

### **6.2.7. Rheology analysis**

The tendency for lipid nanoparticles to aggregate in colloidal dispersions can be assessed by measuring changes in the rheological properties of the systems. For this reason, the shear viscosity of the NLC suspensions was characterized using a dynamic shear rheometer equipped with a cup-and-bob measurement cell (Kinexus Rheometer, Malvern Instruments Ltd., MA, U.S.A.). A shear rate from 0.1 to 100 s<sup>-1</sup> was applied to samples incubated at 25 °C. The instrumental software (Kinexus rSpace, version 1.30, Malvern Instruments Ltd., MA) was used to control the measurement parameters and acquire the data. The apparent shear viscosity results were reported at 10 s<sup>-1</sup>.

### **6.2.8. Color measurements and physical appearance**

The tristimulus color coordinates of the NLC suspensions were determined using a benchtop instrumental colorimeter (ColorFlez EZ, HunterLab, Reston, VA). An aliquot of NLC suspension (~ 10 mL) was placed in a transparent disposable petri dish and the sample was exposed to an illuminant/observer combination of D65/10. A black cup was used as a background to obtain the  $L^*$  values (lightness) of the samples.

### **6.2.9. Aggregation stability**

The stability of the NLCs to aggregation was studied at a number of selected temperatures where the particles were believed to have different physical states, which was identified by DSC analysis. After preparation, the final nanoemulsion was cooled to specific temperatures at which the lipid nanoparticles were liquid (40 °C), partially crystalline (32–36 °C), or fully crystalline (20 °C). NLC suspensions were stirred

(75 rpm) continuously at these temperatures for 24 h and then the particle size was analyzed as described in section 2.4.

#### **6.2.10. Transmission electron microscopy (TEM)**

NLC samples were diluted with Milli-Q water at a ratio of 1:5000, stained with uranyl acetate, and then dried on carbon film (CF400-Cu-UL, Electron Microscopy Science, Hatfield, PA). Their structure was then examined using a TEM instrument (JEOL JEM-2200FS).

#### **6.2.11. Temperature-dependent optical microscopy analysis**

The temperature-dependence of the phase transitions in the NLCs were studied using optical microscopy. For this, NLC suspensions (30% HSO, 6% QN, 64% phosphate buffer) were formulated from coarse emulsions using a hand-held blender but not passed through the microfluidizer (see Section 5.2.3 ). Microfluidization was not used so that it was possible to obtain lipid particles large enough to observe using optical microscopy. A glass slide containing the diluted sample was placed inside a covered heating stage (Linkam LTS120, Tadworth, Surrey, UK) and equilibrated at 70 °C for 5 min. The temperature was then decreased gradually to 30 °C using a temperature control device (Linkam PE94). After equilibration at specific temperatures, polarized light images were captured on a microscope (Nikon D-Eclipse C1 80i, Nikon, Melville, NY, USA) equipped with a 40× objective lens and 10× eyepiece. Image analysis software (NIS-Elements and EZ-CS1, Nikon, Melville, NY) was used to record the microstructure of the samples.



### 6.2.12. Statistical analysis

Experiments were carried out in replicates (minimum 2). At least two samples were freshly prepared and were measured twice in each replicate. Microsoft Excel was used to calculate the mean and the standard deviations. The significant differences among treatments were evaluated using the Tukey multiple-comparison test at a significance level of  $p \leq 0.05$  (SPSS ver.19, SPSS Inc., Chicago, IL, USA).

## 6.3 Results and discussions

### 6.3.1. Thermal behavior of lipid phase

The crystallization and melting characteristics of a fat depend on its fatty acid composition. Initially, we therefore characterized the thermal behavior of a number of hydrogenated bulk fats to identify the one that had the most appropriate melting/crystallization properties for forming NLCs. The bulk fats examined included hydrogenated soybean oil, palm oil, cottonseed oil, coconut oil, and palm kernel oil: HSO, HPO, HCtO, HCO, and HPKO, respectively. The HSO, HPO, and HCtO all showed fairly similar behavior: there was a single endothermic peak during crystallization and two exothermal peaks during melting (see Appendix: **Figure S8**). Based on previous studies, the crystallization peak observed during cooling was associated with the conversion of the liquid melt into fat crystals in either the  $\alpha$ - and/or  $\beta'$ -polymorphic form (Nelis, Declercle, De Neve, Moens, Dewettinck, & Van der Meeren, 2019). The two melting peaks seen during heating were associated with melting of the  $\alpha/\beta'$ -form crystals (lower temperature) and then melting of the  $\beta$ -form crystals (higher temperature), suggesting that there was a  $\alpha/\beta'$ -to- $\beta$  transformation during

incubation at the lower temperatures. The crystallization and melting peaks were broader for the bulk HCO and HPKO, possibly due to the presence of a wider range of lipids with different melting points, which is in agreement with previous studies (Nassu & Guaraldo Gonçalves, 1999). The enthalpy changes and onset temperatures for the melting and crystallization transitions of the bulk fats obtained from the DSC data are summarized in **Table 9**.

**Table 9.** Enthalpy changes and onset temperatures for the melting and crystallization of hydrogenated bulk fats.

	Melting enthalpy (J/g)	Crystallization enthalpy (J/g)	Onset temperature (°C)	
			Melting	Crystallization
HCO	108	94	16.1	16.1
HCtO	132	120	48.9	46.9
HPKO	100	84	22.3	24.8
HPO	115	119	48.2	44.0
HSO	97	106	51.7	48.7

Ideally, we wanted to use a lipid phase that would remain in the solid state in the NLCs when they were stored at ambient temperature. Secondly, it is better to choose a hydrogenated fat that has high stearic acid content and low concentration of other saturated fats. This is because stearic acid is known to be non-atherogenic (Bonanome & Grundy, 1988) and it does not pose a risk for heart disease when compared to other saturated fatty acids (Hunter, Zhang, & Kris-Etherton, 2010; L. Wang et al., 2003). For these reasons, we used the fully hydrogenated soybean oil for the remainder of the experiments.

## **6.3.2. Optimizing NLC formation**

### **6.3.2.1. Number of passes through microfluidizer**

A hot oil-in-water nanoemulsion was prepared from the HSO as a template for formation of the NLCs. Ideally, this nanoemulsion should contain small uniform lipid droplets that are stable to aggregation and gravitational separation prior to NLC formation. Initially, we therefore examined the impact of the number of passes of the hot nanoemulsion through the microfluidizer. Previous studies have shown that increasing the number of times a nanoemulsion is passed through a microfluidizer decreases the particle size and polydispersity (Qian & McClements, 2011). We found that there was a decrease in mean particle diameter when the hot nanoemulsion obtained after the first pass was recirculated through the microfluidizer. But, a cream/oil layer was observed at the top of the nanoemulsion after repeated circulation, which was presumably because the relatively high homogenization temperature used (75 °C) promoted droplet coalescence. For this reason, the coarse emulsions were only passed through the microfluidizer once in the remainder of the experiments. Despite this, the nanoemulsions obtained containing relatively small droplet sizes and monomodal particle size distributions, provided sufficient emulsifier was used.

### **6.3.2.2. Cooling rate and stirring conditions**

Another factor expected to impact the formation of stable NLCs was the conditions employed to cool the hot nanoemulsions and promote lipid phase crystallization. The impact of cooling rate and stirring conditions on the formation and stability of the NLCs was therefore examined. We hypothesized that the cooling rate

might impact the stability of the nanoemulsions to partial coalescence. Partial coalescence leads to the formation of clumps of particles because crystals from one droplet penetrate into the liquid region of another droplet, thereby forming a link between them (Fredrick, Walstra, & Dewettinck, 2010). We therefore anticipated that faster cooling would lead to smaller particles being formed in the NLCs because the lipid phase would remain in a partially crystalline state for a shorter time, thereby limiting partial coalescence. We also hypothesized that stirring would increase the collision frequency of the oil droplets during cooling, which would again promote partial coalescence (Fredrick et al., 2010).

In practice, no significant difference was observed in the mean particle diameter of the NLC suspensions (6% QN) when the hot nanoemulsions were cooled at different cooling rates (*i.e.*, slow, moderate, and fast = 1, 5, and 10 °C /min) with or without stirring (Appendix, **Figure S9**). Even so, the NLCs formed by cooling at the moderate rate had slightly smaller mean particle diameters:  $D_{43} = 0.525 \pm 0.017 \mu\text{m}$ . For this reason, NLCs were prepared by cooling at a moderate rate under non-stirring conditions in the remainder of the studies, as these were the most practical and convenient preparation conditions. The reason that cooling conditions had little impact of the stability of the NLCs may have been because the interfacial coating formed around the lipid particles by the quillaja saponin prevented partial coalescence. Indeed, previous studies have shown that certain types of emulsifier are able to prevent the fat crystals from one droplet penetrating into another droplet (Goibier, Lecomte, Leal-Calderon, & Faure, 2017; Thanasukarn, Pongsawatmanit, & McClements, 2004).

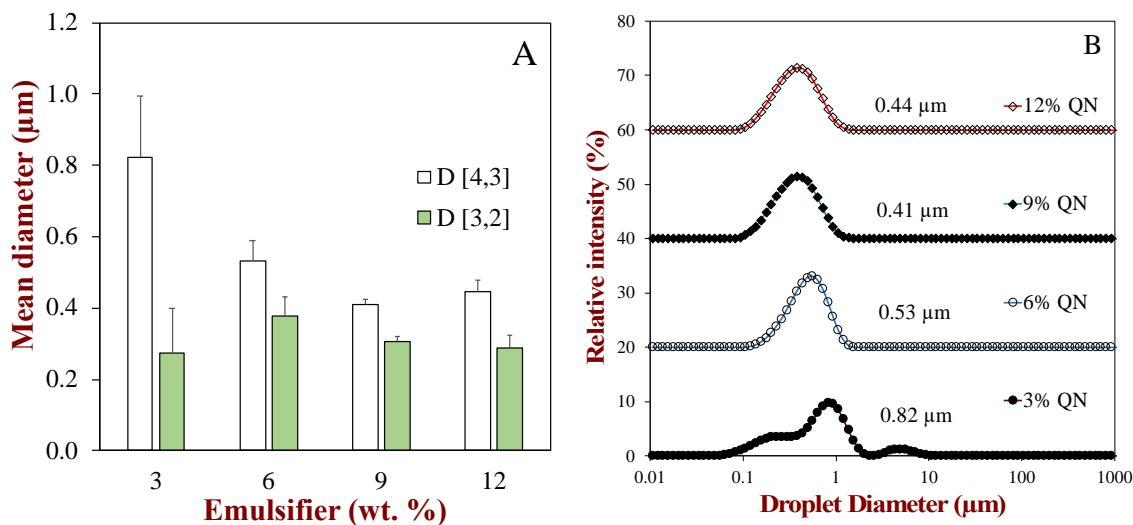


**Figure 33.** Effect of emulsifier concentration on the mean particle diameter (A) and particle size distribution (B) of 30 wt% fully hydrogenated soybean oil-in-water emulsions prepared using a high-pressure homogenizer (microfluidizer).

### 6.3.2.3. Effect of emulsifier concentration on droplet size

The mean particle diameter of the NLCs decreased as the concentration of Quillaja saponin used to prepare them was increased from 3 to 12 wt. % (**Figure 33.A**). The reduction in particle size was greatest (from  $0.82 \pm 0.17$  to  $0.53 \pm 0.06$  μm) when the emulsifier concentration was increased from 3 to 6 wt. %, but then did not change considerably when the emulsifier level was raised further. This suggests that the lipid droplet surfaces were completely covered by emulsifier molecules above this level and that the microfluidizer could not break down the droplets any further.

At the lowest Quillaja saponin concentration used, the particle size distribution was multimodal, which suggests that there was insufficient emulsifier present to cover all the droplets formed inside the microfluidizer. Conversely, at higher emulsifier levels, all the NLCs had monomodal particle size distributions (**Figure 33.B**), which is often an

advantage for commercial applications. The NLC suspension formulated using 6% QN was therefore used for the remainder of the studies because it contained the lowest emulsifier level required to form stable suspensions with small particles.

### **6.3.3. Properties of NLC suspensions**

#### **6.3.3.1. Thermal behavior of NLC**

Knowledge of the thermal behavior of the lipid phase of NLCs is important for optimizing their formation, stability, and functional performance. For this reason, we characterized the thermal properties of the NLCs using both DSC and temperature-scanning spectrophotometry (**Figure 34**). The thermal transitions of the emulsified fat were clearly different from those observed in bulk fat and depended on emulsifier concentration (**Table 9**). Compared to the bulk fat, there was a bigger difference between the onset crystallization and onset melting temperatures for the emulsified fat (**Figure 34.A**). This phenomenon can be explained by the different nucleation mechanisms occurring inside the lipid droplets. During cooling of melted bulk fat, even a small number of impurities can act as nucleation sites that initiate the formation of crystals that spread through the entire volume of the system. As a result, nucleation occurs through a heterogeneous mechanism and the crystallization temperature is relatively high. Conversely, after emulsification, the impurities in the lipid phase are spread throughout a huge number of different lipid droplets and so the probability of finding a nucleus within any particular droplet is very low. In this case, nucleation occurs through a homogeneous mechanism and the crystallization temperature is greatly suppressed *i.e.*, a high degree of supercooling occurs (McClements, 2012). This phenomenon of deep supercooling of

emulsified lipids has been reported in numerous earlier studies (Siva A. Vanapalli, Jirin Palanuwech, & John N. Coupland, 2002).

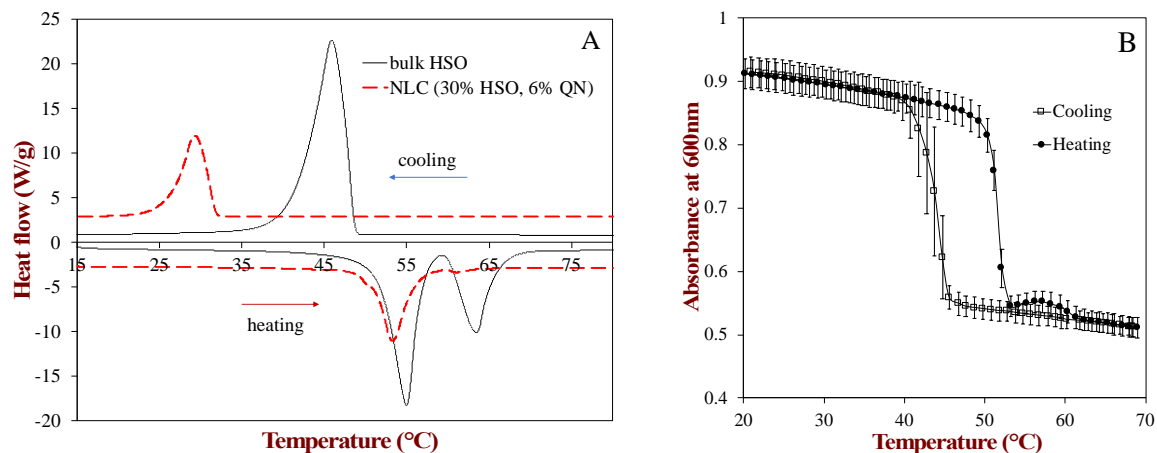


**Figure 34.** DSC profiles of hydrogenated soybean oil (HSO) in bulk form and NLC suspension form (30% HSO, 6% QN) during heating and cooling at a controlled rate of 10 °C min<sup>-1</sup>; (B) Turbidity analysis of the same NLC suspensions.

Interestingly, the emulsified lipids in the NLC suspension exhibited a distinct melting peak around 53 °C and a rather small peak around 61 °C during heating, whereas the bulk fat exhibited two distinct melting peaks at 55 °C and 63 °C. This suggests that the emulsification of the lipids altered their thermal transition behavior. As mentioned earlier, the lower peak is associated with the melting of  $\alpha/\beta'$  crystals, whereas the higher peak is due to melting of  $\beta$  crystals. Consequently, there may have been a reduction in the fraction of  $\beta$  crystals generated inside the lipid droplets compared to within the bulk fat. The slight decrease in the melting temperature for the emulsified lipids can be attributed to a thermodynamic effect: the melting point of a material is known to decrease as the droplet size decreases due to curvature effects (McClements, 2012).

Temperature-scanning spectrophotometry was used to provide additional information about the thermal transitions occurring inside the NLCs during heating and cooling (**Figure 34.B**). The turbidity of a colloidal dispersion depends on the refractive index contrast between the particles and surrounding liquid (Bohren & Huffman, 2008). When a lipid undergoes a liquid-to-solid transition its refractive index increases, which causes more intense light scattering and therefore an increase in turbidity (Linke & Drusch, 2018). Moreover, there may also be changes in the size and shape of the particles after a phase transition (Bunjies, Steiniger, & Richter, 2007), which also causes changes in light scattering and turbidity (Bohren et al., 2008). As a result, turbidity measurements can provide valuable information about the phase transitions occurring inside the particles in colloidal dispersions.

When the NLC suspension was heated from 20 to 50 °C, there was a slight decrease in turbidity, which can be attributed to expansion of the solid lipid particles, which reduces their refractive index (Alvarado, 1995). However, when the NLCs were heated further, there was a steep fall in the turbidity around 50 to 53 °C, which can be attributed to melting of the solid lipid particles. As discussed earlier, the lipid phase would be expected to be in the  $\alpha/\beta'$ -form in the solidified lipid particles, and so this first transition was probably caused by the melting of this polymorphic form. Interestingly, there was a very small peak in the turbidity scan around 58 °C when the NLCs were heated further, which was attributed to the formation and subsequent melting of the  $\beta$ -polymorphic crystalline form. As pointed out previously, a relatively large peak was observed around 53 °C and a small peak around 61 °C in the DSC thermograms (**Figure 34.A**), which supports this hypothesis.



During cooling, the absorbance of the NLC suspensions increased steeply when the temperature fell below about 45 °C, which is indicative of the onset of crystallization, and is fairly similar to the temperature where crystallization was observed by DSC.

The NLCs formulated with different levels of Quillaja saponin exhibited different thermal profiles in the DSC ( **Table 10** and **Figure 35.A**). The solid fat content (SFC) versus temperature profile of the samples was calculated by integration of the heat flow curves measured by DSC during cooling (**Figure 35.B**)

**Table 10.** Comparison of thermal behavior (transition enthalpies and onset temperatures) of NLCs and bulk fats formulated from hydrogenated soybean oil. The NLCs were formulated using different Q-naturale levels

	Melting enthalpy (J/g)	Crystallization enthalpy (J/g)	Onset temperature (°C)	
			Melting	Crystallization
Bulk	97	106	51.7	48.7
3% QN	39	37	51.0	39.0
6% QN	36	40	50.5	34.5
9% QN	30	35	51.8	30.5
12% QN	32	36	50.7	30.5

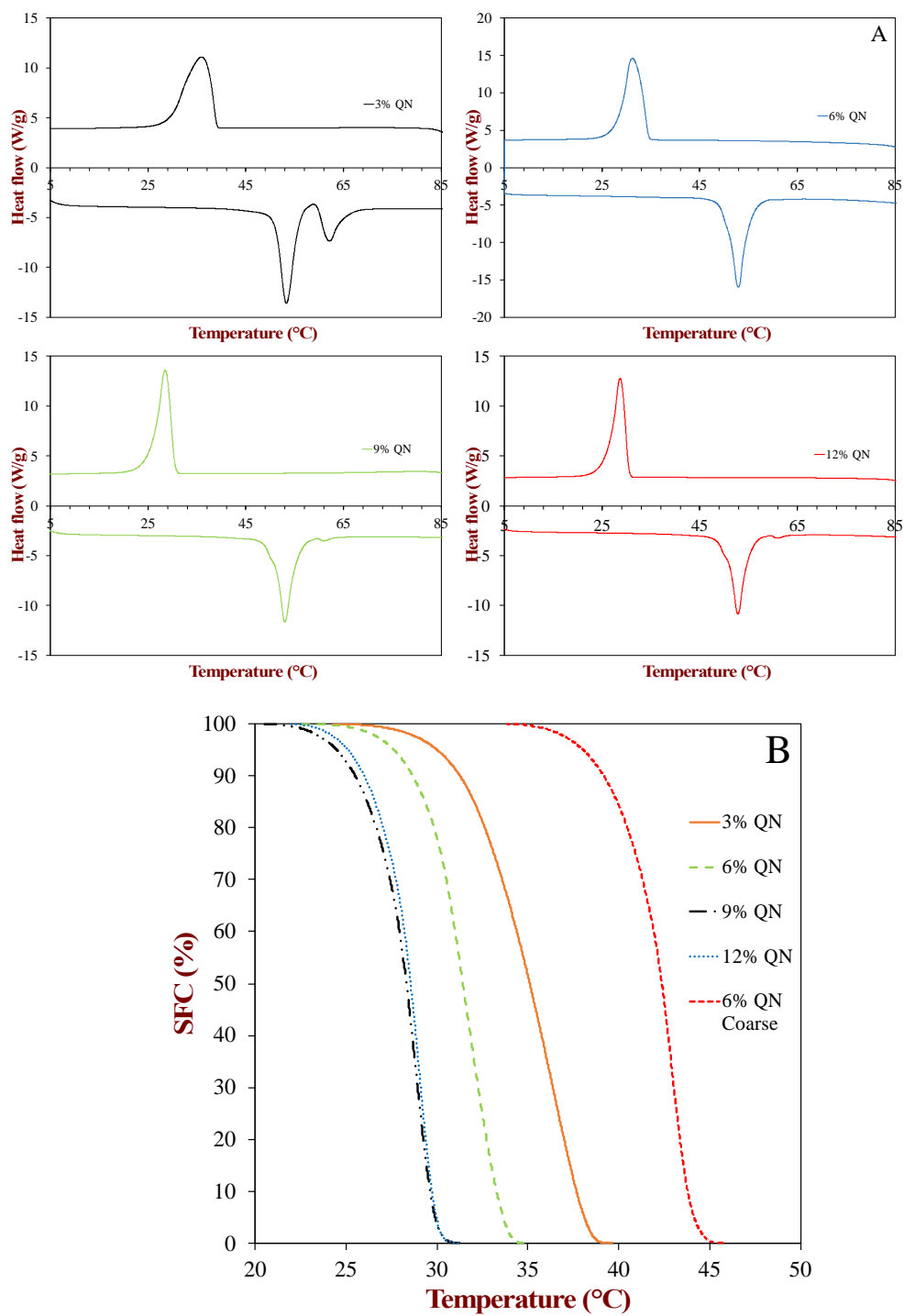


**Figure 35.** DSC profiles (A), and solid fat content as a function of temperature (B) in emulsified HSO (30 wt. %) prepared with varying emulsifier concentrations. Samples were analyzed at a rate of 10 °C min<sup>-1</sup>.

The crystallization temperature decreased with increasing emulsifier concentration, which can at least partly be attributed to the reduction in droplet size. From a thermodynamic point of view, the crystallization point of materials is known to decrease as their droplet size decreases due to changes in the interfacial curvature (McClements, 2012). From a kinetic point of view, the temperature where crystals are first observed may decrease as the droplet size decreases because homogeneous nucleation is more likely for smaller droplets. Other studies have also reported that the crystallization temperature of emulsified fats decreases with decreasing droplet size (McClements et al., 1993).

There were also differences in the melting behavior of the emulsions depending on emulsifier concentration and, therefore, droplet size (**Figure 35**). For the system containing the largest lipid particles (3% QN), two distinct peaks were observed during heating: a relatively large one at 53 °C and a smaller one at 62 °C. This behavior was fairly similar to that observed for the bulk hydrogenated soybean oil. Conversely, for the systems with the smaller lipid particles (6 to 12% QN), a large peak was also observed around 53 °C but a much smaller one was observed at 62 °C. This suggests that the melting behavior of the lipids was different in the smaller droplets, presumably because of their more confined interiors. In particular, it seems like the formation and melting of the  $\beta$ -form of the lipids was suppressed in the NLCs containing the small lipid particles. When the NLC samples were heated and cooled a second time, the crystallization peak did not coincide with that observed in bulk fat, which suggested that they were stable to coalescence and oiling off during the DSC measurements (data not shown).

### 6.3.3.2. Rheology of NLC

The flow behavior of the NLC suspensions was characterized using shear rheology (**Figure 36.A**). For all suspensions, the applied shear stress increased linearly ( $R_2 > 0.999$ ) with increasing shear rate (0.1 to 100  $s^{-1}$ ), which suggested they had ideal (Newtonian) characteristics in the shear range studied. In all samples, the shear viscosity was relatively low ( $< 5$  mP.s), which suggested that extensive droplet flocculation did not occur. The shear viscosity appeared to increase slightly with increasing emulsifier concentration (**Figure 36.B**). This may be because the effective volume of the particles in a colloidal dispersion increased as the droplet size decreased, due to the contribution of the emulsifier layer (McClements, 2015b).

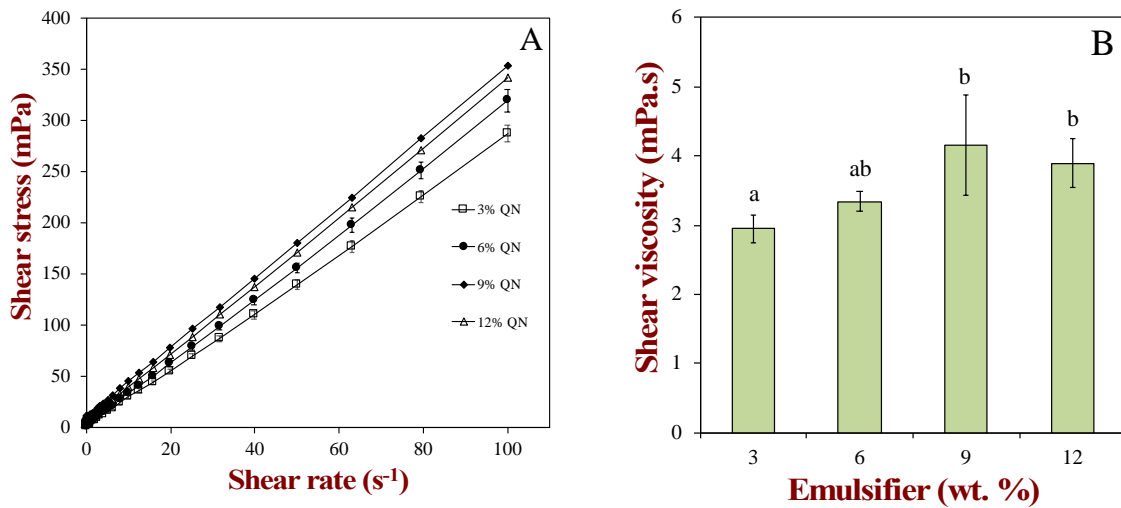


**Figure 36.** Rheological properties of NLC suspensions. (A) Flow behavior studied by measuring shear stress at variable shear rates; (B) Effect of emulsifier concentration on shear viscosity of NLC suspensions.

### 6.3.3.3. Appearance of NLC suspensions

Visually, the NLC suspensions had a uniform milky appearance and no phase separation was observed (**Figure 37**). They therefore looked very similar to conventional

emulsions. Their lightness ( $L^*$ ) decreased with increasing emulsifier concentration while their perceived yellowness increased. This effect was mainly attributed to the brownish color of the Quillaja saponin solution used to formulate the NLCs. These color changes may be important in some food and beverage products because it could negatively impact their desired appearance.

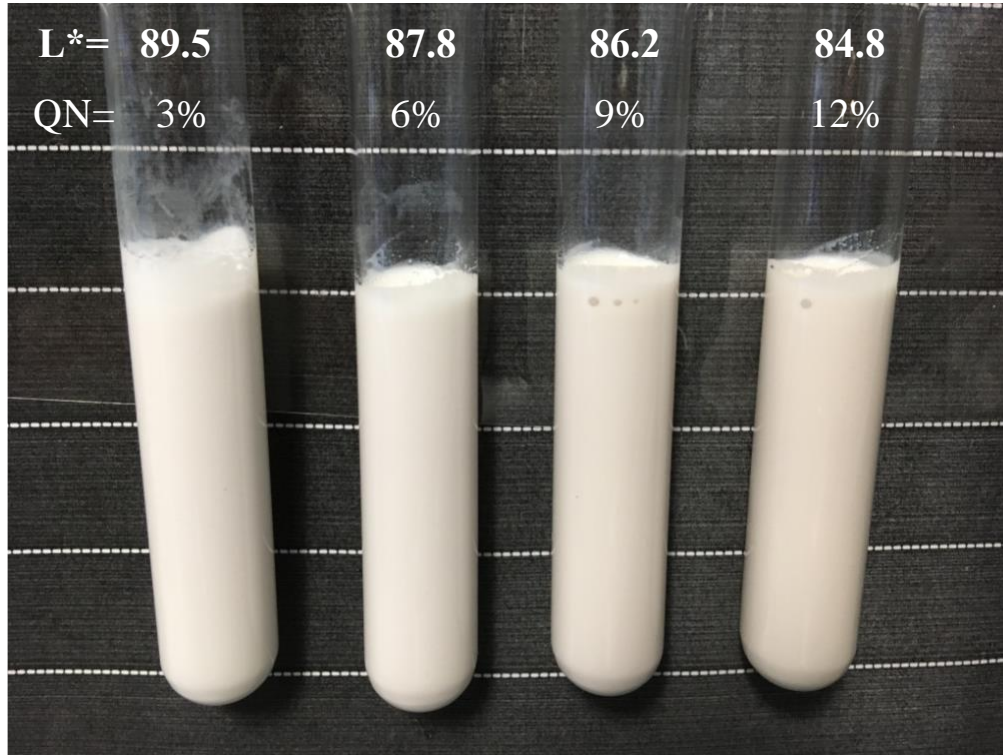


**Figure 37.** Visual appearance of NLC suspensions with QN contents of 3, 6, 9, and 12 wt. % (left to right).  $L^*$  values represent lightness of dispersion.

#### 6.3.3.4. Microstructure of coarse NLCs during thermal transitions

The small particles in conventional NLCs ( $d < 500$  nm) are too small to be seen using conventional optical microscopy. For this reason, we prepared NLCs from coarse emulsions so that we could visualize the changes occurring in the lipid particles during melting and crystallization (**Figure 38**). Polarized light microscopy images showed that

the lipid droplets were spherical at 70 °C and contained no visible crystals (white regions). When these emulsions were cooled using a temperature-controlled microscopy stage, the first evidence of crystal formation inside the droplets was observed at 50 °C. When these systems were cooled to 40 °C and below, there was evidence of many crystalline lipid particles within the emulsions. The crystallization of the lipid phase in oil-in-water emulsions may occur via homogeneous or heterogeneous nucleation mechanisms. Homogeneous nucleation occurs when the lipid droplets are so small that the chance of finding an impurity within a single droplet is infinitesimal. The presence of impurities is important because they act as nucleation sites where subsequent crystal growth can occur. Conversely, heterogeneous nucleation occurs when each lipid droplet is likely to contain one or more impurities. The emulsified lipids in emulsions undergoing homogeneous nucleation typically exhibit a much higher degree of supercooling than bulk oils. This phenomenon is highlighted in the SFS *versus* temperature profiles, which showed that droplet crystallization occurred at a much higher temperature in the coarse emulsions than for any of the nanoemulsions that had been passed through the microfluidizer (**Figure 35.B**).

During heating, some of the crystalline lipid particles in the coarse NLCs melted around 50 °C, as demonstrated by the fact that the number of white dots in the polarized light images decreased (**Figure 38**). Upon further heating, all the lipid particles melted when the temperature exceeded 65 °C. The *Mean Gray Value* (MGV) of the microscopy images was used to provide some information about changes in the fraction of crystalline lipid particles with temperature during heating and cooling. The MGV is the number of pixels with grey values below some critical value divided by the total number of pixels

within the selected area. The MGV was obtained for each image after processing for background thresholding (**Figure 39.A**). As expected, the MGV decreased during heating as more lipid particles melted and increased during cooling as more fat droplets crystallized. The data obtained from polarized light microscopy analysis of the coarse NLC suspensions therefore agrees with that obtained from DSC (**Figure 39.B**).

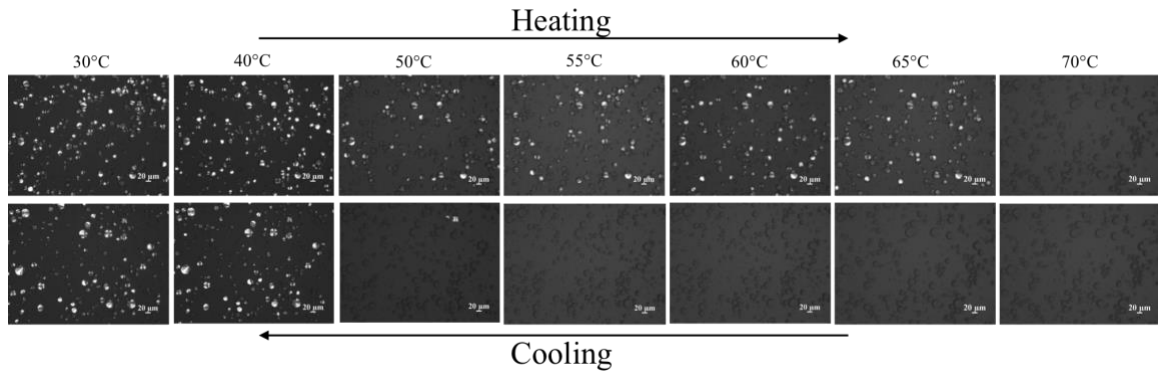


**Figure 38.** Microscopy images of coarse NLC suspensions during heating and cooling on an optical microscopy stage with crossed-polarizers (30% HSO, 6% QN, 64% phosphate buffer).

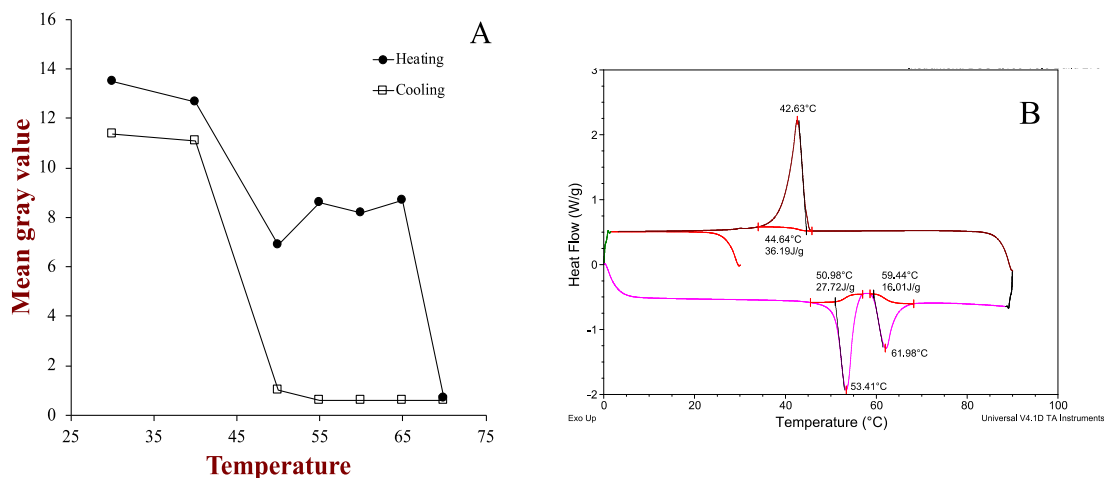


**Figure 39.** Mean Grey Value analysis of optical microscopy images (A) and DSC analysis (B) of coarse NLC (30% HSO, 6% QN, 64% phosphate buffer).

### 6.3.3.5. Transition electron microscopy

The morphology of the lipid nanoparticles within the NLCs produced from oil-in-water nanoemulsions (6% QN) was determined using TEM (**Figure 40**). These images showed that the lipid particles had a roughly spherical appearance, but that they also had some plate-like dark structures at certain locations on their surfaces. We postulated that these platelet structures were small fat crystals adsorbed to the oil-water interface. Previous studies have shown that the appearance of platelets in electron microscopy images depends on their alignment relative to the electron beam (Jores, Mehnert, Drechsler, Bunjes, Johann, & Mäder, 2004). As a result, some platelets can have needle-like structures in the images.



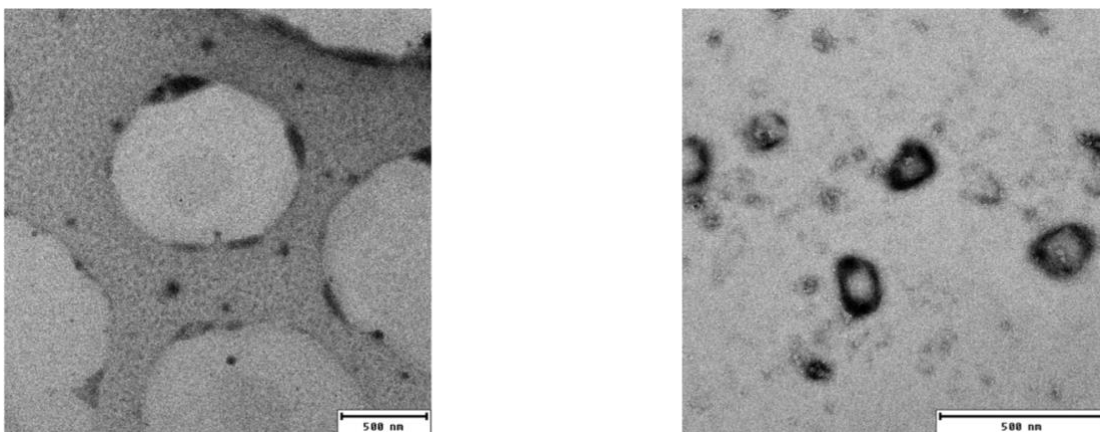


**Figure 40.** Transmission electron microscopy images of NLC suspensions (30% HSO, 6% QN). The scale bar represents 500 nm.

#### **6.3.4. Stability of NLC to thermal stress**

The long-term stability of the NLC suspensions was measured by storing them for one-month at ambient temperature. There was no significant change in the mean particle diameter of the NLCs after 1 month of storage. Also, visible phase separation of the suspensions was not observed at the end of storage. Together, results suggest that the NLCs had good stability to flocculation, coalescence, partial coalescence, and gravitational separation. This was probably because the adsorbed layer of quillaja saponin was effective at increasing the steric and electrostatic repulsion between the lipid particles.

When the NLC (6% QN) suspension was heated and cooled repeatedly in hermetically sealed aluminum pans using the DSC instrument, it was found that both the heating and cooling peaks overlapped each other. Previous studies have shown that the thermal profiles of emulsions change appreciably if they undergo droplet coalescence because this alters the nucleation mechanism (Thanasukarn et al., 2004). Our results therefore indicate that the NLC suspensions were relatively stable to thermal stresses.

When different cooling rates (1, 5, 10, and 20 °C/min) were applied to the NLC (6% QN) suspensions, the onset crystallization temperature decreased slightly as the cooling rate was reduced (**Figure S10**). For instance, the onset crystallization temperatures were 33.5, 32.0, 31.2, and 30.1 °C at cooling rates of 1, 5, 10, 20 °C/min, which may have been due to more supercooling at faster rates. Conversely, the onset melting temperature remained relatively constant ( $50.5 \pm 0.1$  °C) at different heating rates. Overall, the heating and cooling rates did not appear to have a major influence on the thermal characteristics of the NLCs.

Changes in the mean diameter of the particles in the NLC (6% QN) dispersion were also measured during cooling over the temperature range where the liquid-to-solid transition occurred (*i.e.*, 36 to 32 °C). The mean particle diameter remained relatively constant ( $0.50 \pm 0.01$  μm) when the emulsions were stirred for 24 h period at the specified incubation temperatures (**Figure S11**), which suggested that the NLCs were highly stable to aggregation. Earlier studies have reported droplet flocculation and coalescence can occur in partially crystalline fat droplets (Vanapalli & Coupland, 2001). In our study, the lipid particles in the NLC suspensions had roughly spherical shapes, with no sharp crystals penetrating into the aqueous phase (**Figure 40**). As a result, it would have been more difficult for a crystal from one droplet to penetrate into another droplet (Siva A. Vanapalli et al., 2002). Moreover, the lipid particles were covered by a layer of natural surfactant (Quillaja saponin) that generated a strong electrostatic and steric repulsion between them, thereby preventing them coming close enough for the crystals in one particle to penetrate into another.

## 6.4 Conclusions

This study showed that NLCs could be successfully prepared using nature-derived ingredients. The solidified lipid phase of the NLCs was formulated using fully hydrogenated oils, which are a good alternative to PHOs. Indeed, PHOs recently lost their GRAS status in the USA due to their link to health problems such as heart disease. NLCs fabricated from completely hydrogenated oils have similar appearances and rheological properties as conventional oil-in-water emulsions, which means that they may be used in many of the same products, such as beverages, creams, sauces, dressings, desserts, and soups.

We showed that stable NLC suspensions containing small particles could be formulated by optimizing the thermal behavior of the hydrogenated oil, homogenization conditions (such as number of passes and emulsifier level), as well as the cooling conditions. In future studies, it will be useful to assess the ability of NLCs to encapsulate bioactive components, as well as to establish their stability in real food products and their behavior under gastrointestinal conditions. Moreover, it will be important to compare their performance with alternative colloidal delivery systems, such as nanoemulsions and solid lipid nanoparticles.

## CHAPTER 7

### CONCLUSION AND FUTURE STUDIES

Our study showed that the chemical stability of curcumin depends greatly on physical factors such as temperature, and chemical factors like pH and the molecular environment. Its stability could be significantly improved by encapsulating in oil droplets that effectively protect curcumin from oxidation and hydrolysis. We showed that oil-in-water emulsion could significantly prevent curcumin from chemical degradation. It was found that factors like emulsifier type affect curcumin stability, and droplet surface area plays an important role in modulating chemical alteration in curcumin that is encapsulated in oil-in-water emulsion. We also found that antioxidants could efficiently control the rate and extent of curcumin degradation in emulsions especially when the antioxidants are water soluble. Another strategy of chemically protecting curcumin is to control the interfacial phenomena such as diffusion and molecular transport. For this purpose, we modified the properties of the lipid phase and successfully optimized the process of fabricating nanostructured lipid carriers using completely hydrogenated soybean oil and saponins.

In the future studies, it may be interesting to encapsulate curcumin in nanostructured lipid carriers and compare their performance with oil-in-water emulsions and solid-lipid-nanoparticles. It will also be important to test these delivery systems for their relative bioavailability *in-vivo* models and possibly in human subjects.

**APPENDIX**

Supplementary Figures

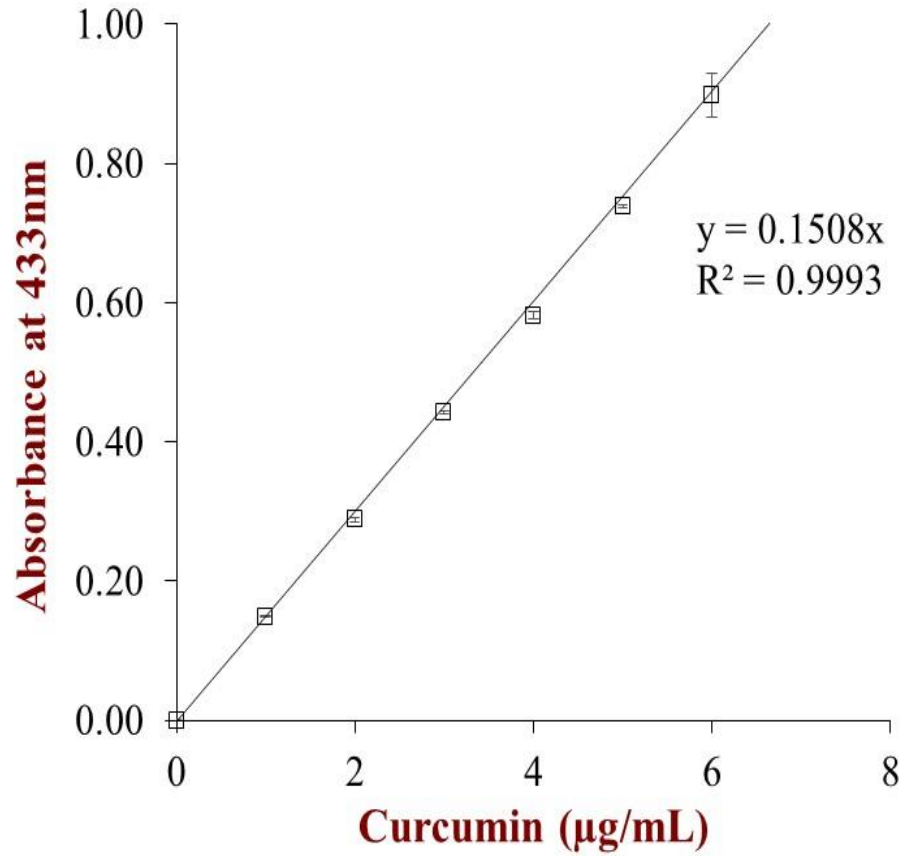


**Figure S1.** Standard curve for curcumin quantification.

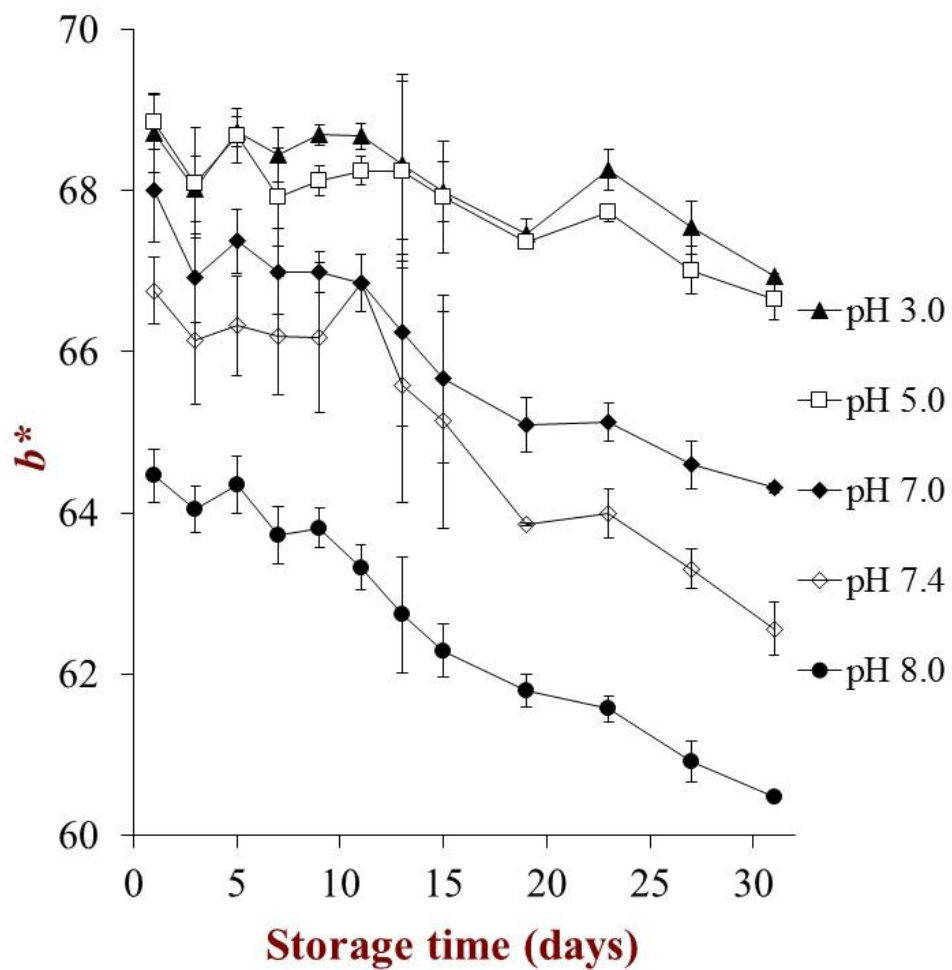


**Figure S2.** Change in yellowness ( $b^*$  value) of oil-in-water emulsions (30% wt% oil) incubated at 37 °C.

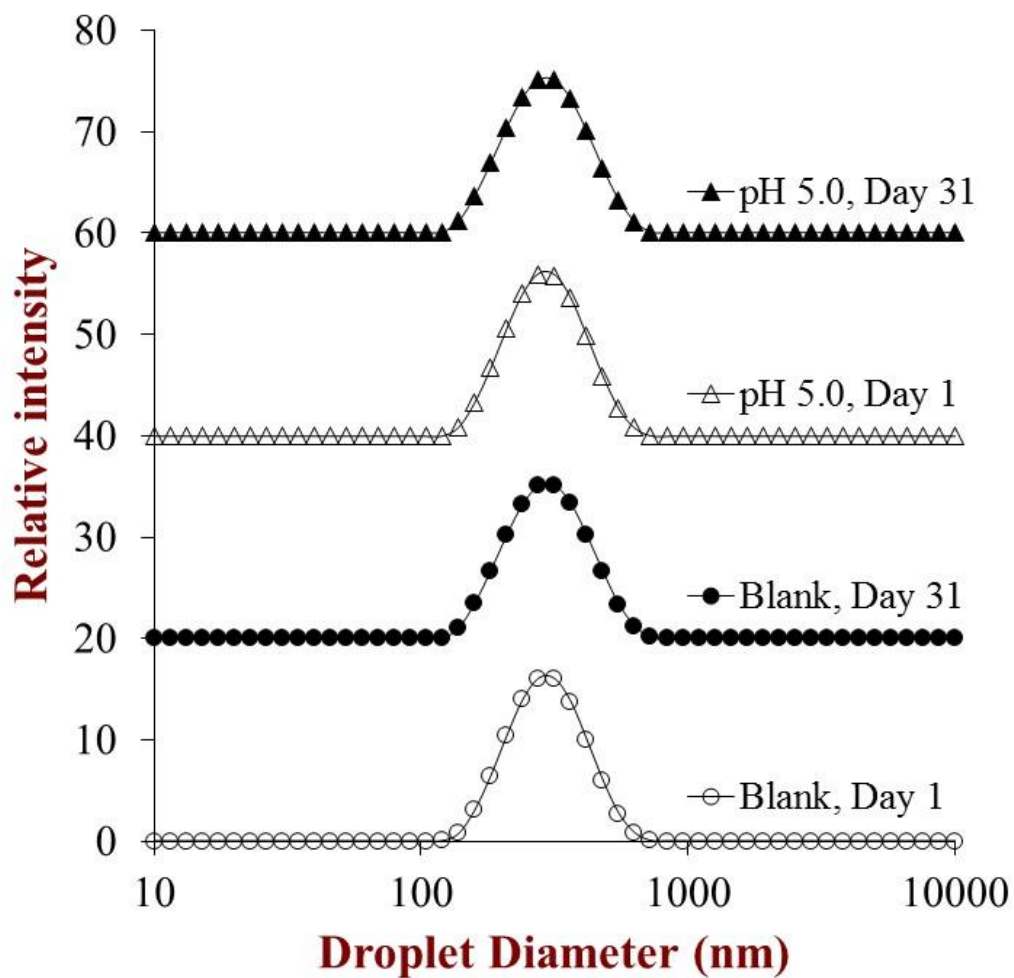


**Figure S3.** Particle size distribution of oil-in-water emulsions (pH 5.0) with and without curcumin at day 1 and day 31. Similar results were obtained for emulsions at other pH values (data not shown).

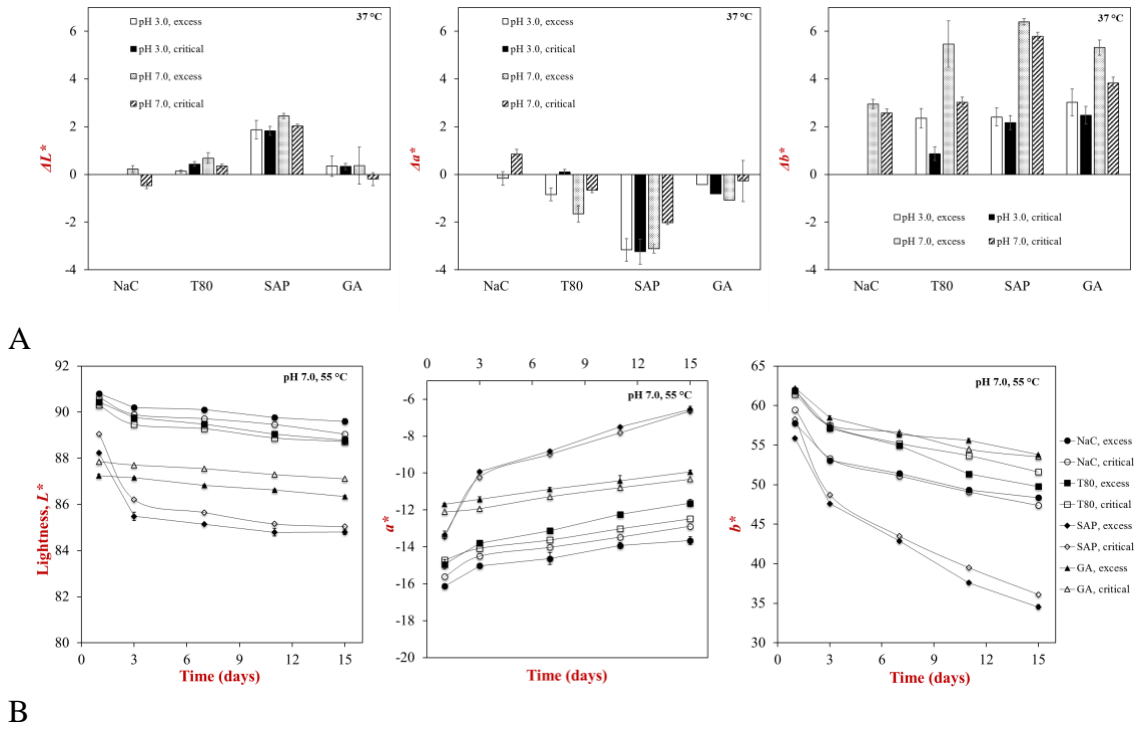
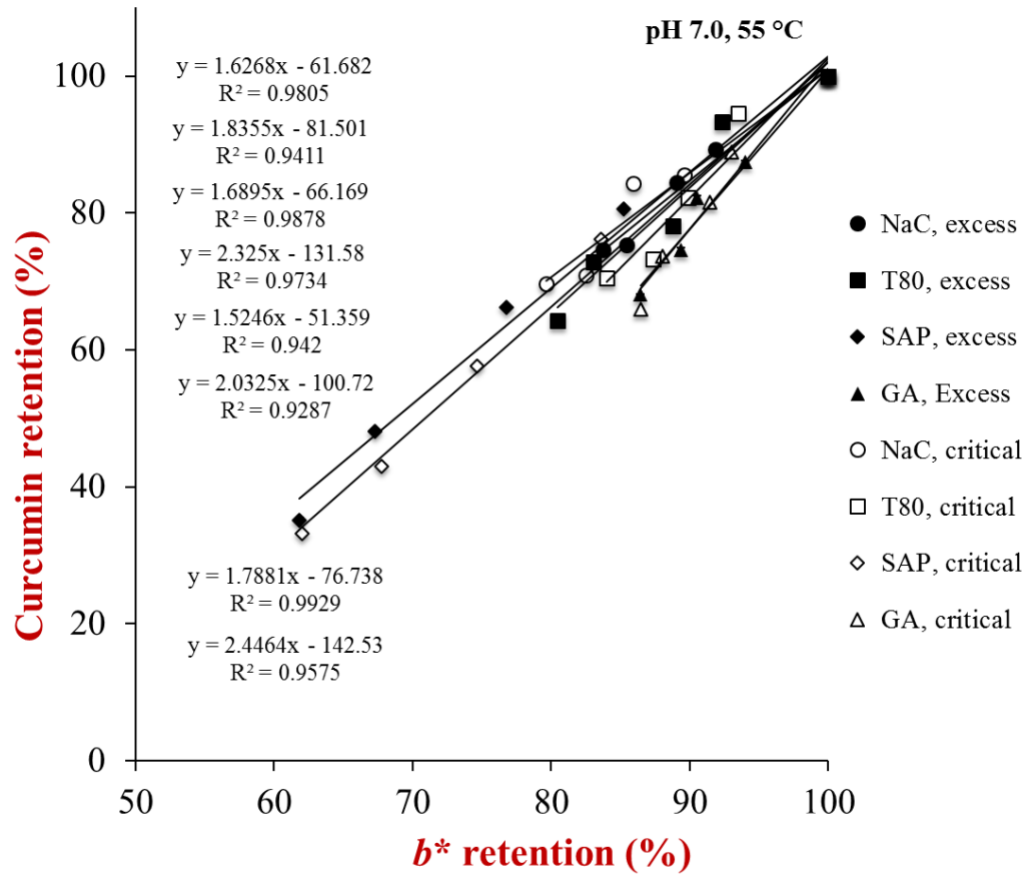
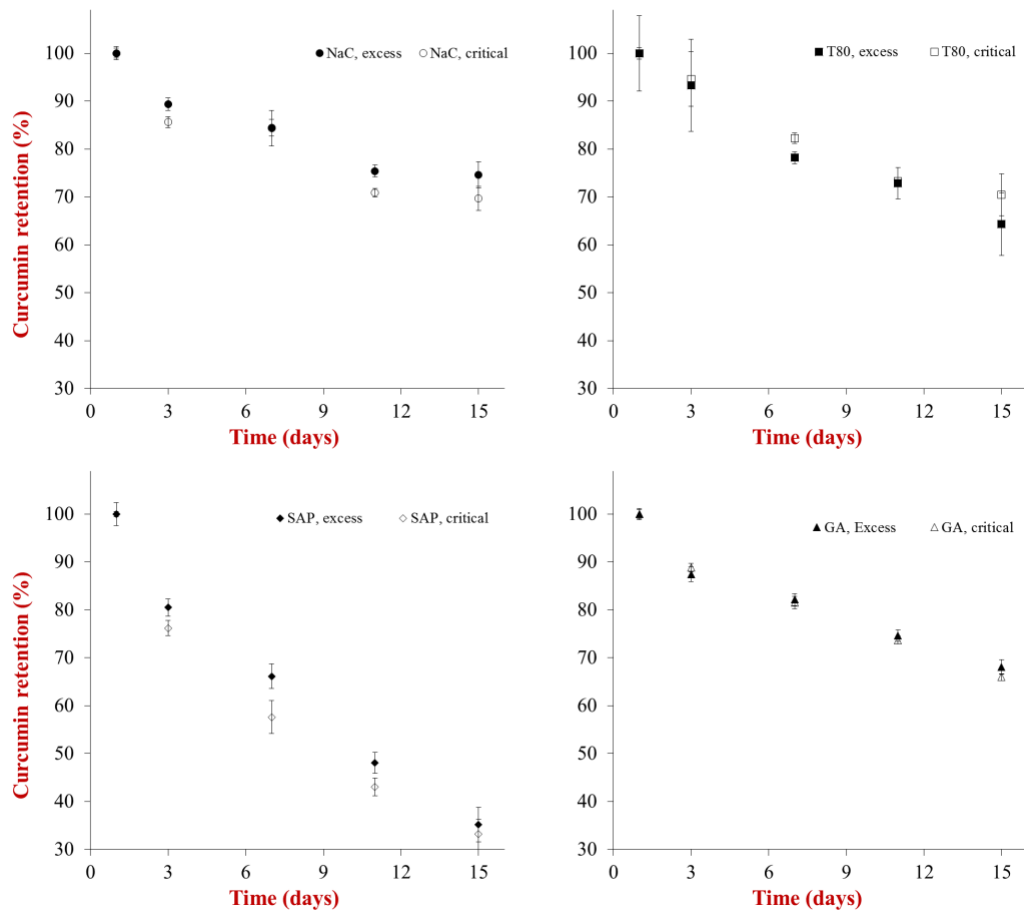


**Figure S4.** Measurement of tristimulus color coordinates ( $L^*$ ,  $a^*$ ,  $b^*$ ) of curcumin emulsions. A) Change in coordinate values ( $\Delta L$ ,  $\Delta a$ ,  $\Delta b$ ) after 15 days of storage at 37 °C; B) color coordinates as a function of storage period (emulsion pH = 7.0, incubation temperature = 55 °C)





A



B

**Figure S5.** A) correlation between retention (%) values of curcumin content and color coordinate  $b^*$ ; B) Effect of emulsifier concentration on retention (%) of curcumin in emulsions at various storage period intervals (emulsion pH = 7.0, incubation temperature = 55 °C)

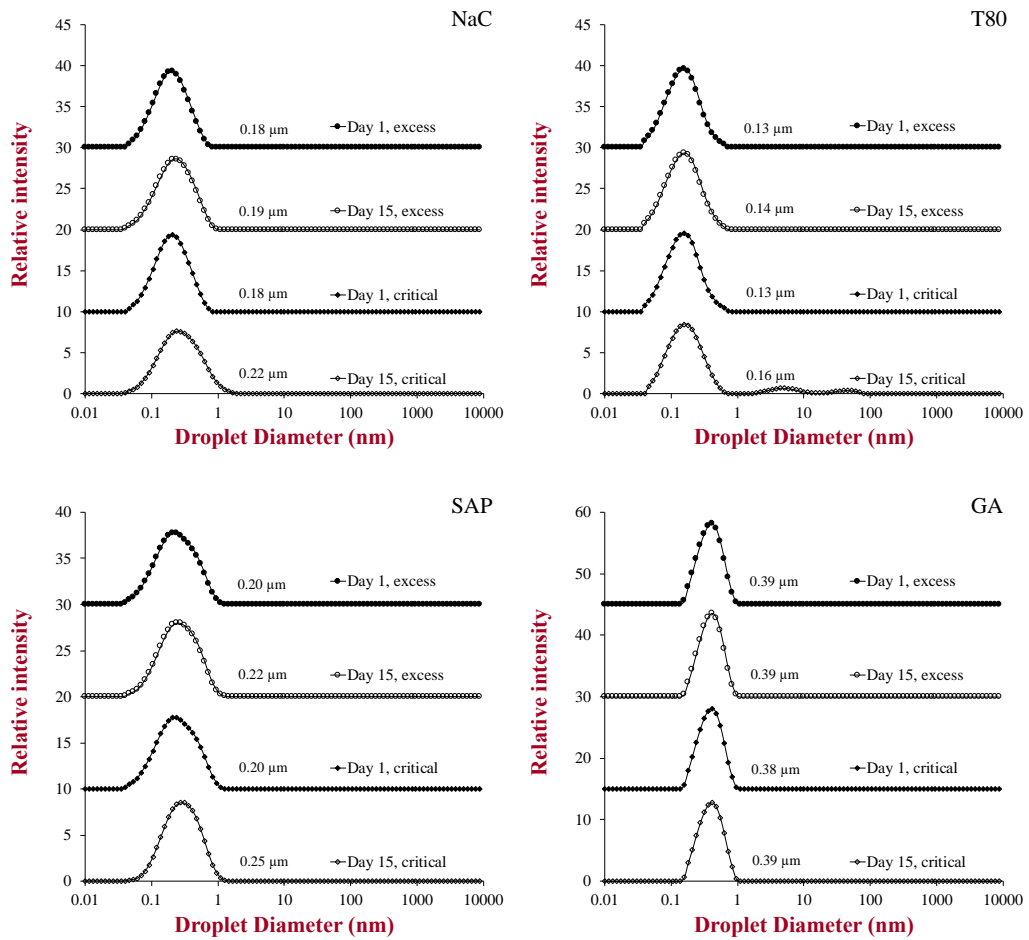


**Figure S6.** Droplet size distribution of curcumin containing MCT-in-water emulsions at Day 1 and Day 15. The number above distribution graph represents corresponding D<sub>32</sub> value. Emulsion was maintained at pH 7.0 and stored at 55 °C

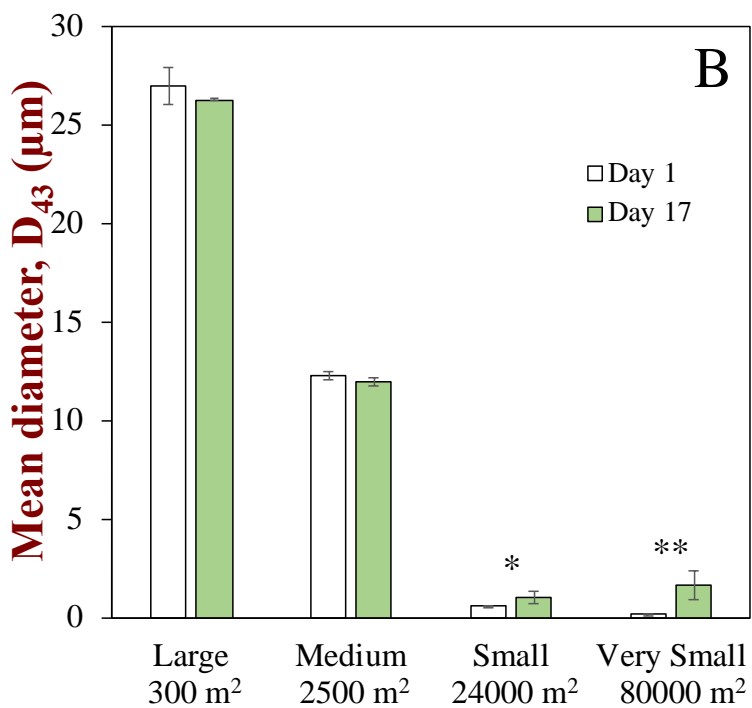
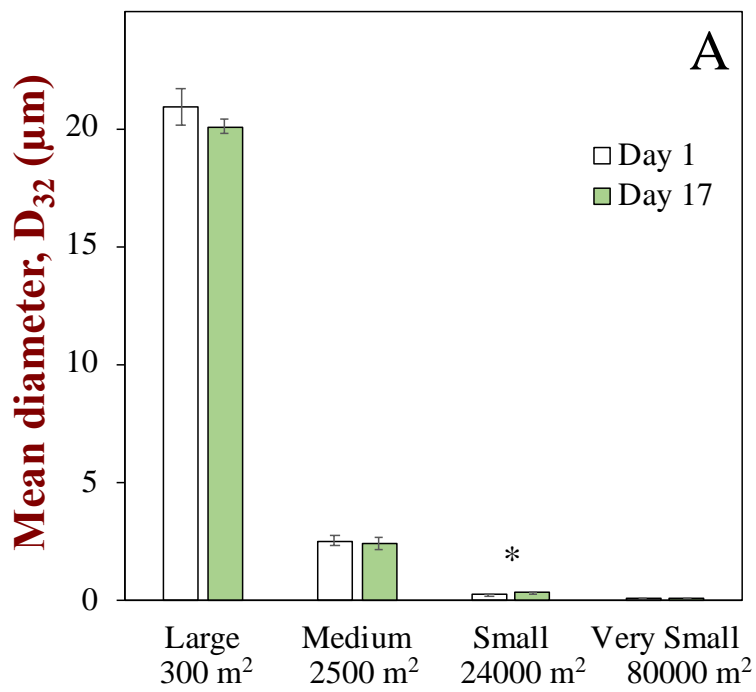


**Figure S7.** Sauter mean,  $D_{32}$  (A) and De Brouckere mean,  $D_{43}$  (B) droplet diameter of MCT oil-in-water emulsions droplets having different specific surface area

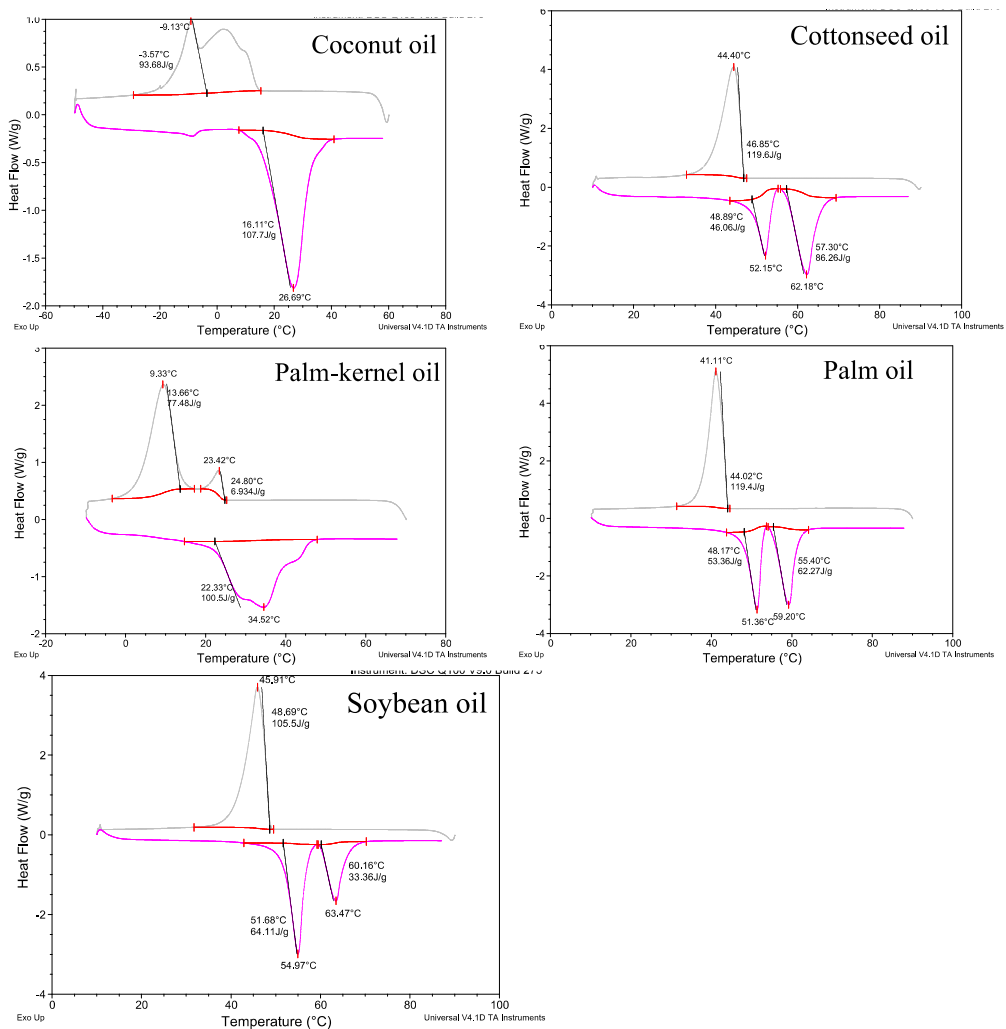


**Figure S8.** DSC analysis of completely hydrogenated fats (coconut, cottonseed, palm-kernel, palm, soybean)

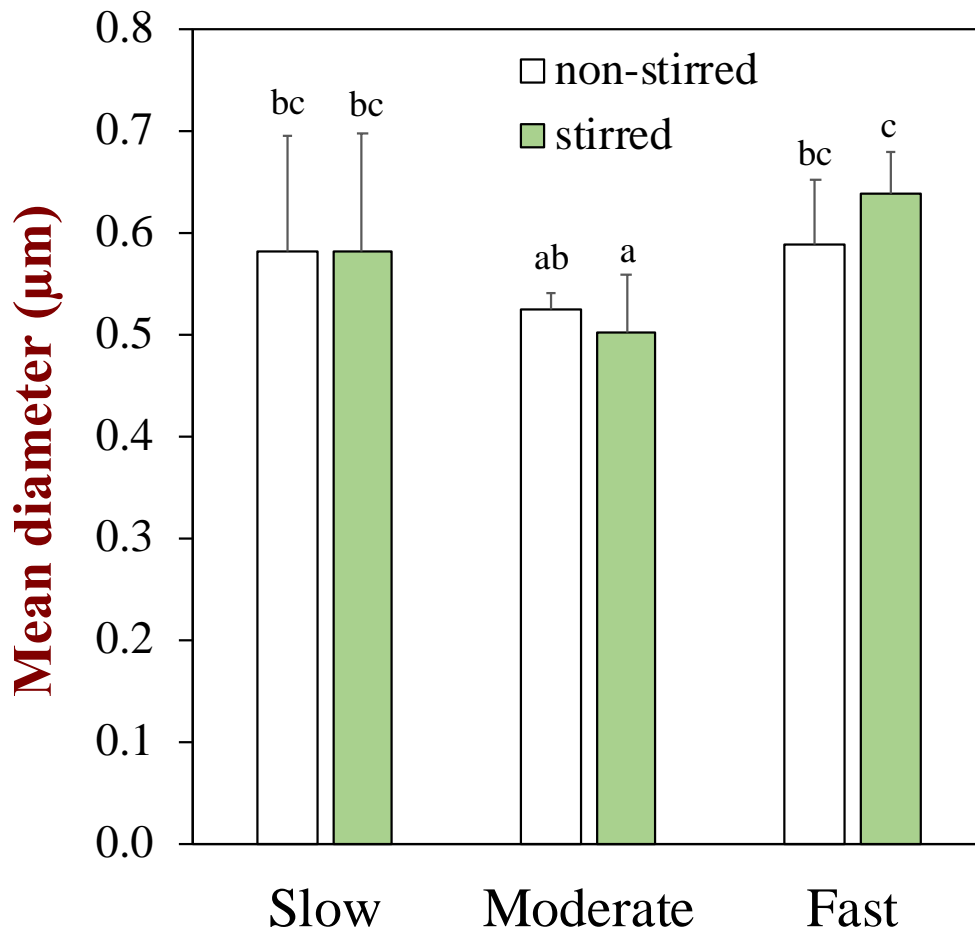


**Figure S9.** Effect of cooling rate and stirring conditions on the mean droplet diameter of 30% completely hydrogenated soybean oil-in-water emulsions (6 wt. % QN) prepared using a high-pressure homogenizer (microfluidizer).

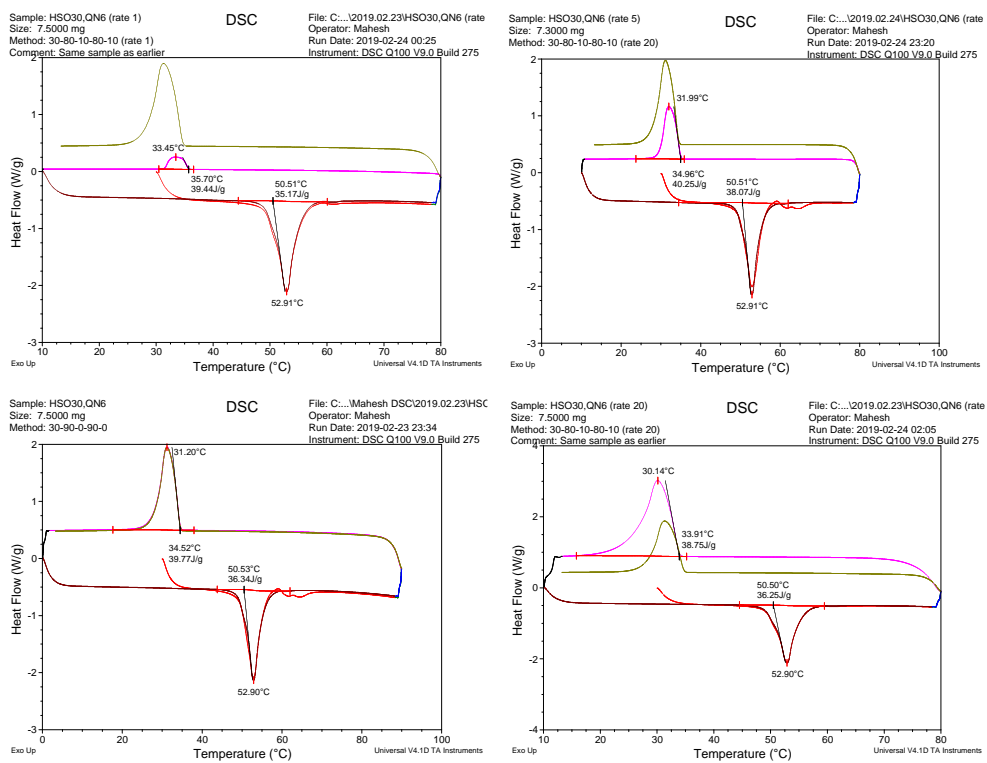


**Figure S10.** DSC analysis of NLC (30% HSO, 6% QN, 64% phosphate buffer) at different thermal rates (1, 5, 10, 20 °C/min)

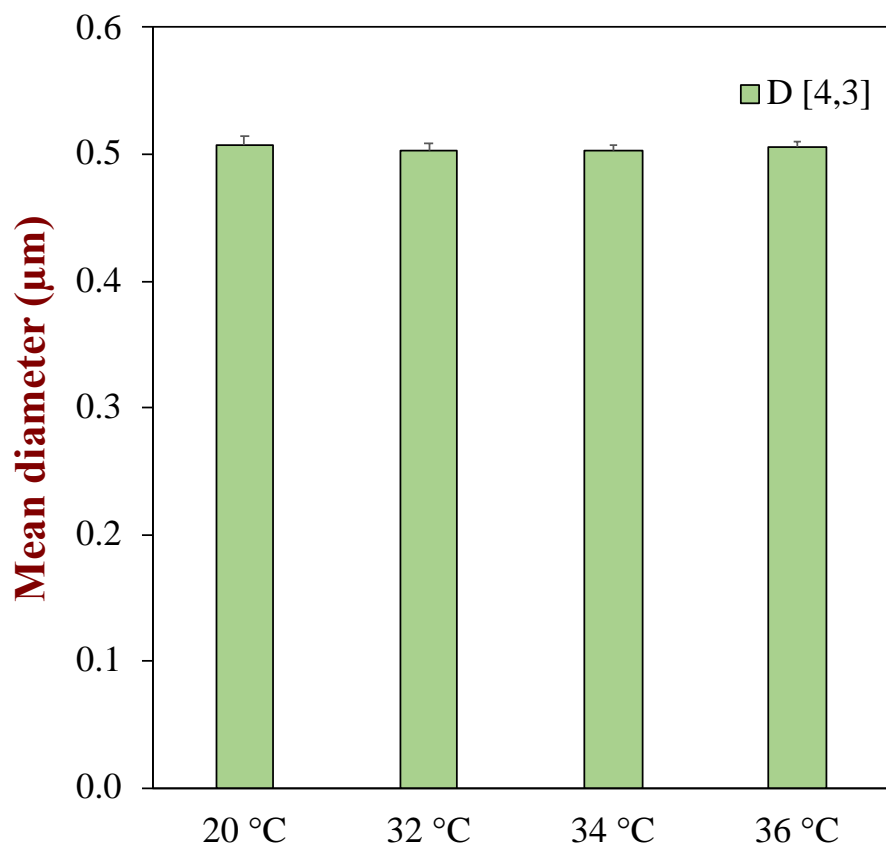


**Figure S11.** Mean droplet diameter of NLC6 measured after stirring at specific temperature for 24 h.



## BIBLIOGRAPHY

- Aditya, N. P., Aditya, S., Yang, H., Kim, H. W., Park, S. O., & Ko, S. (2015). Co-delivery of hydrophobic curcumin and hydrophilic catechin by a water-in-oil-in-water double emulsion. *Food Chemistry*, *173*, 7-13. <https://doi.org/10.1016/j.foodchem.2014.09.131>.
- Aditya, N. P., Macedo, A. S., Doktorovova, S., Souto, E. B., Kim, S., Chang, P.-S., & Ko, S. (2014). Development and evaluation of lipid nanocarriers for quercetin delivery: A comparative study of solid lipid nanoparticles (SLN), nanostructured lipid carriers (NLC), and lipid nanoemulsions (LNE). *LWT - Food Science and Technology*, *59*(1), 115-121. <https://doi.org/http://doi.org/10.1016/j.lwt.2014.04.058>.
- Aditya, N. P., Shim, M., Lee, I., Lee, Y., Im, M. H., & Ko, S. (2013). Curcumin and Genistein Coloaded Nanostructured Lipid Carriers: in Vitro Digestion and Antiprostata Cancer Activity. *Journal of Agricultural and Food Chemistry*, *61*(8), 1878-1883. <https://doi.org/10.1021/jf305143k>.
- Aguilar, F., Crebelli, R., Di Domenico, A., Dusemund, B., Frutos, M. J., Galtier, P., . . . Sou, E. P. F. A. N. (2015). Scientific Opinion on the re-evaluation of ascorbic acid (E 300), sodium ascorbate (E 301) and calcium ascorbate (E 302) as food additives. *Efsa Journal*, *13*(5). <https://doi.org/10.2903/j.efsa.2015.4087>.
- Ahmed, K., Li, Y., McClements, D. J., & Xiao, H. (2012). Nanoemulsion- and emulsion-based delivery systems for curcumin: Encapsulation and release properties. *Food Chemistry*, *132*(2), 799-807. <https://doi.org/10.1016/j.foodchem.2011.11.039>.
- Alvarado, J. D. (1995). Mechanical properties of vegetable oils and fats. *Grasas Y Aceites*, *46*(4-5), 264-269.
- Anand, P., Kunnumakkara, A. B., Newman, R. A., & Aggarwal, B. B. (2007). Bioavailability of curcumin: Problems and promises. *Molecular Pharmaceutics*, *4*(6), 807-818. <https://doi.org/10.1021/mp700113r>.
- Anitha, A., Deepagan, V. G., Rani, V. V. D., Menon, D., Nair, S. V., & Jayakumar, R. (2011). Preparation, characterization, in vitro drug release and biological studies of curcumin loaded dextran sulphate-chitosan nanoparticles. *Carbohydrate Polymers*, *84*(3), 1158-1164. <https://doi.org/10.1016/j.carbpol.2011.01.005>.
- Ansari, M. J., Ahmad, S., Kohli, K., Ali, J., & Khar, R. K. (2005). Stability-indicating HPTLC determination of curcumin in bulk drug and pharmaceutical formulations. *Journal of Pharmaceutical and Biomedical Analysis*, *39*(1-2), 132-138. <https://doi.org/10.1016/j.jpba.2005.03.021>.

- Araiza-Calahorra, A., Akhtar, M., & Sarkar, A. (2018). Recent advances in emulsion-based delivery approaches for curcumin: From encapsulation to bioaccessibility. *Trends in Food Science & Technology*, 71, 155-169. <https://doi.org/https://doi.org/10.1016/j.tifs.2017.11.009>.
- Astrup, A., Dyerberg, J., Elwood, P., Hermansen, K., Hu, F. B., Jakobsen, M. U., . . . Willett, W. C. (2011). The role of reducing intakes of saturated fat in the prevention of cardiovascular disease: where does the evidence stand in 2010? *American Journal of Clinical Nutrition*, 93(4), 684-688. <https://doi.org/10.3945/ajcn.110.004622>.
- Babazadeh, A., Ghanbarzadeh, B., & Hamishehkar, H. (2016). Novel nanostructured lipid carriers as a promising food grade delivery system for rutin. *Journal of Functional Foods*, 26, 167-175. <https://doi.org/10.1016/j.jff.2016.07.017>.
- Babu, S. P. S., Sarkar, D., Ghosh, N. K., Saha, A., Sukul, N. C., & Bhattacharya, S. (1997). Enhancement of Membrane Damage by Saponins Isolated from *Acacia auriculiformis*. *The Japanese Journal of Pharmacology*, 75(4), 451-454. <https://doi.org/10.1254/jjp.75.451>.
- Bai, L., Huan, S., Gu, J., & McClements, D. J. (2016). Fabrication of oil-in-water nanoemulsions by dual-channel microfluidization using natural emulsifiers: Saponins, phospholipids, proteins, and polysaccharides. *Food Hydrocolloids*, 61, 703-711. <https://doi.org/http://doi.org/10.1016/j.foodhyd.2016.06.035>.
- Balasubramanian, K. (2006). Molecular orbital basis for yellow curry spice curcumin's prevention of Alzheimer's disease. *Journal of Agricultural and Food Chemistry*, 54(10), 3512-3520. <https://doi.org/10.1021/jf0603533>.
- Barber-Chamoux, N., Milenkovic, D., Verny, M. A., Habauzit, V., Pereira, B., Lambert, C., . . . Morand, C. (2018). Substantial Variability Across Individuals in the Vascular and Nutrigenomic Response to an Acute Intake of Curcumin: A Randomized Controlled Trial. *Molecular Nutrition & Food Research*, 62(5). <https://doi.org/10.1002/mnfr.201700418>.
- Bates, T. R., Nightingale, C. H., & Dixon, E. (1973). KINETICS OF HYDROLYSIS OF POLYOXYETHYLENE (20) SORBITAN FATTY-ACID ESTER SURFACTANTS. *Journal of Pharmacy and Pharmacology*, 25(6), 470-477. <https://doi.org/10.1111/j.2042-7158.1973.tb09135.x>.
- Bele, C., Matea, C. T., Raducu, C., Miresan, V., & Negrea, O. (2013). Tocopherol Content in Vegetable Oils Using a Rapid HPLC Fluorescence Detection Method. *Notulae Botanicae Horti Agrobotanici Cluj-Napoca*, 41(1), 93-96.
- Bergonzi, M. C., Hamdouch, R., Mazzacuva, F., Isacchi, B., & Bilia, A. R. (2014). Optimization, characterization and in vitro evaluation of curcumin

- microemulsions. *Lwt-Food Science and Technology*, 59(1), 148-155.  
<https://doi.org/10.1016/j.lwt.2014.06.009>.
- Bernabe-Pineda, M., Ramirez-Silva, M. T., Romero-Romo, M., Gonzadlez-Vergara, E., & Rojas-Hernandez, A. (2004). Determination of acidity constants of curcumin in aqueous solution and apparent rate constant of its decomposition. *Spectrochimica Acta Part a-Molecular and Biomolecular Spectroscopy*, 60(5), 1091-1097.  
[https://doi.org/10.1016/s1386-1425\(03\)00342-1](https://doi.org/10.1016/s1386-1425(03)00342-1).
- Bohren, C. F., & Huffman, D. R. (2008). *Absorption and Scattering of Light by Small Particles*: Wiley.
- Bonanome, A., & Grundy, S. M. (1988). EFFECT OF DIETARY STEARIC-ACID ON PLASMA-CHOLESTEROL AND LIPOPROTEIN LEVELS. *New England Journal of Medicine*, 318(19), 1244-1248.  
<https://doi.org/10.1056/nejm198805123181905>.
- Bonnaud, M., Weiss, J., & McClements, D. J. (2010). Interaction of a Food-Grade Cationic Surfactant (Lauric Arginate) with Food-Grade Biopolymers (Pectin, Carrageenan, Xanthan, Alginate, Dextran, and Chitosan). *Journal of Agricultural and Food Chemistry*, 58(17), 9770-9777. <https://doi.org/10.1021/jf101309h>.
- Bos, M. A., & van Vliet, T. (2001). Interfacial rheological properties of adsorbed protein layers and surfactants: a review. *Advances in Colloid and Interface Science*, 91(3), 437-471. [https://doi.org/https://doi.org/10.1016/S0001-8686\(00\)00077-4](https://doi.org/https://doi.org/10.1016/S0001-8686(00)00077-4).
- Bunjes, H., Steiniger, F., & Richter, W. (2007). Visualizing the structure of triglyceride nanoparticles in different crystal modifications. *Langmuir*, 23(7), 4005-4011.  
<https://doi.org/10.1021/la062904p>.
- Chanamai, R., & McClements, D. J. (2001). Depletion flocculation of beverage emulsions by gum arabic and modified starch. *Journal of Food Science*, 66(3), 457-463. <https://doi.org/10.1111/j.1365-2621.2001.tb16129.x>.
- Chantrapornchai, W., Clydesdale, F., & McClements, D. J. (1998). Influence of droplet size and concentration on the color of oil-in-water emulsions. *Journal of Agricultural and Food Chemistry*, 46(8), 2914-2920.  
<https://doi.org/10.1021/jf980278z>.
- Chassaing, B., Koren, O., Goodrich, J. K., Poole, A. C., Srinivasan, S., Ley, R. E., & Gewirtz, A. T. (2015). Dietary emulsifiers impact the mouse gut microbiota promoting colitis and metabolic syndrome. *Nature*, 519(7541), 92-U192.  
<https://doi.org/10.1038/nature14232>.
- Chaurasia, S., Patel, R. R., Chaubey, P., Kumar, N., Khan, G., & Mishra, B. (2015). Lipopolysaccharide based oral nanocarriers for the improvement of bioavailability

- and anticancer efficacy of curcumin. *Carbohydrate Polymers*, 130, 9-17.  
<https://doi.org/10.1016/j.carbpol.2015.04.062>.
- Chazelas, S., Razafindralambo, H., Dumont de Chassart, Q., & Paquot, M. (1995). Surface Properties of the Milk Fat Globule Membrane: Competition between Casein and Membrane Material. In *Food Macromolecules and Colloids* (pp. 95-98): The Royal Society of Chemistry.
- Chen, F. P., Li, B. S., & Tang, C. H. (2015). Nanocomplexation between Curcumin and Soy Protein Isolate: Influence on Curcumin Stability/Bioaccessibility and in Vitro Protein Digestibility. *Journal of Agricultural and Food Chemistry*, 63(13), 3559-3569. <https://doi.org/10.1021/acs.jafc.5b00448>.
- Cheng, C., Peng, S. F., Li, Z. L., Zou, L. Q., Liu, W., & Liu, C. M. (2017). Improved bioavailability of curcumin in liposomes prepared using a pH-driven, organic solvent-free, easily scalable process. *Rsc Advances*, 7(42), 25978-25986.  
<https://doi.org/10.1039/c7ra02861j>.
- Combs, G. F., & McClung, J. P. (2017). Chapter 8 - Vitamin E. In G. F. Combs & J. P. McClung (Eds.), *The Vitamins (Fifth Edition)* (pp. 207-242): Academic Press.
- Cui, J., Yu, B., Zhao, Y., Zhu, W. W., Li, H. L., Lou, H. X., & Zhai, G. X. (2009). Enhancement of oral absorption of curcumin by self-microemulsifying drug delivery systems. *International Journal of Pharmaceutics*, 371(1-2), 148-155.  
<https://doi.org/10.1016/j.ijpharm.2008.12.009>.
- Cuvelier, M. E., Richard, H., & Berset, C. (1992). COMPARISON OF THE ANTIOXIDATIVE ACTIVITY OF SOME ACID-PHENOLS - STRUCTURE ACTIVITY RELATIONSHIP. *Bioscience Biotechnology and Biochemistry*, 56(2), 324-325. <https://doi.org/10.1271/bbb.56.324>.
- Das, S., Ng, W. K., & Tan, R. B. H. (2012). Are nanostructured lipid carriers (NLCs) better than solid lipid nanoparticles (SLNs): Development, characterizations and comparative evaluations of clotrimazole-loaded SLNs and NLCs? *European Journal of Pharmaceutical Sciences*, 47(1), 139-151.  
<https://doi.org/http://doi.org/10.1016/j.ejps.2012.05.010>.
- Davidov-Pardo, G., Gumus, C. E., & McClements, D. J. (2016). Lutein-enriched emulsion-based delivery systems: Influence of pH and temperature on physical and chemical stability. *Food Chemistry*, 196, 821-827.  
<https://doi.org/http://dx.doi.org/10.1016/j.foodchem.2015.10.018>.
- Dhillon, N., Aggarwal, B. B., Newman, R. A., Wolf, R. A., Kunnumakkara, A. B., Abbruzzese, J. L., . . . Kurzrock, R. (2008). Phase II trial of curcumin in patients with advanced pancreatic cancer. *Clinical Cancer Research*, 14(14), 4491-4499.  
<https://doi.org/10.1158/1078-0432.ccr-08-0024>.

- Dickinson, E. (2003). Hydrocolloids at interfaces and the influence on the properties of dispersed systems. *Food Hydrocolloids*, 17(1), 25-39. [https://doi.org/10.1016/s0268-005x\(01\)00120-5](https://doi.org/10.1016/s0268-005x(01)00120-5).
- Etzel, M. R. (2004). Manufacture and use of dairy protein fractions. *Journal of Nutrition*, 134(4), 996S-1002S.
- Euston, S. R., & Hirst, R. L. (2000). The Emulsifying Properties of Commercial Milk Protein Products in Simple Oil-in-Water Emulsions and in a Model Food System. *Journal of Food Science*, 65(6), 934-940. <https://doi.org/10.1111/j.1365-2621.2000.tb09396.x>.
- Fisher, A. N., Brown, K., Davis, S. S., Parr, G. D., & Smith, D. A. (1987). THE EFFECT OF MOLECULAR-SIZE ON THE NASAL ABSORPTION OF WATER-SOLUBLE COMPOUNDS IN THE ALBINO-RAT. *Journal of Pharmacy and Pharmacology*, 39(5), 357-362. <https://doi.org/10.1111/j.2042-7158.1987.tb03398.x>.
- Fredrick, E., Walstra, P., & Dewettinck, K. (2010). Factors governing partial coalescence in oil-in-water emulsions. *Advances in Colloid and Interface Science*, 153(1-2), 30-42. <https://doi.org/10.1016/j.cis.2009.10.003>.
- Goibier, L., Lecomte, S., Leal-Calderon, F., & Faure, C. (2017). The effect of surfactant crystallization on partial coalescence in O/W emulsions. *Journal of Colloid and Interface Science*, 500, 304-314. <https://doi.org/10.1016/j.jcis.2017.04.021>.
- Gordon, O. N., Luis, P. B., Ashley, R. E., Osheroff, N., & Schneider, C. (2015). Oxidative Transformation of Demethoxy- and Bisdemethoxycurcumin: Products, Mechanism of Formation, and Poisoning of Human Topoisomerase II $\alpha$ . *Chemical Research in Toxicology*, 28(5), 989-996. <https://doi.org/10.1021/acs.chemrestox.5b00009>.
- Gordon, O. N., Luis, P. B., Sintim, H. O., & Schneider, C. (2015). Unraveling Curcumin Degradation AUTOXIDATION PROCEEDS THROUGH SPIROEPOXIDE AND VINYLETHYR INTERMEDIATES EN ROUTE TO THE MAIN BICYCLOPENTADIONE. *Journal of Biological Chemistry*, 290(8), 4817-4828. <https://doi.org/10.1074/jbc.M114.618785>.
- Gordon, O. N., & Schneider, C. (2012). Vanillin and ferulic acid: not the major degradation products of curcumin. *Trends in Molecular Medicine*, 18(7), 361-363. <https://doi.org/10.1016/j.molmed.2012.04.011>.
- Gumus, C. E., Decker, E. A., & McClements, D. J. (2017). Impact of legume protein type and location on lipid oxidation in fish oil-in-water emulsions: Lentil, pea, and faba bean proteins. *Food Research International*, 100, 175-185. <https://doi.org/10.1016/j.foodres.2017.08.029>.

- Hartel, R. W., & Hasenhuettl, G. L. (2013). *Food Emulsifiers and Their Applications*: Springer US.
- Heger, M., van Golen, R. F., Broekgaarden, M., & Michel, M. C. (2014). The Molecular Basis for the Pharmacokinetics and Pharmacodynamics of Curcumin and Its Metabolites in Relation to Cancers. *Pharmacological Reviews*, 66(1), 222-307. <https://doi.org/10.1124/pr.110.004044>.
- Helgason, T., Awad, T. S., Kristbergsson, K., McClements, D. J., & Weiss, J. (2009). Effect of surfactant surface coverage on formation of solid lipid nanoparticles (SLN). *Journal of Colloid and Interface Science*, 334(1), 75-81. <https://doi.org/10.1016/j.jcis.2009.03.012>.
- Helgason, T., Salminen, H., Kristbergsson, K., McClements, D. J., & Weiss, J. (2015). Formation of transparent solid lipid nanoparticles by microfluidization: Influence of lipid physical state on appearance. *Journal of Colloid and Interface Science*, 448, 114-122. <https://doi.org/10.1016/j.jcis.2015.02.010>.
- Hu, K., Huang, X. X., Gao, Y. Q., Huang, X. L., Xiao, H., & McClements, D. J. (2015). Core-shell biopolymer nanoparticle delivery systems: Synthesis and characterization of curcumin fortified zein-pectin nanoparticles. *Food Chemistry*, 182, 275-281. <https://doi.org/10.1016/j.foodchem.2015.03.009>.
- Hu, L. D., Jia, Y. H., Niu, F., Jia, Z., Yang, X., & Jiao, K. L. (2012). Preparation and Enhancement of Oral Bioavailability of Curcumin Using Microemulsions Vehicle. *Journal of Agricultural and Food Chemistry*, 60(29), 7137-7141. <https://doi.org/10.1021/jf204078t>.
- Hunter, J. E., Zhang, J., & Kris-Etherton, P. M. (2010). Cardiovascular disease risk of dietary stearic acid compared with trans, other saturated, and unsaturated fatty acids: a systematic review. *American Journal of Clinical Nutrition*, 91(1), 46-63. <https://doi.org/10.3945/ajcn.2009.27661>.
- Huyskens, P. L., & Haulaitpirson, M. C. (1985). A NEW EXPRESSION FOR THE COMBINATORIAL ENTROPY OF MIXING IN LIQUID-MIXTURES. *Journal of Molecular Liquids*, 31(3), 135-151. [https://doi.org/10.1016/0167-7322\(85\)80030-1](https://doi.org/10.1016/0167-7322(85)80030-1).
- Jagannathan, R., Abraham, P. M., & Poddar, P. (2012). Temperature-Dependent Spectroscopic Evidences of Curcumin in Aqueous Medium: A Mechanistic Study of Its Solubility and Stability. *Journal of Physical Chemistry B*, 116(50), 14533-14540. <https://doi.org/10.1021/jp3050516>.
- Jia, Q., Ivanov, I., Zlatev, Z. Z., Alaniz, R. C., Weeks, B. R., Callaway, E. S., . . . Chapkin, R. S. (2011). Dietary fish oil and curcumin combine to modulate colonic cytokinetics and gene expression in dextran sodium sulphate-treated mice. *British*



*Journal of Nutrition*, 106(4), 519-529.  
<https://doi.org/10.1017/s0007114511000390>.

- Jores, K., Mehnert, W., Drechsler, M., Bunjes, H., Johann, C., & Mäder, K. (2004). Investigations on the structure of solid lipid nanoparticles (SLN) and oil-loaded solid lipid nanoparticles by photon correlation spectroscopy, field-flow fractionation and transmission electron microscopy. *Journal of Controlled Release*, 95(2), 217-227.  
<https://doi.org/https://doi.org/10.1016/j.jconrel.2003.11.012>.
- Joung, H. J., Choi, M.-J., Kim, J. T., Park, S. H., Park, H. J., & Shin, G. H. (2016). Development of Food-Grade Curcumin Nanoemulsion and its Potential Application to Food Beverage System: Antioxidant Property and In Vitro Digestion. *Journal of Food Science*, 81(3), N745-N753.  
<https://doi.org/10.1111/1750-3841.13224>.
- Jourdain, L., Leser, M. E., Schmitt, C., Michel, M., & Dickinson, E. (2008). Stability of emulsions containing sodium caseinate and dextran sulfate: Relationship to complexation in solution. *Food Hydrocolloids*, 22(4), 647-659.  
<https://doi.org/10.1016/j.foodhyd.2007.01.007>.
- Jovanovic, S. V., Steenken, S., Boone, C. W., & Simic, M. G. (1999). H-atom transfer is a preferred antioxidant mechanism of curcumin. *Journal of the American Chemical Society*, 121(41), 9677-9681. <https://doi.org/10.1021/ja991446m>.
- Joye, I. J., & McClements, D. J. (2014). Biopolymer-based nanoparticles and microparticles: Fabrication, characterization, and application. *Current Opinion in Colloid & Interface Science*, 19(5), 417-427.  
<https://doi.org/10.1016/j.cocis.2014.07.002>.
- Kabalnov, A., & Wennerstrom, H. (1996). Macroemulsion stability: The oriented wedge theory revisited. *Langmuir*, 12(2), 276-292. <https://doi.org/10.1021/la950359e>.
- Kakkar, V., Singh, S., Singla, D., & Kaur, I. P. (2011). Exploring solid lipid nanoparticles to enhance the oral bioavailability of curcumin. *Molecular Nutrition & Food Research*, 55(3), 495-503. <https://doi.org/10.1002/mnfr.201000310>.
- Karewicz, A., Bielska, D., Loboda, A., Gzyl-Malcher, B., Bednar, J., Jozkowicz, A., . . . Nowakowska, M. (2013). Curcumin-containing liposomes stabilized by thin layers of chitosan derivatives. *Colloids and Surfaces B-Biointerfaces*, 109, 307-316. <https://doi.org/10.1016/j.colsurfb.2013.03.059>.
- Karimi, N., Ghanbarzadeh, B., Hamishehkar, H., Mehramuz, B., & Kafil, H. S. (2018). Antioxidant, Antimicrobial and Physicochemical Properties of Turmeric Extract-Loaded Nanostructured Lipid Carrier (NLC). *Colloid and Interface Science Communications*, 22, 18-24. <https://doi.org/10.1016/j.colcom.2017.11.006>.

- Kharat, M., Du, Z., Zhang, G., & McClements, D. J. (2017). Physical and Chemical Stability of Curcumin in Aqueous Solutions and Emulsions: Impact of pH, Temperature, and Molecular Environment. *Journal of Agricultural and Food Chemistry*, 65(8), 1525-1532. <https://doi.org/10.1021/acs.jafc.6b04815>.
- Kharat, M., & McClements, D. J. (2019). Recent advances in colloidal delivery systems for nutraceuticals: A case study – Delivery by Design of curcumin. *Journal of Colloid and Interface Science*, 557, 506-518. <https://doi.org/10.1016/j.jcis.2019.09.045>.
- Kharat, M., Zhang, G., & McClements, D. J. (2018). Stability of curcumin in oil-in-water emulsions: Impact of emulsifier type and concentration on chemical degradation. *Food Research International*, 111, 178-186. <https://doi.org/10.1016/j.foodres.2018.05.021>.
- Kharat, M., Zhang, G. D., & McClements, D. J. (2018). Stability of curcumin in oil-in-water emulsions: Impact of emulsifier type and concentration on chemical degradation. *Food Research International*, 111, 178-186. <https://doi.org/10.1016/j.foodres.2018.05.021>.
- Kocher, A., Schiborr, C., Behnam, D., & Frank, J. (2015). The oral bioavailability of curcuminoids in healthy humans is markedly enhanced by micellar solubilisation but not further improved by simultaneous ingestion of sesamin, ferulic acid, naringenin and xanthohumol. *Journal of Functional Foods*, 14, 183-191. <https://doi.org/10.1016/j.jff.2015.01.045>.
- Kontush, A., Finckh, B., Karten, B., Kohlschutter, A., & Beisiegel, U. (1996). Antioxidant and prooxidant activity of alpha-tocopherol in human plasma and low density lipoprotein. *Journal of Lipid Research*, 37(7), 1436-1448.
- Krickau, D. P., Mueller, R. H., & Thomsen, J. (2007). Degradation kinetics of hydrolytically susceptible drugs in O/W emulsions - Effects of interfacial area and lecithin. *International Journal of Pharmaceutics*, 342(1-2), 62-71. <https://doi.org/10.1016/j.ijpharm.2007.04.033>.
- Kumar, A., Kaur, G., Kansal, S. K., Chaudhary, G. R., & Mehta, S. K. (2016). Enhanced solubilization of curcumin in mixed surfactant vesicles. *Food Chemistry*, 199, 660-666. <https://doi.org/10.1016/j.foodchem.2015.12.077>.
- Kunwar, A., Barik, A., Pandey, R., & Priyadarsini, K. I. (2006). Transport of liposomal and albumin loaded curcumin to living cells: An absorption and fluorescence spectroscopic study. *Biochimica Et Biophysica Acta-General Subjects*, 1760(10), 1513-1520. <https://doi.org/10.1016/j.bbagen.2006.06.012>.
- LaClair, C. E., & Etzel, M. R. (2010). Ingredients and pH are Key to Clear Beverages that Contain Whey Protein. *Journal of Food Science*, 75(1), C21-C27.



<https://doi.org/10.1111/j.1750-3841.2009.01400.x>.

- Lesmes, U., Baudot, P., & McClements, D. J. (2010). Impact of Interfacial Composition on Physical Stability and In Vitro Lipase Digestibility of Triacylglycerol Oil Droplets Coated with Lactoferrin and/or Caseinate. *Journal of Agricultural and Food Chemistry*, 58(13), 7962-7969. <https://doi.org/10.1021/jf100703c>.
- Leung, M. H. M., Colangelo, H., & Kee, T. W. (2008). Encapsulation of curcumin in cationic micelles suppresses alkaline hydrolysis. *Langmuir*, 24(11), 5672-5675. <https://doi.org/10.1021/la800780w>.
- Li, J. Y., Liu, D. D., Tan, G. X., Zhao, Z. N., Yang, X. G., & Pan, W. S. (2016). A comparative study on the efficiency of chitosan-N-acetylcysteine, chitosan oligosaccharides or carboxymethyl chitosan surface modified nanostructured lipid carrier for ophthalmic delivery of curcumin. *Carbohydrate Polymers*, 146, 435-444. <https://doi.org/10.1016/j.carbpol.2016.03.079>.
- Linke, C., & Drusch, S. (2018). Re-Designing Clouds to Increase Turbidity in Beverage Emulsions. *Food Biophysics*, 13(1), 91-101. <https://doi.org/10.1007/s11483-018-9515-x>.
- Ma, P. H., Zeng, Q. H., Tai, K. D., He, X. Y., Yao, Y. Y., Hong, X. F., & Yuan, F. (2017). Preparation of curcumin-loaded emulsion using high pressure homogenization: Impact of oil phase and concentration on physicochemical stability. *Lwt-Food Science and Technology*, 84, 34-46. <https://doi.org/10.1016/j.lwt.2017.04.074>.
- Maherani, B., Arab-Tehrany, E., Mozafari, M. R., Gaiani, C., & Linder, M. (2011). Liposomes: A Review of Manufacturing Techniques and Targeting Strategies. *Current Nanoscience*, 7(3), 436-452. <https://doi.org/10.2174/157341311795542453>.
- Makino, K., Yamada, T., Kimura, M., Oka, T., Ohshima, H., & Kondo, T. (1991). TEMPERATURE-INDUCED AND IONIC STRENGTH-INDUCED CONFORMATIONAL-CHANGES IN THE LIPID HEAD GROUP REGION OF LIPOSOMES AS SUGGESTED BY ZETA-POTENTIAL DATA. *Biophysical Chemistry*, 41(2), 175-183. [https://doi.org/10.1016/0301-4622\(91\)80017-l](https://doi.org/10.1016/0301-4622(91)80017-l).
- Mandal, S., Banerjee, C., Ghosh, S., Kuchlyan, J., & Sarkar, N. (2013). Modulation of the Photophysical Properties of Curcumin in Nonionic Surfactant (Tween-20) Forming Micelles and Niosomes: A Comparative Study of Different Microenvironments. *Journal of Physical Chemistry B*, 117(23), 6957-6968. <https://doi.org/10.1021/jp403724g>.
- Matloob, A. H., Mourtas, S., Klepetsanis, P., & Antimisiaris, S. G. (2014). Increasing the stability of curcumin in serum with liposomes or hybrid drug-in-cyclodextrin-in-liposome systems: A comparative study. *International Journal of Pharmaceutics*,

- 476(1-2), 108-115. <https://doi.org/10.1016/j.ijpharm.2014.09.041>.
- McClements, D. J. (2005). *Food Emulsions: Principles, Practice, and Techniques*. (2nd ed.). Boca Raton: CRC Press.
- McClements, D. J. (2007). Critical review of techniques and methodologies for characterization of emulsion stability. *Critical Reviews in Food Science and Nutrition*, 47(7), 611-649. <https://doi.org/10.1080/10408390701289292>.
- McClements, D. J. (2011). Edible nanoemulsions: fabrication, properties, and functional performance. *Soft Matter*. <https://doi.org/10.1039/C0SM00549E>.
- McClements, D. J. (2012). Crystals and crystallization in oil-in-water emulsions: Implications for emulsion-based delivery systems. *Advances in Colloid and Interface Science*, 174, 1-30. <https://doi.org/10.1016/j.cis.2012.03.002>.
- McClements, D. J. (2015a). *Food Emulsions: Principles, Practice, and Techniques*. (2nd ed.). Boca Raton: CRC Press.
- McClements, D. J. (2015b). *Food Emulsions: Principles, Practices, and Techniques, Third Edition*: CRC Press.
- McClements, D. J. (2018). Delivery by Design (DbD): A Standardized Approach to the Development of Efficacious Nanoparticle- and Microparticle-Based Delivery Systems. *Comprehensive Reviews in Food Science and Food Safety*, 17(1), 200-219. <https://doi.org/10.1111/1541-4337.12313>.
- McClements, D. J., Decker, E. A., & Weiss, J. (2007). Emulsion-based delivery systems for lipophilic bioactive components. *J Food Sci*, 72(8), R109-124. <https://doi.org/10.1111/j.1750-3841.2007.00507.x>.
- McClements, D. J., Dungan, S. R., German, J. B., Simoneau, C., & Kinsella, J. E. (1993). DROPLET SIZE AND EMULSIFIER TYPE AFFECT CRYSTALLIZATION AND MELTING OF HYDROCARBON-IN-WATER EMULSIONS. *Journal of Food Science*, 58(5), 1148-&. <https://doi.org/10.1111/j.1365-2621.1993.tb06135.x>.
- McClements, D. J., & Gumus, C. E. (2016). Natural Emulsifiers - Biosurfactants, Phospholipids, Biopolymers, and Colloidal Particles: Molecular and Physicochemical Basis of Functional Performance. *Advances in Colloid and Interface Science*, *In press*.
- McClements, D. J., & Gumus, C. E. (2016). Natural emulsifiers — Biosurfactants, phospholipids, biopolymers, and colloidal particles: Molecular and physicochemical basis of functional performance. *Advances in Colloid and Interface Science*, 234, 3-26. <https://doi.org/http://doi.org/10.1016/j.cis.2016.03.002>.

- McClements, D. J., & Rao, J. (2011). Food-Grade Nanoemulsions: Formulation, Fabrication, Properties, Performance, Biological Fate, and Potential Toxicity. *Critical Reviews in Food Science and Nutrition*, 51(4), 285-330. <https://doi.org/10.1080/10408398.2011.559558>.
- McClements, D. J., & Xiao, H. (2012). Potential biological fate of ingested nanoemulsions: influence of particle characteristics. *Food & Function*, 3(3), 202-220. <https://doi.org/10.1039/c1fo10193e>.
- Mehnert, W., & Mäder, K. (2001). Solid lipid nanoparticles: Production, characterization and applications. *Advanced Drug Delivery Reviews*, 47(2), 165-196. [https://doi.org/https://doi.org/10.1016/S0169-409X\(01\)00105-3](https://doi.org/https://doi.org/10.1016/S0169-409X(01)00105-3).
- Mohammadi, M., Pezeshki, A., Abbasi, M. M., Ghanbarzadeh, B., & Hamishehkar, H. (2017). Vitamin D-3-Loaded Nanostructured Lipid Carriers as a Potential Approach for Fortifying Food Beverages; in Vitro and in Vivo Evaluation. *Advanced Pharmaceutical Bulletin*, 7(1), 61-71. <https://doi.org/10.15171/apb.2017.008>.
- Mondal, S., Ghosh, S., & Moulik, S. P. (2016). Stability of curcumin in different solvent and solution media: UV-visible and steady-state fluorescence spectral study. *Journal of Photochemistry and Photobiology B-Biology*, 158, 212-218. <https://doi.org/10.1016/j.jphotobiol.2016.03.004>.
- Muller, R. H., Radtke, M., & Wissing, S. A. (2002). Nanostructured lipid matrices for improved microencapsulation of drugs. *International Journal of Pharmaceutics*, 242(1-2), 121-128. [https://doi.org/10.1016/s0378-5173\(02\)00180-1](https://doi.org/10.1016/s0378-5173(02)00180-1).
- Müller, R. H., Radtke, M., & Wissing, S. A. (2002). Solid lipid nanoparticles (SLN) and nanostructured lipid carriers (NLC) in cosmetic and dermatological preparations. *Advanced Drug Delivery Reviews*, 54, Supplement, S131-S155. [https://doi.org/http://doi.org/10.1016/S0169-409X\(02\)00118-7](https://doi.org/http://doi.org/10.1016/S0169-409X(02)00118-7).
- Nassu, R. T., & Guaraldo Gonçalves, L. A. (1999). Determination of melting point of vegetable oils and fats by differential scanning calorimetry (DSC) technique. *Grasas y Aceites; Vol 50, No 1 (1999)DO - 10.3989/gya.1999.v50.i1.630*.
- Nelis, V., Declercle, A., De Neve, L., Moens, K., Dewettinck, K., & Van der Meeren, P. (2019). Fat crystallization and melting in W/O/W double emulsions: Comparison between bulk and emulsified state. *Colloids and Surfaces a-Physicochemical and Engineering Aspects*, 566, 196-206. <https://doi.org/10.1016/j.colsurfa.2019.01.019>.
- Nimiya, Y., Wang, W., Du, Z., Sukamtoh, E., Zhu, J., Decker, E., & Zhang, G. (2015). Redox modulation of curcumin stability: Redox active antioxidants increase chemical stability of curcumin. *Molecular Nutrition & Food Research*, n/a-n/a.

<https://doi.org/10.1002/mnfr.201500681>.

- Niu, Y. M., Ke, D., Yang, Q. Q., Wang, X. Y., Chen, Z. Y., An, X. Q., & Shen, W. G. (2012). Temperature-dependent stability and DPPH scavenging activity of liposomal curcumin at pH 7.0. *Food Chemistry*, 135(3), 1377-1382. <https://doi.org/10.1016/j.foodchem.2012.06.018>.
- Niu, Y. M., Wang, X. Y., Chai, S. H., Chen, Z. Y., An, X. Q., & Shen, W. G. (2012). Effects of Curcumin Concentration and Temperature on the Spectroscopic Properties of Liposomal Curcumin. *Journal of Agricultural and Food Chemistry*, 60(7), 1865-1870. <https://doi.org/10.1021/jf204867v>.
- Pabon, H. J. J. (1964). A synthesis of curcumin and related compounds. *Recueil des Travaux Chimiques des Pays-Bas*, 83(4), 379-386. <https://doi.org/10.1002/recl.19640830407>.
- Pan, K., Luo, Y. C., Gan, Y. D., Baek, S. J., & Zhong, Q. X. (2014). pH-driven encapsulation of curcumin in self-assembled casein nanoparticles for enhanced dispersibility and bioactivity. *Soft Matter*, 10(35), 6820-6830. <https://doi.org/10.1039/c4sm00239c>.
- Patsahan, T., Ilnytskyi, J. M., & Pizio, O. (2017). On the properties of a single OPLS-UA model curcumin molecule in water, methanol and dimethyl sulfoxide. Molecular dynamics computer simulation results. *Condensed Matter Physics*, 20(2). <https://doi.org/10.5488/cmp.20.23003>.
- Peng, S. F., Li, Z. L., Zou, L. Q., Liu, W., Liu, C. M., & McClements, D. J. (2018). Enhancement of Curcumin Bioavailability by Encapsulation in Sphorolipid-Coated Nanoparticles: An in Vitro and in Vivo Study. *Journal of Agricultural and Food Chemistry*, 66(6), 1488-1497. <https://doi.org/10.1021/acs.jafc.7605478>.
- Peng, S. F., Zou, L. Q., Liu, W., Liu, C. M., & McClements, D. J. (2018). Fabrication and Characterization of Curcumin-Loaded Liposomes Formed from Sunflower Lecithin: Impact of Composition and Environmental Stress. *Journal of Agricultural and Food Chemistry*, 66(46), 12421-12430. <https://doi.org/10.1021/acs.jafc.8b04136>.
- Pezeshki, A., Hamishehkar, H., Ghanbarzadeh, B., Fathollahy, I., Nahr, F. K., Heshmati, M. K., & Mohammadi, M. (2019). Nanostructured lipid carriers as a favorable delivery system for beta-carotene. *Food Bioscience*, 27, 11-17. <https://doi.org/10.1016/j.fbio.2018.11.004>.
- Price, L. C., & Buescher, R. W. (1997). Kinetics of alkaline degradation of the food pigments curcumin and curcuminoids. *Journal of Food Science*, 62(2), 267-269. <https://doi.org/10.1111/j.1365-2621.1997.tb03982.x>.

- Priyadarsini, K. I., Maity, D. K., Naik, G. H., Kumar, M. S., Unnikrishnan, M. K., Satav, J. G., & Mohan, H. (2003). Role of phenolic O-H and methylene hydrogen on the free radical reactions and antioxidant activity of curcumin. *Free Radical Biology and Medicine*, 35(5), 475-484. [https://doi.org/10.1016/s0891-5849\(03\)00325-3](https://doi.org/10.1016/s0891-5849(03)00325-3).
- Qian, C., Decker, E. A., Xiao, H., & McClements, D. J. (2013). Impact of lipid nanoparticle physical state on particle aggregation and beta-carotene degradation: Potential limitations of solid lipid nanoparticles. *Food Research International*, 52(1), 342-349. <https://doi.org/10.1016/j.foodres.2013.03.035>.
- Qian, C., & McClements, D. J. (2011). Formation of nanoemulsions stabilized by model food-grade emulsifiers using high-pressure homogenization: Factors affecting particle size. *Food Hydrocolloids*, 25(5), 1000-1008. <https://doi.org/10.1016/j.foodhyd.2010.09.017>.
- Ramalingam, P., Yoo, S. W., & Ko, Y. T. (2016). Nanodelivery systems based on mucoadhesive polymer coated solid lipid nanoparticles to improve the oral intake of food curcumin. *Food Research International*, 84, 113-119. <https://doi.org/10.1016/j.foodres.2016.03.031>.
- Rao, P. H., & He, M. (2006). Adsorption of anionic and nonionic surfactant mixtures from synthetic detergents on soils. *Chemosphere*, 63(7), 1214-1221. <https://doi.org/10.1016/j.chemosphere.2005.08.067>.
- Reichert, C. L., Salminen, H., & Weiss, J. (2019). Quillaja Saponin Characteristics and Functional Properties. *Annual Review of Food Science and Technology*, Vol 10, 10, 43-73. <https://doi.org/10.1146/annurev-food-032818-122010>.
- Renard, D., Lavenant-Gourgeon, L., Ralet, M.-C., & Sanchez, C. (2006). Acacia senegal Gum: Continuum of Molecular Species Differing by Their Protein to Sugar Ratio, Molecular Weight, and Charges. *Biomacromolecules*, 7(9), 2637-2649. <https://doi.org/10.1021/bm060145j>.
- Roberts, D. D., Elmore, J. S., Langley, K. R., & Bakker, J. (1996). Effects of sucrose, guar gum, and carboxymethylcellulose on the release of volatile flavor compounds under dynamic conditions. *Journal of Agricultural and Food Chemistry*, 44(5), 1321-1326. <https://doi.org/10.1021/jf950567c>.
- Roughley, P. J., & Whiting, D. A. (1973). EXPERIMENTS IN BIOSYNTHESIS OF CURCUMIN. *Journal of the Chemical Society-Perkin Transactions 1*(20), 2379-2388. <https://doi.org/10.1039/p19730002379>.
- Salminen, H., Ankenbrand, J., Zeeb, B., Bonisch, G. B., Schafer, C., Kohlus, R., & Weiss, J. (2019). Influence of spray drying on the stability of food-grade solid lipid nanoparticles. *Food Research International*, 119, 741-750. <https://doi.org/10.1016/j.foodres.2018.10.056>.

- Salminen, H., Gommel, C., Leuenberger, B. H., & Weiss, J. (2016). Influence of encapsulated functional lipids on crystal structure and chemical stability in solid lipid nanoparticles: Towards bioactive-based design of delivery systems. *Food Chemistry*, *190*, 928-937. <https://doi.org/10.1016/j.foodchem.2015.06.054>.
- Santos, V. D., Ribeiro, A. P. B., & Santana, M. H. A. (2019). Solid lipid nanoparticles as carriers for lipophilic compounds for applications in foods. *Food Research International*, *122*, 610-626. <https://doi.org/10.1016/j.foodres.2019.01.032>.
- Sarika, P. R., & James, N. R. (2016). Polyelectrolyte complex nanoparticles from cationised gelatin and sodium alginate for curcumin delivery. *Carbohydrate Polymers*, *148*, 354-361. <https://doi.org/10.1016/j.carbpol.2016.04.073>.
- Schiborr, C., Kocher, A., Behnam, D., Jandasek, J., Toelstede, S., & Frank, J. (2014). The oral bioavailability of curcumin from micronized powder and liquid micelles is significantly increased in healthy humans and differs between sexes. *Molecular Nutrition & Food Research*, *58*(3), 516-527. <https://doi.org/10.1002/mnfr.201300724>.
- Seo, T. R., Lee, I., Chun, Y. G., Park, D. J., Lee, S. H., & Kim, B. K. (2019). Improved Stability of Polyglycerol Polyricinoleate-Substituted Nanostructured Lipid Carrier Cholecalciferol Emulsions with Different Carrier Oils. *Journal of Food Science*, *84*(4), 782-791. <https://doi.org/10.1111/1750-3841.14423>.
- Shah, B. R., Zhang, C. L., Li, Y., & Li, B. (2016). Bioaccessibility and antioxidant activity of curcumin after encapsulated by nano and Pickering emulsion based on chitosan-tripolyphosphate nanoparticles. *Food Research International*, *89*, 399-407. <https://doi.org/10.1016/j.foodres.2016.08.022>.
- Sharma, R. A., McLelland, H. R., Hill, K. A., Ireson, C. R., Euden, S. A., Manson, M. M., . . . Steward, W. P. (2001). Pharmacodynamic and pharmacokinetic study of oral Curcuma extract in patients with colorectal cancer. *Clinical Cancer Research*, *7*(7), 1894-1900.
- Silva, H. D., Cerqueira, M. A., & Vicente, A. A. (2012). Nanoemulsions for Food Applications: Development and Characterization. *Food and Bioprocess Technology*, *5*(3), 854-867. <https://doi.org/10.1007/s11947-011-0683-7>.
- Silvestre, M. P. C., Chaiyasit, W., Brannan, R. G., McClements, D. J., & Decker, E. A. (2000). Ability of surfactant headgroup size to alter lipid and antioxidant oxidation in oil-in-water emulsions. *Journal of Agricultural and Food Chemistry*, *48*(6), 2057-2061. <https://doi.org/10.1021/jf991162l>.
- Sun, J. B., Bi, C., Chan, H. M., Sun, S. P., Zhang, Q. W., & Zheng, Y. (2013). Curcumin-loaded solid lipid nanoparticles have prolonged in vitro antitumour activity, cellular uptake and improved in vivo bioavailability. *Colloids and Surfaces B-*



*Biointerfaces*, 111, 367-375. <https://doi.org/10.1016/j.colsurfb.2013.06.032>.

- Takahashi, M., Uechi, S., Takara, K., Asikin, Y., & Wada, K. (2009). Evaluation of an Oral Carrier System in Rats: Bioavailability and Antioxidant Properties of Liposome-Encapsulated Curcumin. *Journal of Agricultural and Food Chemistry*, 57(19), 9141-9146. <https://doi.org/10.1021/jf9013923>.
- Tamjidi, F., Shahedi, M., Varshosaz, J., & Nasirpour, A. (2013). Nanostructured lipid carriers (NLC): A potential delivery system for bioactive food molecules. *Innovative Food Science & Emerging Technologies*, 19, 29-43. <https://doi.org/http://doi.org/10.1016/j.ifset.2013.03.002>.
- Tapal, A., & Tiku, P. K. (2012). Complexation of curcumin with soy protein isolate and its implications on solubility and stability of curcumin. *Food Chemistry*, 130(4), 960-965. <https://doi.org/10.1016/j.foodchem.2011.08.025>.
- Taylor, T. M., Davidson, P. M., Bruce, B. D., & Weiss, J. (2005). Liposomal nanocapsules in food science and agriculture. *Critical Reviews in Food Science and Nutrition*, 45(7-8), 587-605. <https://doi.org/10.1080/10408390591001135>.
- Thanasukarn, P., Pongsawatmanit, R., & McClements, D. J. (2004). Influence of emulsifier type on freeze-thaw stability of hydrogenated palm oil-in-water emulsions. *Food Hydrocolloids*, 18(6), 1033-1043. <https://doi.org/10.1016/j.foodhyd.2004.04.010>.
- Tonnesen, H. H. (2002). Solubility, chemical and photochemical stability of curcumin in surfactant solutions - Studies of curcumin and curcuminoids, XXVIII. *Pharmazie*, 57(12), 820-824.
- Tonnesen, H. H., & Karlsen, J. (1985a). STUDIES ON CURCUMIN AND CURCUMINOIDS .5. ALKALINE-DEGRADATION OF CURCUMIN. *Zeitschrift Fur Lebensmittel-Untersuchung Und-Forschung*, 180(2), 132-134. <https://doi.org/10.1007/bf01042637>.
- Tonnesen, H. H., & Karlsen, J. (1985b). STUDIES ON CURCUMIN AND CURCUMINOIDS .6. KINETICS OF CURCUMIN DEGRADATION IN AQUEOUS-SOLUTION. *Zeitschrift Fur Lebensmittel-Untersuchung Und-Forschung*, 180(5), 402-404. <https://doi.org/10.1007/bf01027775>.
- Tonnesen, H. H., Karlsen, J., Adhikary, S. R., & Pandey, R. (1989). STUDIES ON CURCUMIN AND CURCUMINOIDS .17. VARIATION IN THE CONTENT OF CURCUMINOIDS IN CURCUMA-LONGA L FROM NEPAL DURING ONE SEASON. *Zeitschrift Fur Lebensmittel-Untersuchung Und-Forschung*, 189(2), 116-118. <https://doi.org/10.1007/bf01332943>.
- Tonnesen, H. H., Masson, M., & Loftsson, T. (2002). Studies of curcumin and

- curcuminoids. XXVII. Cyclodextrin complexation: solubility, chemical and photochemical stability. *International Journal of Pharmaceutics*, 244(1-2), 127-135. [https://doi.org/10.1016/s0378-5173\(02\)00323-x](https://doi.org/10.1016/s0378-5173(02)00323-x).
- Tonnesen, H. H., Smistad, G., Agren, T., & Karlsen, J. (1993). STUDIES ON CURCUMIN AND CURCUMINOIDS .23. EFFECTS OF CURCUMIN ON LIPOSOMAL LIPID-PEROXIDATION. *International Journal of Pharmaceutics*, 90(3), 221-228.
- Topping, D. L. (1991). SOLUBLE FIBER POLYSACCHARIDES - EFFECTS ON PLASMA-CHOLESTEROL AND COLONIC FERMENTATION. *Nutrition Reviews*, 49(7), 195-203.
- Uluata, S., McClements, D. J., & Decker, E. A. (2015). Physical Stability, Autoxidation, and Photosensitized Oxidation of omega-3 Oils in Nanoemulsions Prepared with Natural and Synthetic Surfactants. *Journal of Agricultural and Food Chemistry*, 63(42), 9333-9340. <https://doi.org/10.1021/acs.jafc.5b03572>.
- Vanapalli, S. A., & Coupland, J. N. (2001). Emulsions under shear - the formation and properties of partially coalesced lipid structures. *Food Hydrocolloids*, 15(4-6), 507-512. [https://doi.org/10.1016/s0268-005x\(01\)00057-1](https://doi.org/10.1016/s0268-005x(01)00057-1).
- Vanapalli, S. A., Palanuwech, J., & Coupland, J. N. (2002). Stability of emulsions to dispersed phase crystallization: effect of oil type, dispersed phase volume fraction, and cooling rate. *Colloids and Surfaces A: Physicochemical and Engineering Aspects*, 204(1), 227-237. [https://doi.org/https://doi.org/10.1016/S0927-7757\(01\)01135-9](https://doi.org/https://doi.org/10.1016/S0927-7757(01)01135-9).
- Vanapalli, S. A., Palanuwech, J., & Coupland, J. N. (2002). Stability of emulsions to dispersed phase crystallization: effect of oil type, dispersed phase volume fraction, and cooling rate. *Colloids and Surfaces a-Physicochemical and Engineering Aspects*, 204(1-3), 227-237. [https://doi.org/10.1016/s0927-7757\(01\)01135-9](https://doi.org/10.1016/s0927-7757(01)01135-9).
- Vecchione, R., Quagliariello, V., Calabria, D., Calcagno, V., De Luca, E., Iaffaioli, R. V., & Netti, P. A. (2016). Curcumin bioavailability from oil in water nano-emulsions: In vitro and in vivo study on the dimensional, compositional and interactional dependence. *Journal of Controlled Release*, 233, 88-100. <https://doi.org/10.1016/j.jconrel.2016.05.004>.
- Wang, L., Folsom, A. R., Eckfeldt, J. H., & Investigators, A. S. (2003). Plasma fatty acid composition and incidence of coronary heart disease in middle aged adults: The Atherosclerosis Risk in Communities (ARIC) Study. *Nutrition Metabolism and Cardiovascular Diseases*, 13(5), 256-266. [https://doi.org/10.1016/s0939-4753\(03\)80029-7](https://doi.org/10.1016/s0939-4753(03)80029-7).



- Wang, M. N., Wu, C. X., Tang, Y. Q., Fan, Y. X., Han, Y. C., & Wang, Y. L. (2014). Interactions of cationic trimeric, gemini and monomeric surfactants with trianionic curcumin in aqueous solution. *Soft Matter*, *10*(19), 3432-3440. <https://doi.org/10.1039/c4sm00086b>.
- Wang, T. R., Ma, X. Y., Lei, Y., & Luo, Y. C. (2016). Solid lipid nanoparticles coated with cross-linked polymeric double layer for oral delivery of curcumin. *Colloids and Surfaces B-Biointerfaces*, *148*, 1-11. <https://doi.org/10.1016/j.colsurfb.2016.08.047>.
- Wang, X. Y., Jiang, Y., Wang, Y. W., Huang, M. T., Ho, C. T., & Huang, Q. R. (2008). Enhancing anti-inflammation activity of curcumin through O/W nanoemulsions. *Food Chemistry*, *108*(2), 419-424. <https://doi.org/10.1016/j.foodchem.2007.10.086>.
- Wang, Y., Lu, Z. X., Lv, F. X., & Bie, X. M. (2009). Study on microencapsulation of curcumin pigments by spray drying. *European Food Research and Technology*, *229*(3), 391-396. <https://doi.org/10.1007/s00217-009-1064-6>.
- Wang, Y. J., Pan, M. H., Cheng, A. L., Lin, L. I., Ho, Y. S., Hsieh, C. Y., & Lin, J. K. (1997). Stability of curcumin in buffer solutions and characterization of its degradation products. *Journal of Pharmaceutical and Biomedical Analysis*, *15*(12), 1867-1876. [https://doi.org/10.1016/s0731-7085\(96\)02024-9](https://doi.org/10.1016/s0731-7085(96)02024-9).
- Wanninger, S., Lorenz, V., Subhan, A., & Edelman, F. T. (2015). Metal complexes of curcumin - synthetic strategies, structures and medicinal applications. *Chemical Society Reviews*, *44*(15), 4986-5002. <https://doi.org/10.1039/c5cs00088b>.
- Weiss, J., Decker, E. A., McClements, D. J., Kristbergsson, K., Helgason, T., & Awad, T. (2008). Solid lipid nanoparticles as delivery systems for bioactive food components. *Food Biophysics*, *3*(2), 146-154. <https://doi.org/10.1007/s11483-008-9065-8>.
- Weiszhar, Z., Czucz, J., Revesz, C., Rosivall, L., Szebeni, J., & Rozsnyay, Z. (2012). Complement activation by polyethoxylated pharmaceutical surfactants: Cremophor-EL, Tween-80 and Tween-20. *European Journal of Pharmaceutical Sciences*, *45*(4), 492-498. <https://doi.org/10.1016/j.ejps.2011.09.016>.
- Wu, M. H., Yan, H. H., Chen, Z. Q., & He, M. (2017). Effects of emulsifier type and environmental stress on the stability of curcumin emulsion. *Journal of Dispersion Science and Technology*, *38*(10), 1375-1380. <https://doi.org/10.1080/01932691.2016.1227713>.
- Wu, W. J., Hu, Y. Y., Guo, Q., Yan, J., Chen, Y. C., & Cheng, J. H. (2015). Sorption/desorption behavior of triclosan in sediment-water-rhamnolipid systems: Effects of pH, ionic strength, and DOM. *Journal of Hazardous Materials*, *297*,

59-65. <https://doi.org/10.1016/j.jhazmat.2015.04.078>.

- Xie, X. X., Tao, Q., Zou, Y. N., Zhang, F. Y., Guo, M., Wang, Y., . . . Yu, S. Q. (2011). PLGA Nanoparticles Improve the Oral Bioavailability of Curcumin in Rats: Characterizations and Mechanisms. *Journal of Agricultural and Food Chemistry*, 59(17), 9280-9289. <https://doi.org/10.1021/jf202135j>.
- Xu, G. R., Wang, C. N., & Yao, P. (2017). Stable emulsion produced from casein and soy polysaccharide compacted complex for protection and oral delivery of curcumin. *Food Hydrocolloids*, 71, 108-117. <https://doi.org/10.1016/j.foodhyd.2017.05.010>.
- Xue, J. Y., Wang, T. R., Hu, Q. B., Zhou, M. Y., & Luo, Y. C. (2018). Insight into natural biopolymer-emulsified solid lipid nanoparticles for encapsulation of curcumin: Effect of loading methods. *Food Hydrocolloids*, 79, 110-116. <https://doi.org/10.1016/j.foodhyd.2017.12.018>.
- Yan, Y. D., Kim, J. A., Kwak, M. K., Yoo, B. K., Yong, C. S., & Choi, H. G. (2011). Enhanced Oral Bioavailability of Curcumin via a Solid Lipid-Based Self-Emulsifying Drug Delivery System Using a Spray-Drying Technique. *Biological & Pharmaceutical Bulletin*, 34(8), 1179-1186.
- Yang, H. X., Du, Z. Y., Wang, W. C., Song, M. Y., Sanidad, K., Sukamtoh, E., . . . Zhang, G. D. (2017). Structure-Activity Relationship of Curcumin: Role of the Methoxy Group in Anti-inflammatory and Anticolitis Effects of Curcumin. *Journal of Agricultural and Food Chemistry*, 65(22), 4509-4515. <https://doi.org/10.1021/acs.jafc.7b01792>.
- Yu, H. L., & Huang, Q. R. (2011). Investigation of the Absorption Mechanism of Solubilized Curcumin Using Caco-2 Cell Monolayers. *Journal of Agricultural and Food Chemistry*, 59(17), 9120-9126. <https://doi.org/10.1021/jf201451m>.
- Yu, H. L., & Huang, Q. R. (2012). Improving the Oral Bioavailability of Curcumin Using Novel Organogel-Based Nanoemulsions. *Journal of Agricultural and Food Chemistry*, 60(21), 5373-5379. <https://doi.org/10.1021/jf300609p>.
- Yuan, Y., Gao, Y., Zhao, J., & Mao, L. (2008). Characterization and stability evaluation of  $\beta$ -carotene nanoemulsions prepared by high pressure homogenization under various emulsifying conditions. *Food Research International*, 41(1), 61-68. <https://doi.org/https://doi.org/10.1016/j.foodres.2007.09.006>.
- Zhang, L., Hayes, D. G., Chen, G., & Zhong, Q. (2013). Transparent Dispersions of Milk-Fat-Based Nanostructured Lipid Carriers for Delivery of  $\beta$ -Carotene. *Journal of Agricultural and Food Chemistry*, 61(39), 9435-9443. <https://doi.org/10.1021/jf403512c>.
- Zheng, B. J., Peng, S. F., Zhang, X. Y., & McClements, D. J. (2018). Impact of Delivery

System Type on Curcumin Bioaccessibility: Comparison of Curcumin-Loaded Nanoemulsions with Commercial Curcumin Supplements. *Journal of Agricultural and Food Chemistry*, 66(41), 10816-10826. <https://doi.org/10.1021/acs.jafc.8b03174>.

Zou, L. Q., Zheng, B. J., Liu, W., Liu, C. M., Xiao, H., & McClements, D. J. (2015). Enhancing nutraceutical bioavailability using excipient emulsions: Influence of lipid droplet size on solubility and bioaccessibility of powdered curcumin. *Journal of Functional Foods*, 15, 72-83. <https://doi.org/10.1016/j.jff.2015.02.044>.